

# Introduction to Scanning Probe Microscopy

**Giacomo Torzo**

Physics Dept. Padova University  
ICIS-CNR



UNIVERSITÀ  
DEGLI STUDI  
DI PADOVA

# Overview

What is a surface ?  
Different types of SPM  
STM: the tunnelling process  
SFM: Beam Bounce Detecting technique  
SPMscanners  
Tip to sample Approaching  
Contact Mode  
Constant height and constant force  
Top-view and 3D-view Images  
Long and short ranging forces  
Non-Contact Mode  
Phase- contrast images  
Microtribology  
MFM, EFM, SCM and other techniques  
Aspect Ratio and Curvature radius  
Tip convolution  
Image resolution  
SPM artifacts  
Image post-processing  
NanoEducator SPM  
Software for SPM

# What is a surface?

The definition of a "surface" in the **microscopic** world is not as trivial as in the **macroscopic** world (in a solid sample the atoms at "surface" are separated by distances much higher than the mean nuclear diameter, with the electrons surrounding the nuclei distributed in orbitals extending much beyond the intra-nuclear distances).

A practical definition is the one used for SPM: "*the **locus of points** traced by a **"point-probe"** while **keeping constant** the probe-sample **interaction***"

The **probe** may be a "tip" (or an "electron beam" associated to a sensor detecting the effect of the beam interaction with the scanned surface, as in SEM).

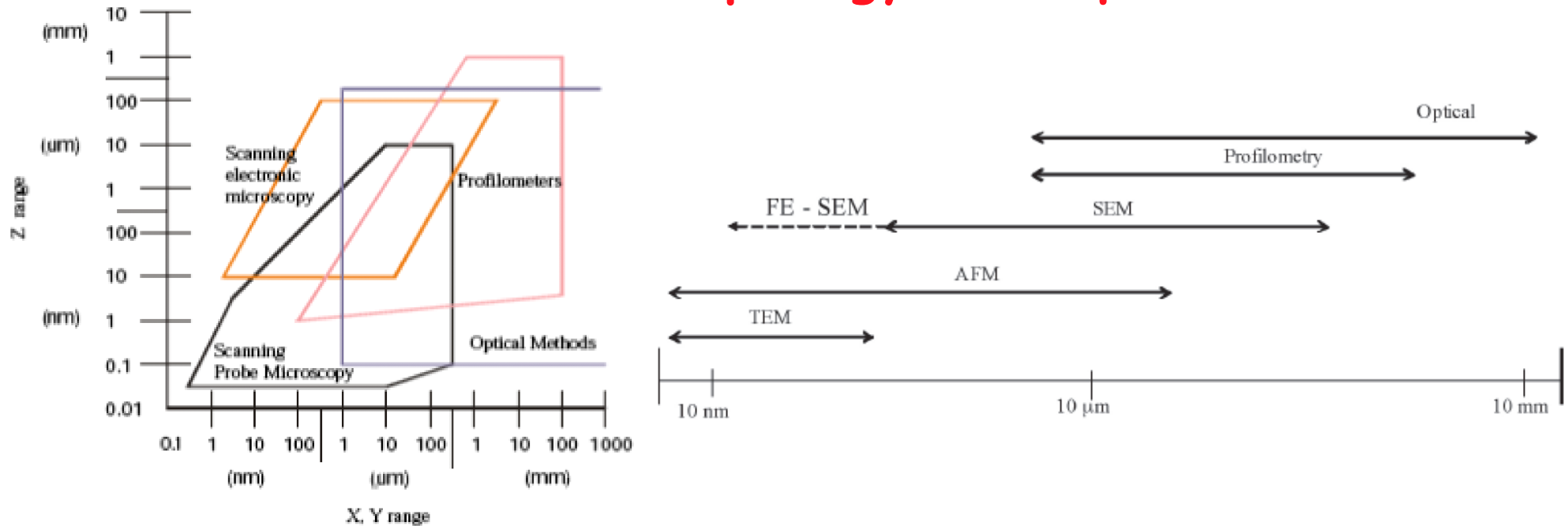
Most SPM use a *piezoelectric scanner* to control the **position (x,y)** of the point-probe over the sample, and the probe-sample **distance (z)**

The probe signal is processed by a computer to build the 3D **image  $I(x,y,z)$**

"**3D topography**" defines the height profile of the sample surface, i.e. the local measurement of the **deviation** from an **ideal flat plane**.

Images at nanometric resolution with **real 3D topography** may only be obtained using **Scanning Probe Microscope**.

# Surface morphology techniques



Comparison of optical, electronic and probe microscopes

|                        | Optical                                      | SEM                                 | SPM   |
|------------------------|--|-------------------------------------|---|
| works in :             | air, liquid, vacuum                          | vacuum                              | air, liquid, vacuum   |
| Field depth :          | small  | large                               | medium  |
| Resolution (x,y) :     | 1.0 $\mu\text{m}$                            | 5nm                                 | 2-10nm (AFM)<br>0.1nm (STM)                                 |
| Resolution (z) :       | absent                                       | absent                              | 0.1nm (AFM)<br>0.01nm (STM)                                 |
| Magnification :        | 1X $\rightarrow$ 2 $\cdot$ 10 <sup>3</sup> X | 10X $\rightarrow$ 10 <sup>6</sup> X | 5 $\cdot$ 10 <sup>2</sup> X $\rightarrow$ 10 <sup>8</sup> X |
| Sample preparation     | small  | important                           | no  |
| Needed sample features | not totally transparent                      | conducting, vacuum compatible       | roughness not large than 10 $\mu\text{m}$                   |



## Different types of SPM

Different kind of **probe-sample interaction** correspond to different types of **SPM**.

In **SEM-STEM** = Scanning (Transmission) Electron Microscope, the signals are produced by detectors that monitor the effect of electron collisions with the sample (*X-rays, reflected or transmitted electrons...*)

In **STM** = Scanning Tunneling Microscope, the signal is the *tunneling electron current*.

In **SFM** = Scanning Force Microscope, the signal is due to some *interactive force* (Van der Waals, magnetic, electric, friction,...).

In **SNOM** = Scanning Near Field Optical Microscope, the signal is the "*evanescent field*" of electromagnetic radiation measured through a small aperture (usually an optical fiber).

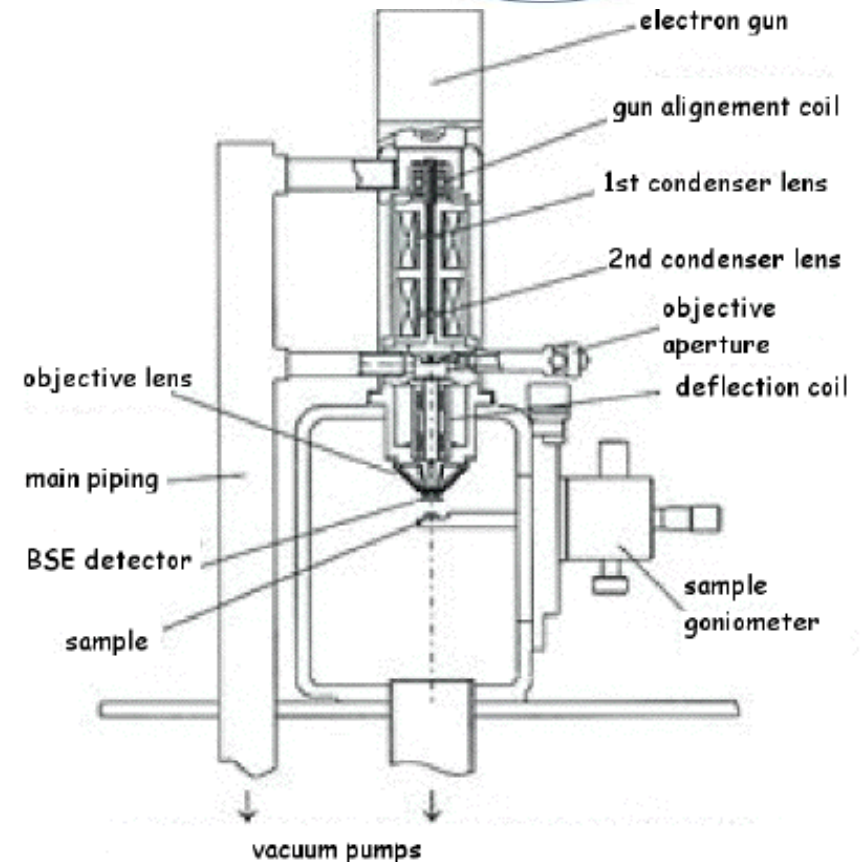
# Electron microscopes

Electron microscopes may be divided into two categories:

**SEM**, for **S**canning (reflection) **E**lectron **M**icroscope  
**(S)TEM** for **(S)**canning **T**ransmission **E**lectron **M**icroscope.

In both the image is normally obtained by **detecting the signal produced by an electron beam** at high energy (10÷500 keV), generated by an electron gun.

The electrons penetrate a region where suitable electrodes (**electromagnetic lenses**) create magnetic or electric fields that track the beam in a **raster scanning** of the sample surface (over an area of few mm<sup>2</sup>).



# SEM

To avoid energy loss and diffusion, which would spoil the monochromatism and the collimation of the electron beam, one must keep the electron gun, lenses and sample inside a **ultra-high vacuum** chamber. ( $\approx 10^{-6} - 10^{-12}$  Pa).

The electron collisions with the sample produce emission of **photons** (or secondary-electrons) that, in the case of SEM, are collected by suitable **photo-detectors** generating an *image* of the swept area.

The electron beam **interacts** with the sample within a **surface layer** whose thickness ranges from **few nm** up to **several  $\mu$ m**. Also primary electrons (backscattered) and secondary electrons are emitted from the sample.

The **secondary electrons** (from the conduction band) are usually the signal used for morphologic SEM analysis. They have low energy ( $< 50$  eV) and only those produced in the first layers (few nm) may escape the surface to be detected by sensors.

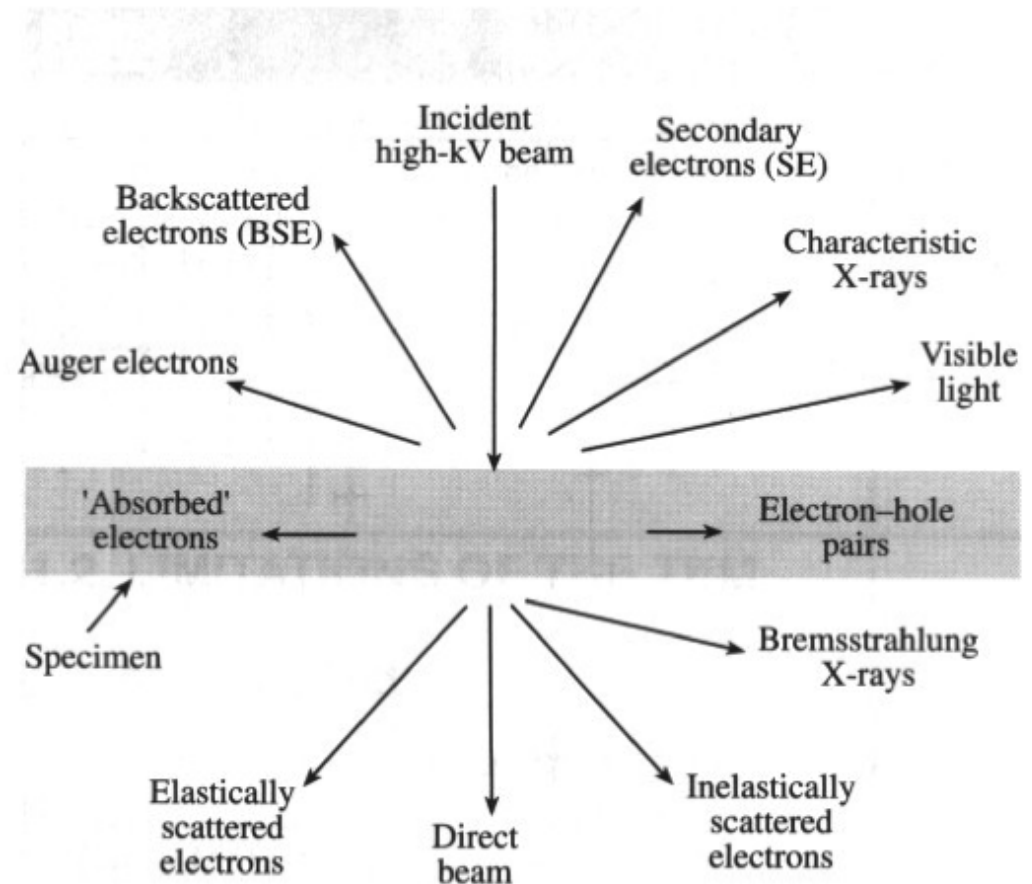
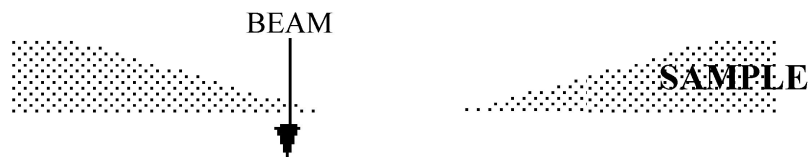
Also **primary electrons** backscattered from deeper layers may produce secondary electrons close to the surface, but far from the entering beam spot.

## SEM-TEM images

The image may be produced also collecting the *current* produced by the electron beam (EBIC = Electron Beam Induced Current), or the AUGER electrons, or X-rays, or cathode-luminescence electrons.

In **STEM** the image is created by electrons *transmitted* through the sample that is made *extremely thin* ( $z < 1\mu\text{m}$ ) in the investigated area.

A *strong interaction* is *therefore unavoidable*: the sample is always damaged.



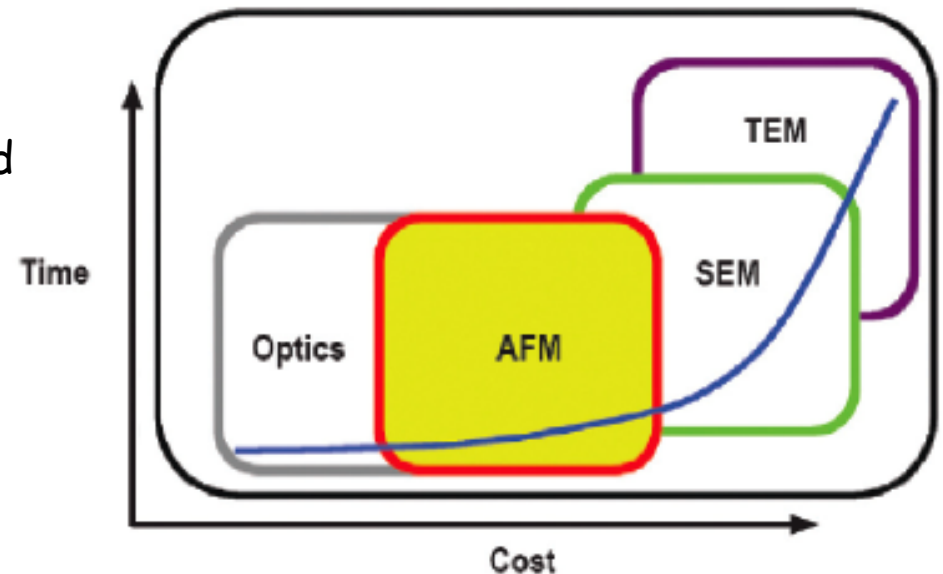
## Comparing SEM-AFM

Any SEM or TEM image bears information produced by a sample **layer** (whose thickness depends on the *sample nature* and by the *beam energy*) which is quite thin, but **never** reaches the limit of a **single atomic layer**.

The SEM e TEM images give information on the **composition and microscopic structure** of the surface layer, but **not a real 3D topography**.

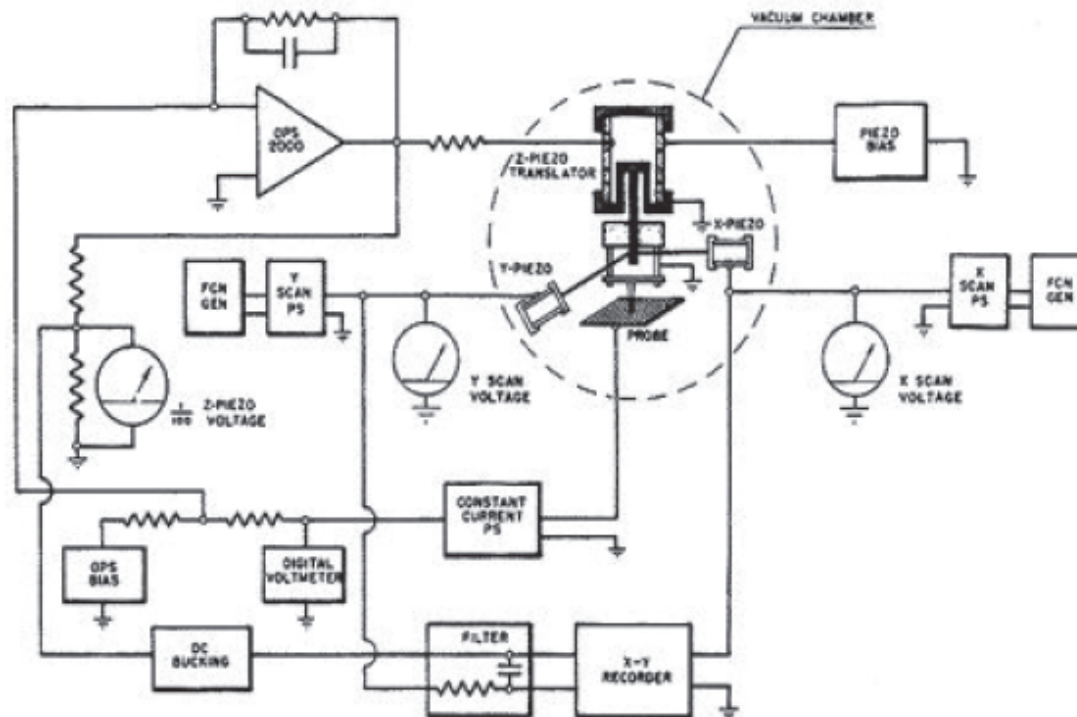
SEM-TEM require advanced skillness of the operator,  
and are intrinsically **very expensive devices** (involve UH-Vacuum and high voltages)

Although the **time** required for making a measurement with the SEM image is typically less than an AFM, the amount of time required to get meaningful images is similar. This is because the SEM/TEM often requires substantial time to prepare a sample. With AFM no sample preparation is required.



## The precursor of STM

The “**topografiner**” was the first device using **electron field emission** to obtain surface topography of a sample  
(electron field emission current between a sharp metal probe and a conductive surface is strongly dependent on the gap)



R. Young, J. Ward, F. Scire, *The Topografiner: An Instrument for Measuring Surface Microtopography*, Rev. Sci. Inst., Vol 43, No 7 (1971)

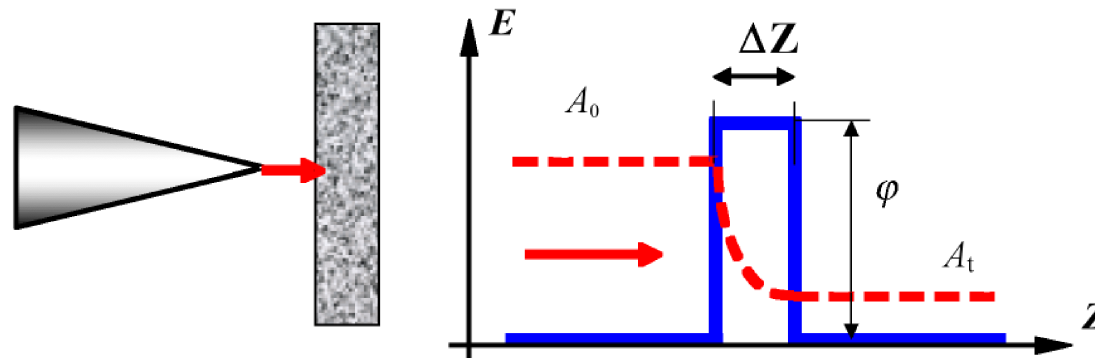
## STM : Scanning Tunneling Microscope

The "tunneling" is a quantum effect: it describes a particle that crosses a potential barrier.

Considering charged particles (electrons) with total energy  $E_0$ , inside a box whose walls are a "shell" at potential  $E_1$ , with  $E_1 > E_0$ , within a classical model it is impossible that these particles escape the box.

To escape they should gain an energy larger than  $E_1$ .

Within quantum model a finite probability exist for a particle with energy  $E_0 < E_1$  to cross the potential barrier: this crossing the barrier is named *tunnel effect*.



The working principle of STM is based on the electron tunneling through the narrow potential barrier between a **metal tip** and a **conducting sample** in an external electric field.



## Tunneling probability

The probability  $W$  of electron tunneling (transmission coefficient) through one-dimensional rectangular barrier is :

$$W = \frac{|A_t|^2}{|A_0|^2} \cong e^{-k\Delta z}$$

where  $A_0$  is the amplitude of electron wave function approaching the barrier;  $A_1$  the amplitude of the transmitted electron wave function,  $k$  the attenuation coefficient of the wave function inside the potential barrier;  $\Delta z$  the barrier width.

In the case of tunneling between two metals, the coefficient  $k$  is:

$$k = \frac{4\pi\sqrt{2m\phi}}{h}$$

where  $m$  is the electron mass,  $\phi$  the average electron emission work function and  $h$  the Planck constant.

For small values of the bias voltage ( $eV \ll \phi$ ), the current density  $j(z)$  can be approximated as:

$$j(z) = j_0(V) e^{-\frac{4\pi}{h} \sqrt{2m\phi} \Delta z}$$

with  $j_0(V) \approx V/\Delta z$



## STM : vertical and lateral resolution

Assuming :

$$j \approx (V/z) \exp(-kz),$$

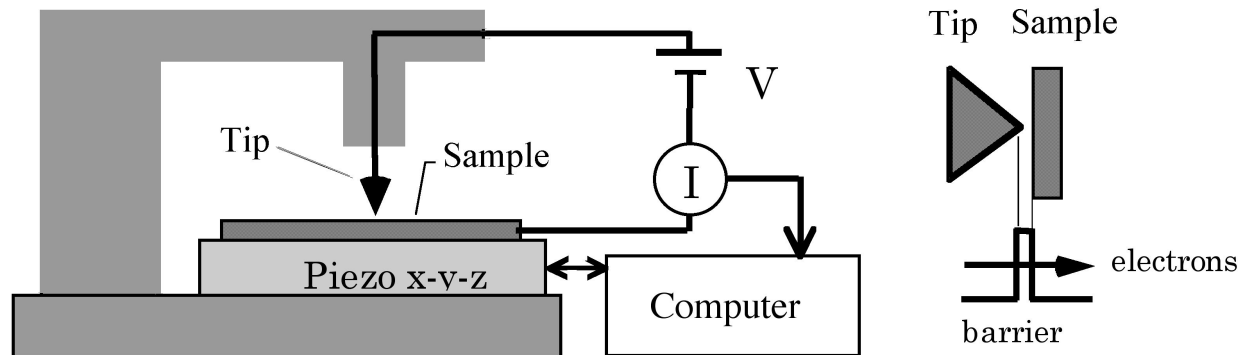
where  $V$  is the tip-sample bias voltage and,  $k$  is of the order of  $10^{-10} \text{ m}$ , by using the tunneling **current** as a measurement of the tip-sample **distance** (the barrier width  $z$ )

we may reach, with a **current resolution of only 10%**, the excellent **vertical resolution of 0.01 nm**.

If we model the tip with a paraboloid with curvature radius  $R$  at the apex, the current density  $j$  has a Gaussian profile along a plane parallel to the sample surface described by the function:

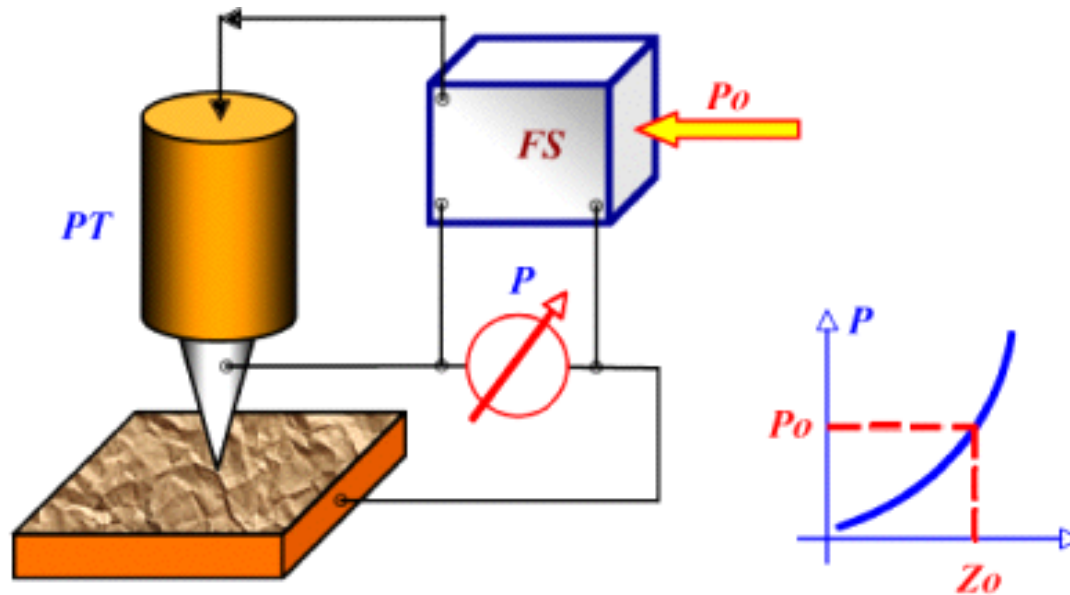
$$j(x) \approx (V/z) \exp(-kx^2/R),$$

giving a **lateral resolution** (for  $R \approx 100 \text{ nm}$ ) of the order of **2 nm**.



## The feedback principle

An extremely accurate positioning of the tip with respect to the sample may be obtained using a **piezo-transducer** (PT) and a **feedback control system** (FS).



For a given function  $P(z)$  of a signal depending on the tip-sample distance  $z$ , the **feedback system keeps constant the value of the parameter  $P$**  (equal to the value  $P_0$ , set by the operator).

If the tip-sample distance changes, the change in the parameter  $P$  is amplified and fed to **the piezo transducer that controls the tip-sample separation**, bringing it back to the preset value. The measured value of the signal fed to the piezo gives the topographic  $z$ -value for each point  $(x,y)$  of the sample surface.

## Tunneling Spectroscopy

The tunneling effect may be used for spectroscopy of electronic states by recording the dependence of the tunneling current on the **local density of states** (LDOS).

The STM allows to acquire the voltage-current characteristics (VCC) in any point of the surface and, therefore, to examine the local electric properties of the sample.

The expression for the tunneling current in the point  $r_0$  on the sample surface is:

$$I(r_0, V) \propto \int_0^{eV} dE \rho_T(E) \rho_S(r_0, E) D(r_0, E)$$

where  $D(r_0, E)$  is the barrier transparency,  $\rho_T(E)$  is the **density of the states** connected with the **tip**,  $\rho_S(r_0, E)$  is the **density of the states** in the  $r_0$  point of the **sample**. The tunneling current is a convolution of density of states of the tip and of the sample, and with an assumption that the density of states near the Fermi level in the tip metal is *practically constant*, the equation for the current may be written as :

$$I(r_0, V) \propto \int_0^{eV} \rho_S(r_0, E) dE$$

The dependence of  $I(r_0, V)$  on the voltage  $V$  is determined by the density of states of the sample. Practically, the  $\rho_S(r_0, E)$  value is estimated by the **voltage derivative of the tunneling current**, taken at **constant tip-sample distance**.

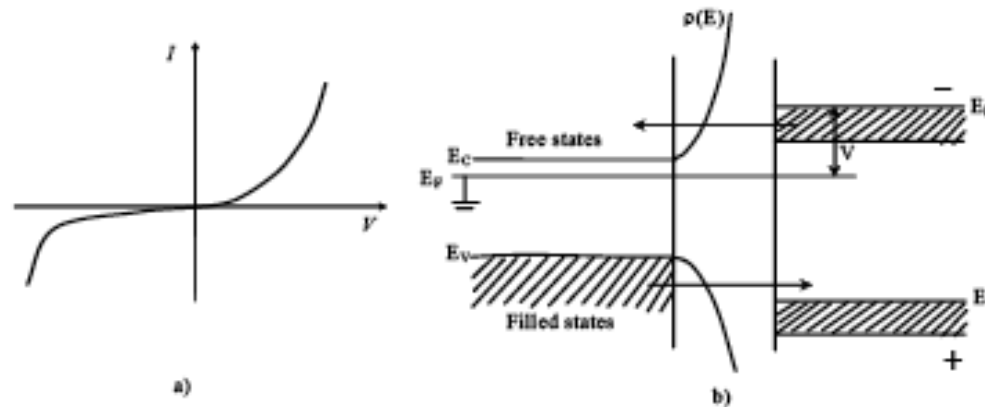
$$\rho_s(eV) \propto \frac{\partial I}{\partial V}$$

## Tunneling current spectra

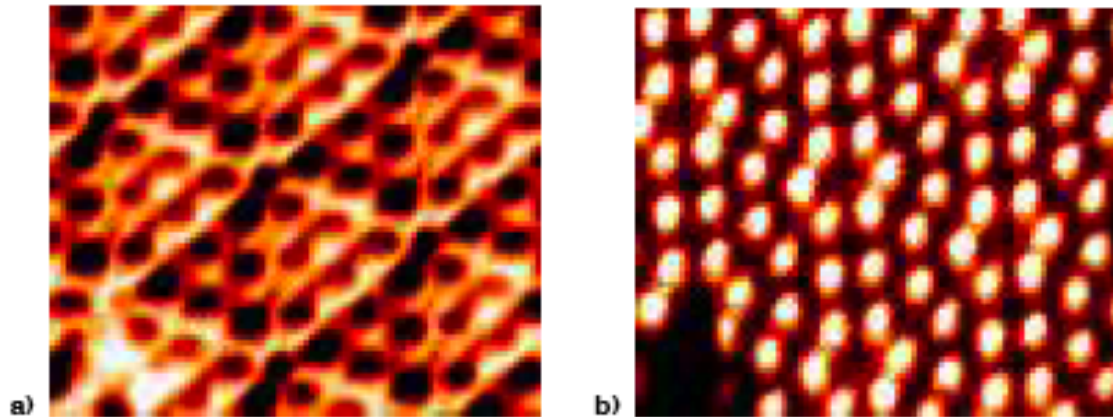
Semiconductor samples have a complex structure of the electron energy spectrum. Presence of the energy band-gap and impurity levels in the semiconductor spectrum makes the VCC of the metal-semiconductor tunneling contact **nonlinear**. A contribution to the tunneling current is also given by surface states and energy levels due to foreign **atoms absorbed on the surface**. This is why examination of local tunneling spectra of semiconductor materials is performed in high vacuum.

Tunneling spectra allow to **determine the arrangement of edges of the conducting and the valence bands with respect to the Fermi level** as well as to identify the peaks connected with the **impurity states** inside the semiconductors band-gap.

The STM surface image depends on the **value** and **polarity** of the voltage applied to the tunneling contact. This is related to the features of electrons tunneling from the tip into the sample free states or from the sample filled states into the tip



## Tunneling current images with different bias voltage



Two STM images of the Si (111)-(7x7) reconstructed with different voltages applied to the contact :  
a)  $V=+0.4V$  b)  $V=-1.4V$

In the **Voltage-modulation mode**, besides the  $V_{\pm}$  constant bias voltage, a  $V_{\sim}$  small alternating voltage is applied to the tunneling contact. The resulting AC modulation of the tunneling current  $I_{\sim}$  is :

$$I_{\sim} = \frac{dI}{dV} \propto \rho(X, Y, E_F + eV_{\pm})$$

In the **constant current mode**, variations of the **work function  $\phi$**  may produce distortion of the topographic image. Those small distortions, (within a few angstroms for  $V$  change in the range 2 ÷ 5 V), may be taken into account by measuring  $\phi(X, Y)$ . To do so, the **tip-sample distance must be modulated** at small amplitude  $d$ , and the AC component  $I_{\sim}$  of the tunneling current is:

$$I_{\sim} = I_{\tau} \frac{\delta}{2} \frac{dI_{\tau}}{dZ} = I_{\tau} \frac{\delta}{\hbar} \sqrt{2m\phi}$$

## The piezo-scanner

It is necessary to control the tip-sample distance and to move the tip over the sample surface with high accuracy (at subnanometric level) in order to make the SPM properly working.

This performance can be achieved using **scanners** made of **piezoceramics** (e.g.  $\text{Pb}(\text{ZrTi})\text{O}_3$  = lead zirconate titanate), material that change size in an external electric field (**inverse piezoelectric effect**).

The piezoceramics is a polarized polycrystalline material, obtained by powder sintering from crystal ferroelectrics.

Polarization of ceramics is performed by heating above its Curie temperature  $T_c$  ( $\approx 300^\circ\text{C}$ ), and then **slowly cooling in a strong electric field** ( $\approx 3 \text{ kV/cm}$ ).

After cooling below  $T_c$ , piezoceramic retains the **induced polarization** and gets the ability to **reversibly change its sizes under an applied electric field**.

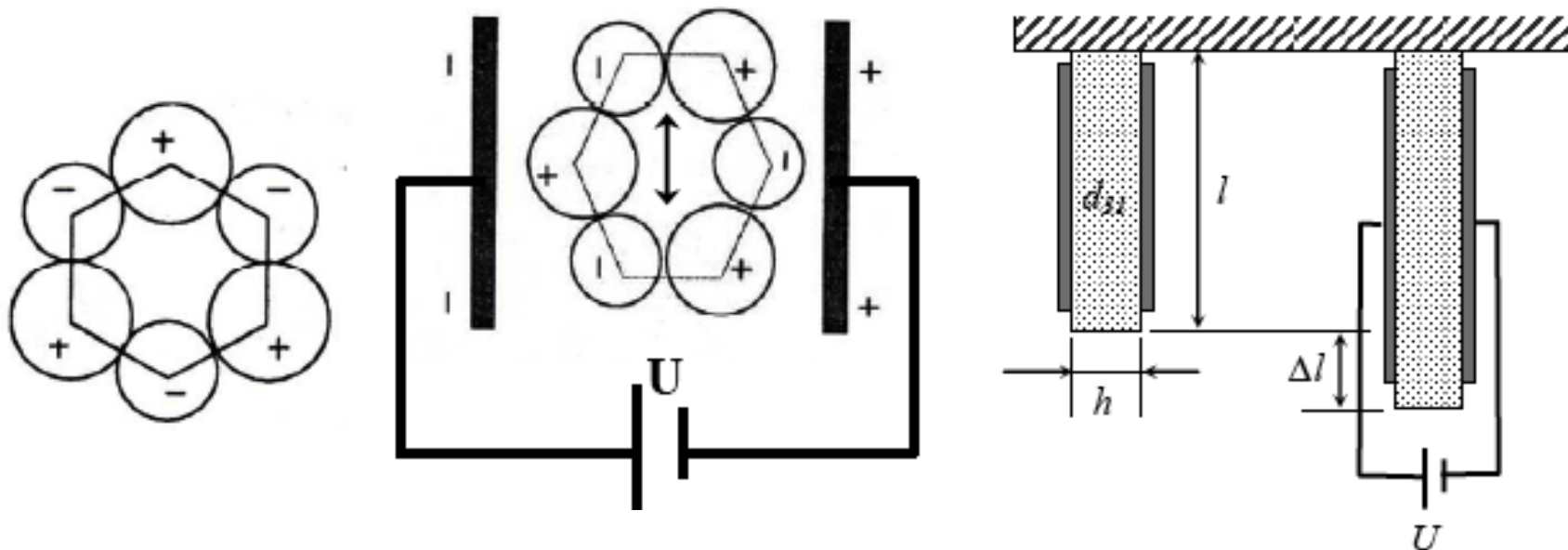
## The inverse piezo-effect

The inverse piezo-effect consists in changes of the piezo-material **geometry** under the effect of an **applied electric field**.

In a simple model imitating the  $\text{SiO}_2$  quartz structure, silicon positive ions in the lattice alternate with negative oxygen ions.

In the non-deformed cell the centers of positive and negative charges coincide.

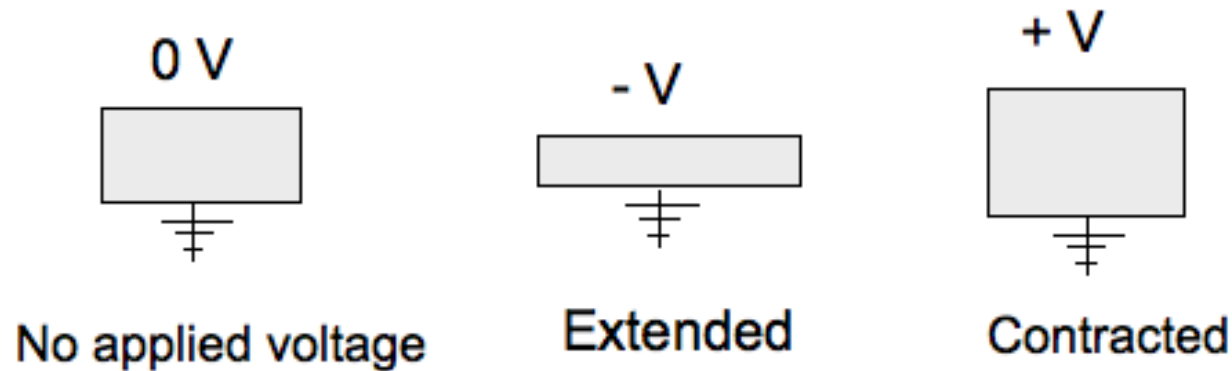
If an external voltage is applied to the metal electrodes located on the opposite faces of the quartz crystal, **the ions are shifted and this causes a deformation of the crystal lattice**.



## The piezo-scanner (2)

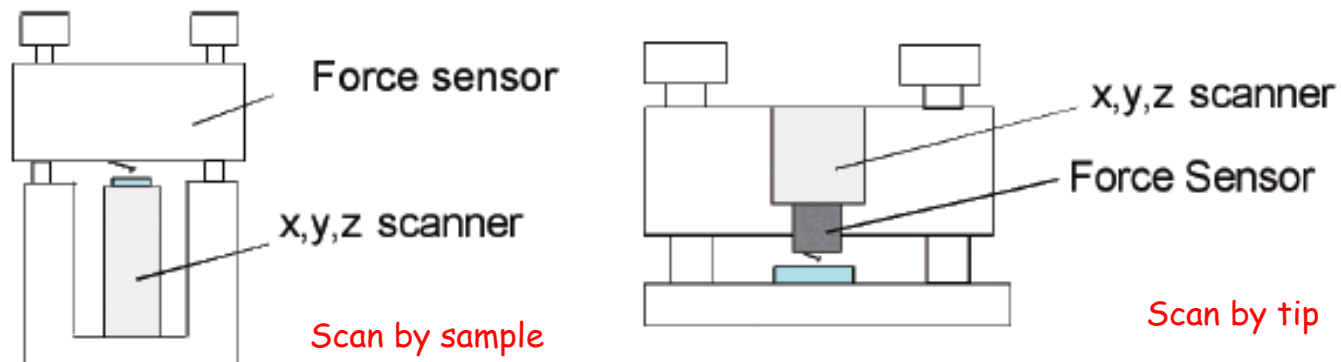
SPM piezo-scanners expand and contract proportionally to the applied voltage.

Whether they expand or contract depends upon the polarity of the applied voltage.



In some versions (**scan by sample**), the piezo tube moves the sample relative to the tip.

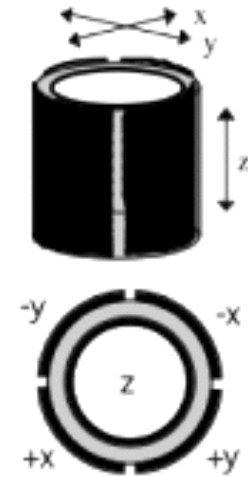
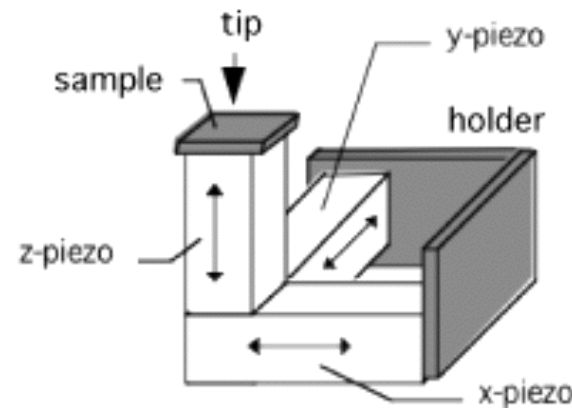
In other models (**scan by tip**), the sample is stationary while the scanner moves the tip.





## Tripod and Tubular scanners

A piezo-scanner may be made as a "tripod", i.e. 3 piezo-elements assembled along 3 orthogonal axes, or as a "tube" with one inner electrode and 4 outer electrodes.



In the **tripod** the 3 piezo bars (x,y,z) are driven independently by applying voltages across each electrode pairs plated onto the lateral faces.

In the **tubular** scanner the lateral displacement (x,y) is obtained as deflection of the cylinder axis by applying opposite voltages to the outer electrodes, and the vertical displacement (z) by applying voltage to the central electrode.

The **piezo-coefficient** is in the range 0.1 to 300 nm/V.

If L, D and  $W \ll D$  are the dimensions (in mm) of the tube height, diameter and wall thickness respectively, the typical displacements  $\Delta x$ ,  $\Delta y$ ,  $\Delta z$  (in nm/volt) are :

$$\Delta x, \approx \Delta y \approx 0.1 (L/D) (L/W), \text{ and } \Delta z \approx 0.2 L / W.$$

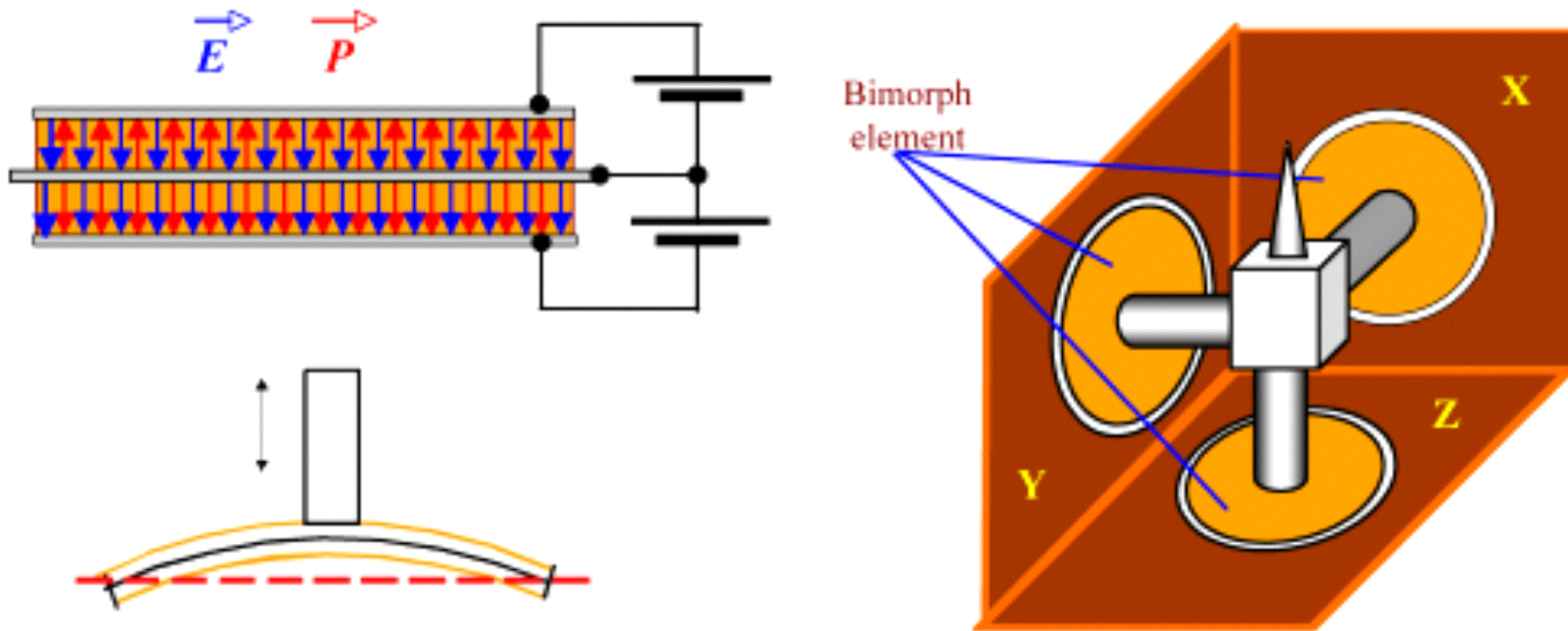
For example with  $L \approx D \approx 1$  cm,  $W \approx 1$  mm, the **vertical sensitivity is about 2nm/volt**.

## Bimorph tripod scanner

Tripod scanners may be made also using **bimorph cells**.

Bimorph is made of **two plates** of piezoelectric material, which have been glued together with opposite polarization vectors .

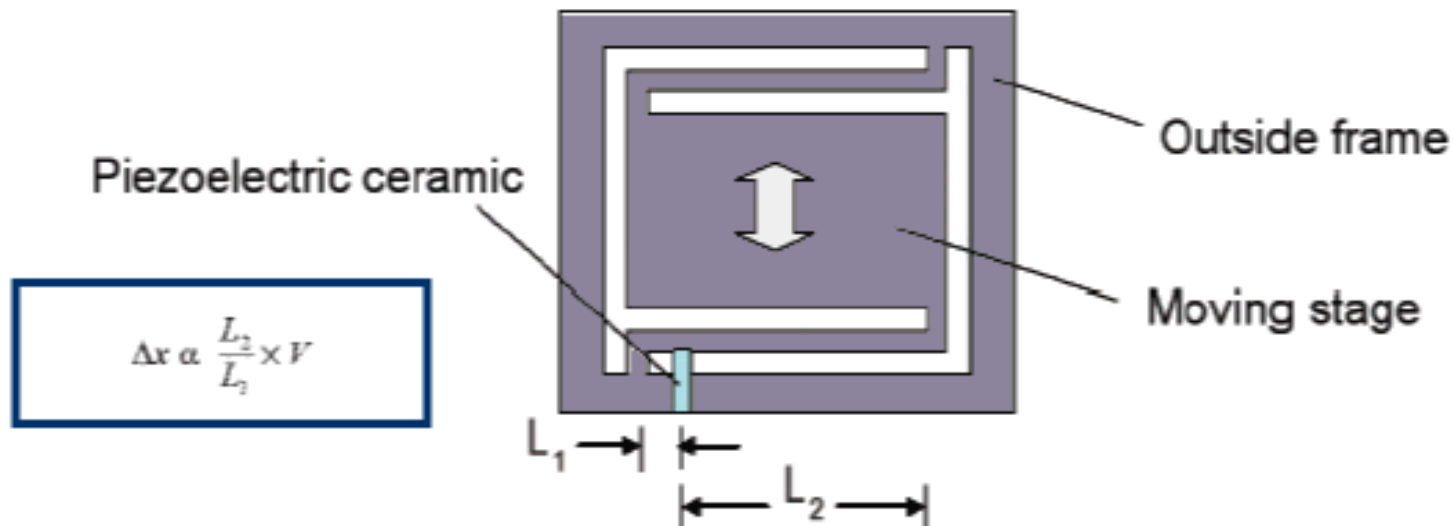
If a voltage is applied to bimorph electrodes, one of the plates will **extend**, and the other one will be **compressed**, resulting in a **bend** of the whole element.



## Flexure scanner

A flexure scanner operates by pushing on a flexure with a PZT. In this design, the ceramic pushes against the flexure which then causes the stage to move.

There is a gain in the motion given by the ratio of  $L_2/L_1$



## Piezoscanner properties

Electronically, piezoscanners act as **capacitors** and store charges on their surface.

Capacitances may be as large as  $100 \mu$  farads.

Once a charge is placed on the piezoceramic, the piezoceramic will stay charged until it is dissipated.

Electronic circuits used for driving the piezoceramics in an AFM must be designed to drive large capacitive loads.

All piezoceramics have a natural **resonance frequency** that depends on the size and shape of the ceramic.

Below the resonance frequency, the ceramic will follow an oscillating frequency, at resonance there is a 90 degree phase change, and above resonance there is a 180 degree phase change.

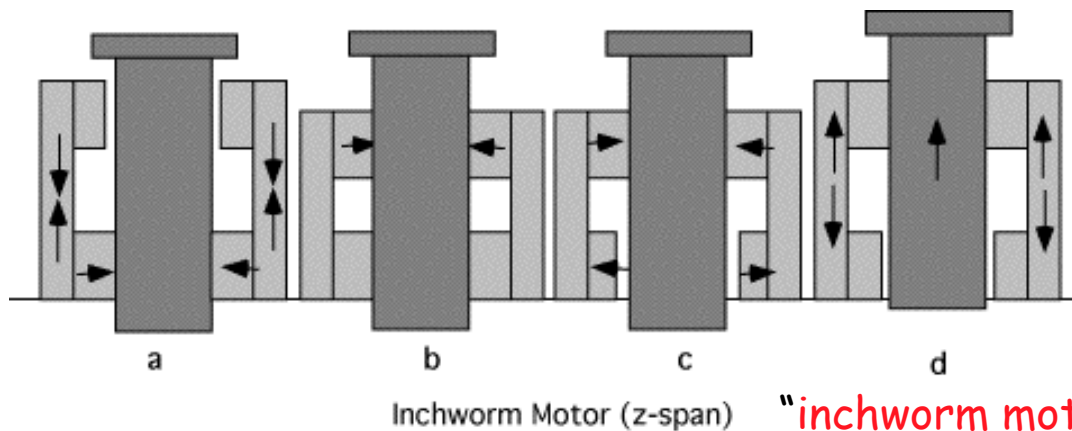
To a great extent, the resonance frequencies of the piezoelectric ceramics limit the scan rates of atomic force microscopes.

## Tip-sample approach

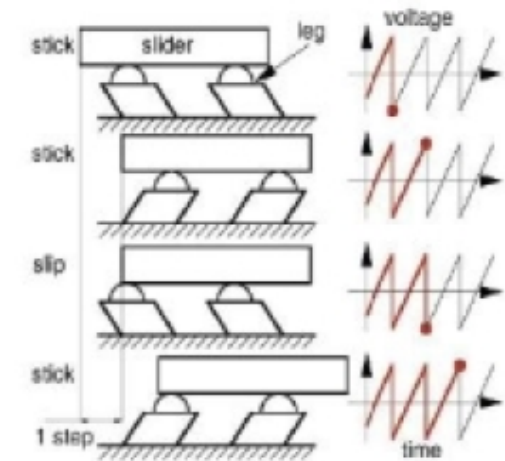
Several techniques are exploited to obtain a precise and **large movement**, to position the tip close to the sample, starting from macroscopic distance (needed to change sample or tip) :

**stepping motors**,  
controlled by encoders or optical sensors,  
or:

**inertial stick-slip** piezo movers  
using "sawtooth" contraction/extension cycles



**"inchworm motors"**,  
using contraction/extension cycles of coupled piezo.

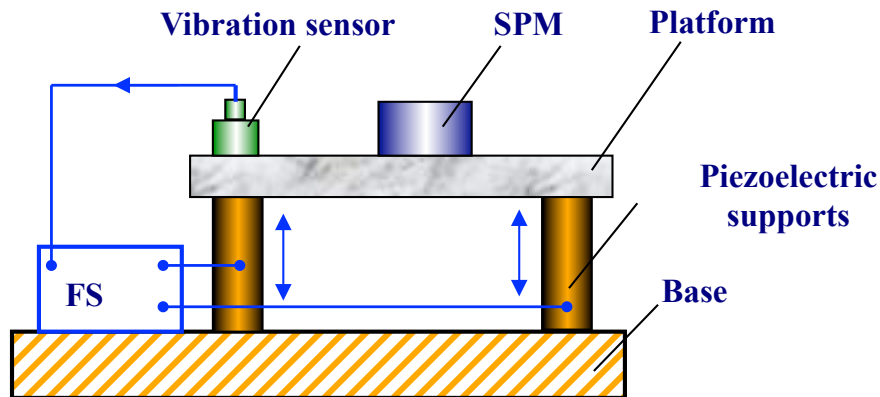


Both inertial and inchworm movers combine **very high resolution** with a **very large range**

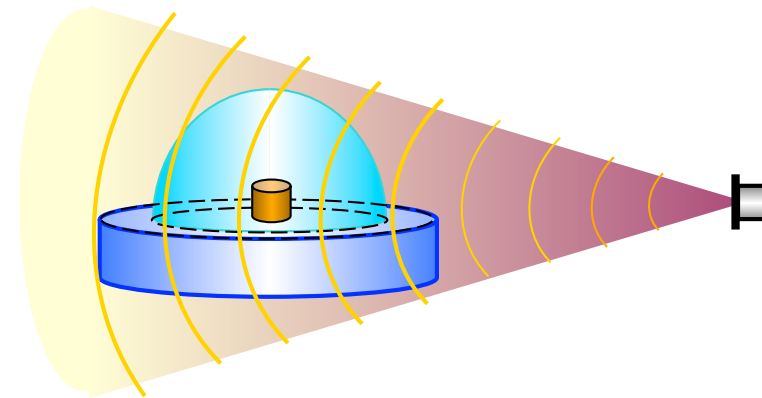
## Vibration insulation

A common feature of SPM is some device for **vibration insulation** :

active or passive pneumatic or piezo suspension tables, hanging springs, magnetic levitation, acoustic enclosures...

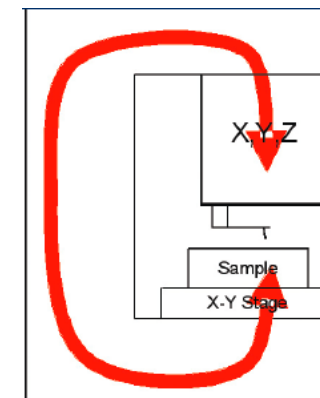


Active piezo suspension table



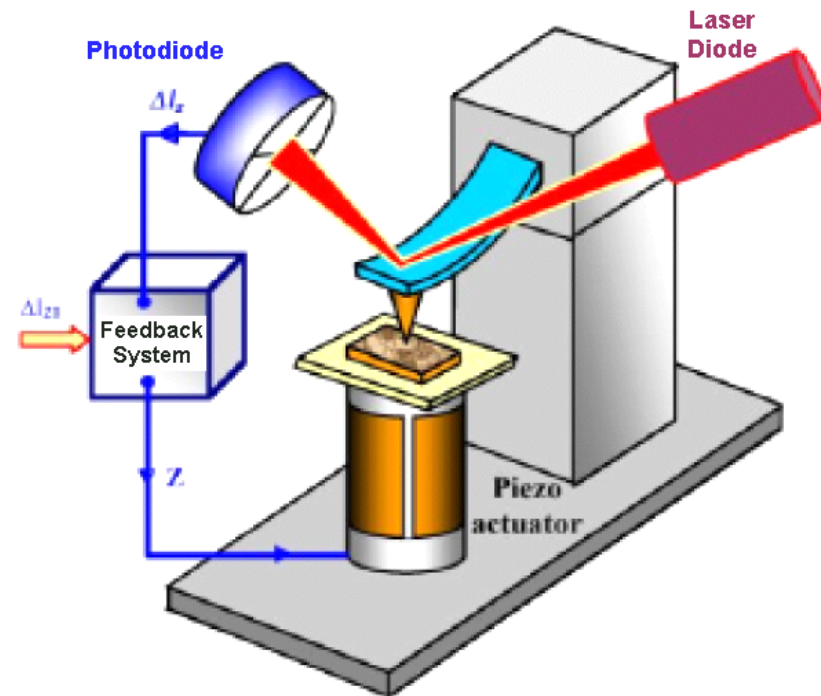
Acoustic insulation enclosure

The **mechanical loop** in an AFM includes all of the structural elements that are required to hold the probe at a fixed distance from the sample. If this loop is not **rigid**, then the probe can vibrate out of phase from the sample, and noise is introduced into images.



## The “reflected beam” force sensor

The most commonly used force sensor in SFM is a **micro-cantilever**, with the tip attached to the free end, and a thin light beam, produced by a **laser diode** which is reflected by the cantilever end, and detected by a **split photo diode**.



The interactive force between the atoms of the tip and of the sample **deflects the cantilever** and **deviates the reflected laser beam**.

The different illumination of the photodiode sectors produces a **differential photocurrent** signal that measures the interactive force.

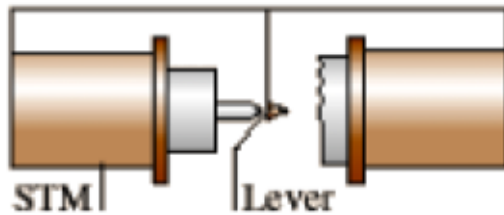
This optical detection technique of the tip-sample interaction force is commonly named “**Beam bounce**”.



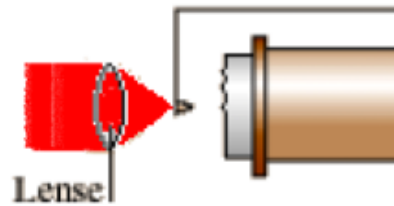
## Different methods for detection of the cantilever deflection

STM current modulation, interferometry, capacitive bridge, piezo strain gauges or piezo-actuators

Electron tunneling



Optical interferometry



Capacitance method

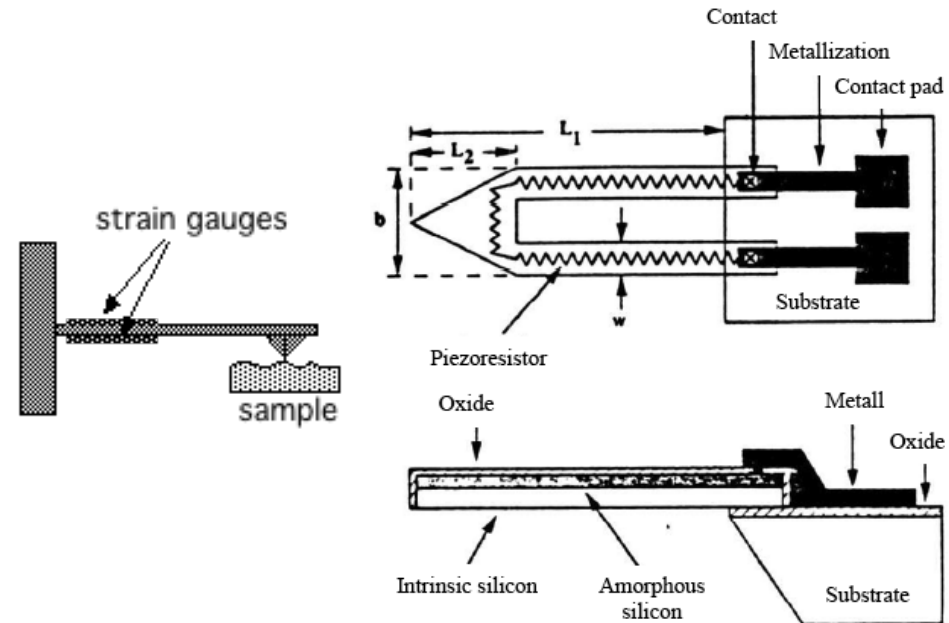
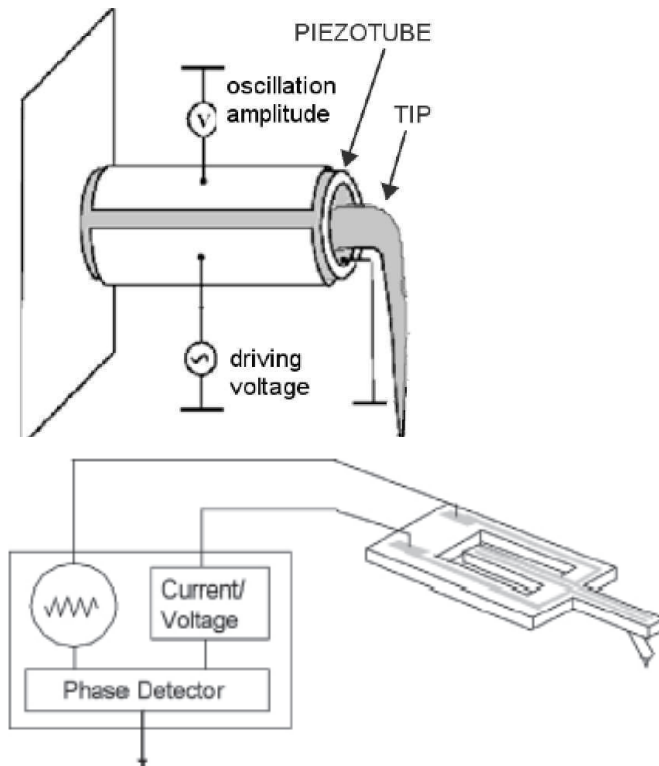
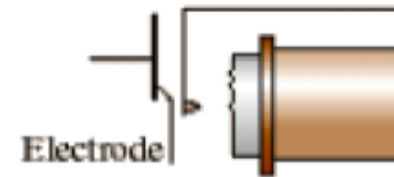




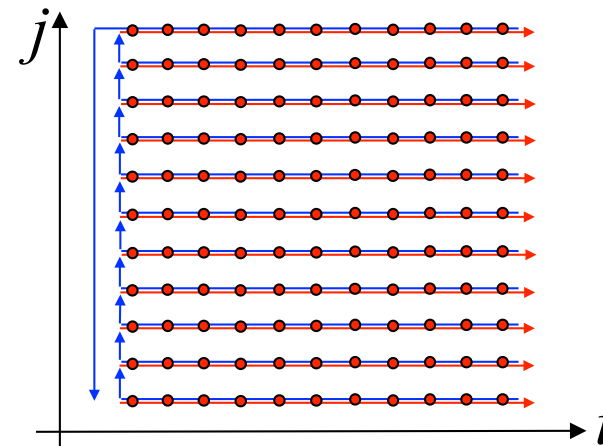
## Image acquisition at "Constant Height in Contact Mode".

The mapping of the interactive force may be obtained by sweeping in a raster scanning the sample area, and by recording in a **bidimensional matrix** the values  $V_i(x_i y_j)$  of the **photodiode output**, for each position  $x_i y_j$  of the tip (i.e. for each pair of voltage values fed to the scanner in order to bring the tip over the point  $x_i y_j$ ).

For example when the tip meets a relief increasing the repulsive force, the cantilever deflects causing the reflected beam to displace its spot on the split photodiode with a consequent change of the photodiode output.

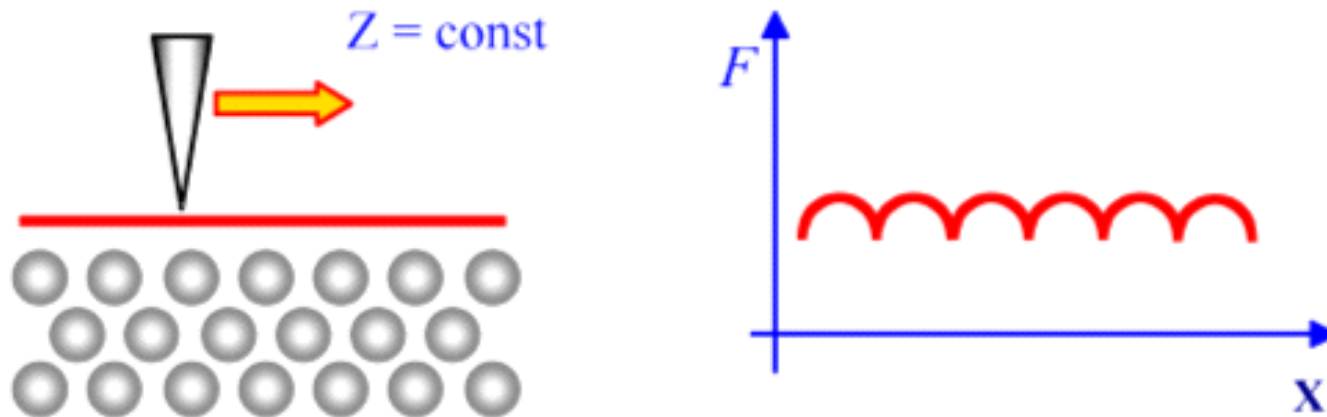
The **matrix of the output values** may be displayed on the computer screen using a grayscale representation of  $V_i(x_i y_j)$ : this is the **map of the interactive force** over the scanned area of the sample.

Pixel by pixel mapping of the sampled area



## Contact Mode at "Constant Height" or "Constant force"

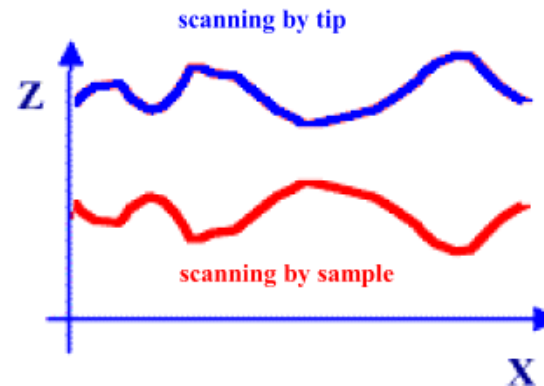
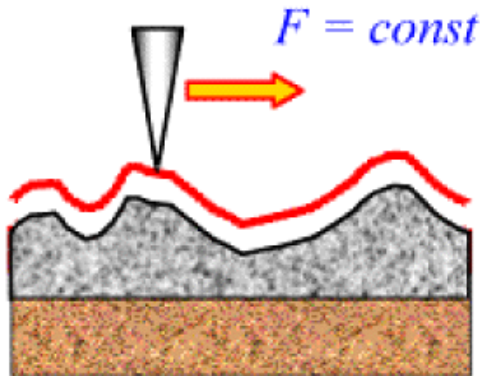
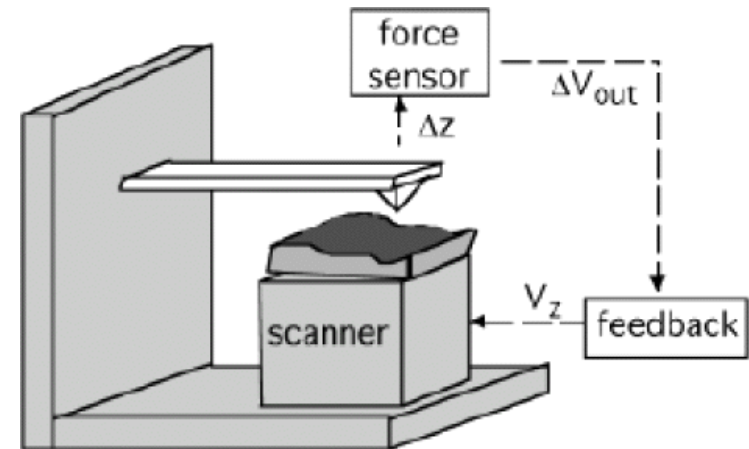
The operating mode that records the force  $F$  [i.e. the photodiode output  $V_i(x,y_j)$ ] is named "Constant Height Mode", because no modulation of the tip-sample distance ( $z$  coordinate of scanner) is made during acquisition.



The **non-linearity** and the **limited range** of the  $V(z)$  response function makes possible this procedure only for sample with **very small roughness**, and with **very small tilt** of the scanned sample plane ( $x, y, z = z_0$ ) with respect to the sample surface plane.

## Acquisition at "Constant Force".

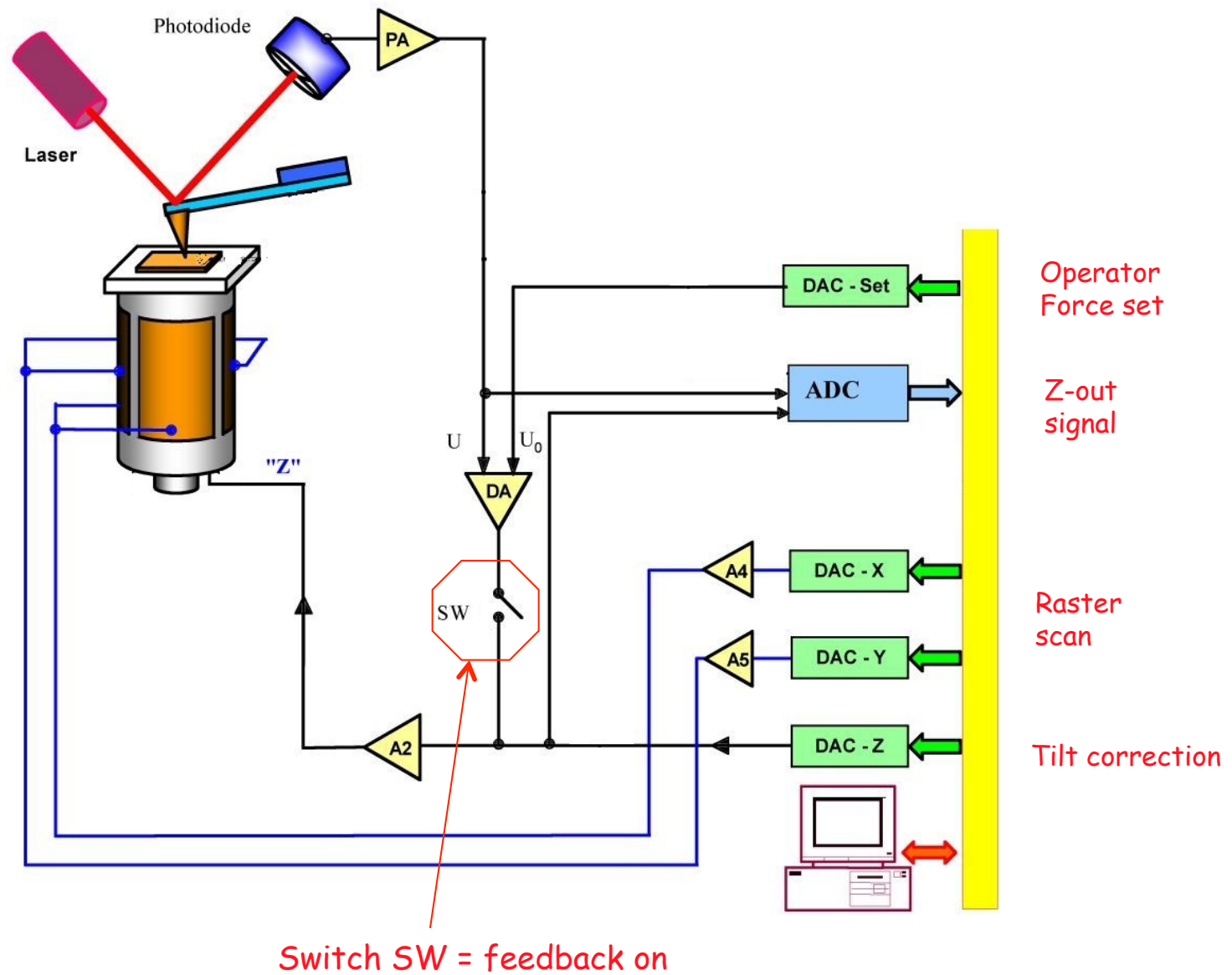
Using the photodiode output to **control** (with a **feedback** system) the **z** value, thus keeping the output signal always at a constant value (i.e. **keeping constant the interaction force**) we increase both the linearity and the dynamic range.



In this case the computer records the matrix  $V_z(x_i y_j)$  of the voltage values fed to the scanner to keep constant the force: this matrix is a **real topographic image** of the scanned area.

The constant force mode is the technique normally used in SFM

## Structure of SPM for constant force feedback



## Top-view and 3D-view images

Once recorded the matrix  $Z(x_i, y_i)$ , with the height values  $z_i$ , we may display it as a grayscale image (2D, or Top view) or as three-dimensional (3D) view seen from a user-defined view-angle, eventually expanding the z axis to enhance the sample details not visible in a proportional representation .

SPM frames are normally square matrixes (typically 256x256, 512x512 or 1024x1024).

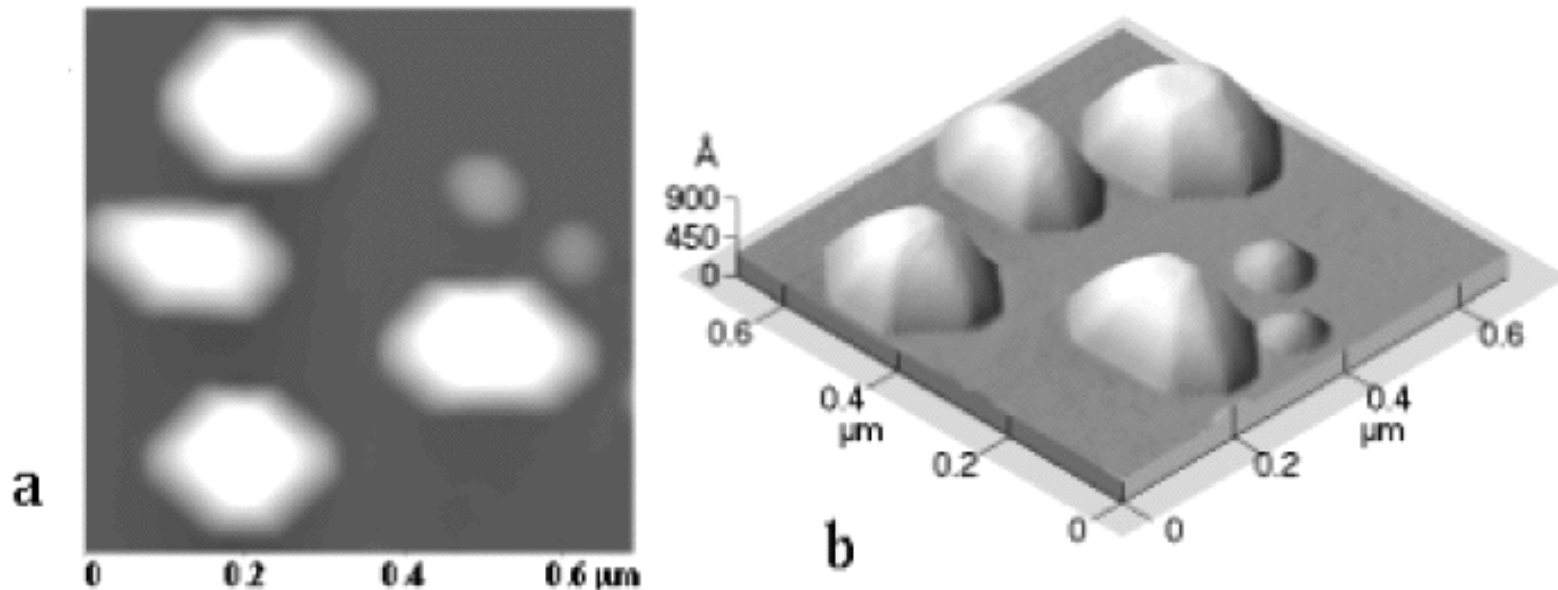


Image of nanostructures of InP grown on a substrate of GaAs

Matrix of 256 x 256 dots:

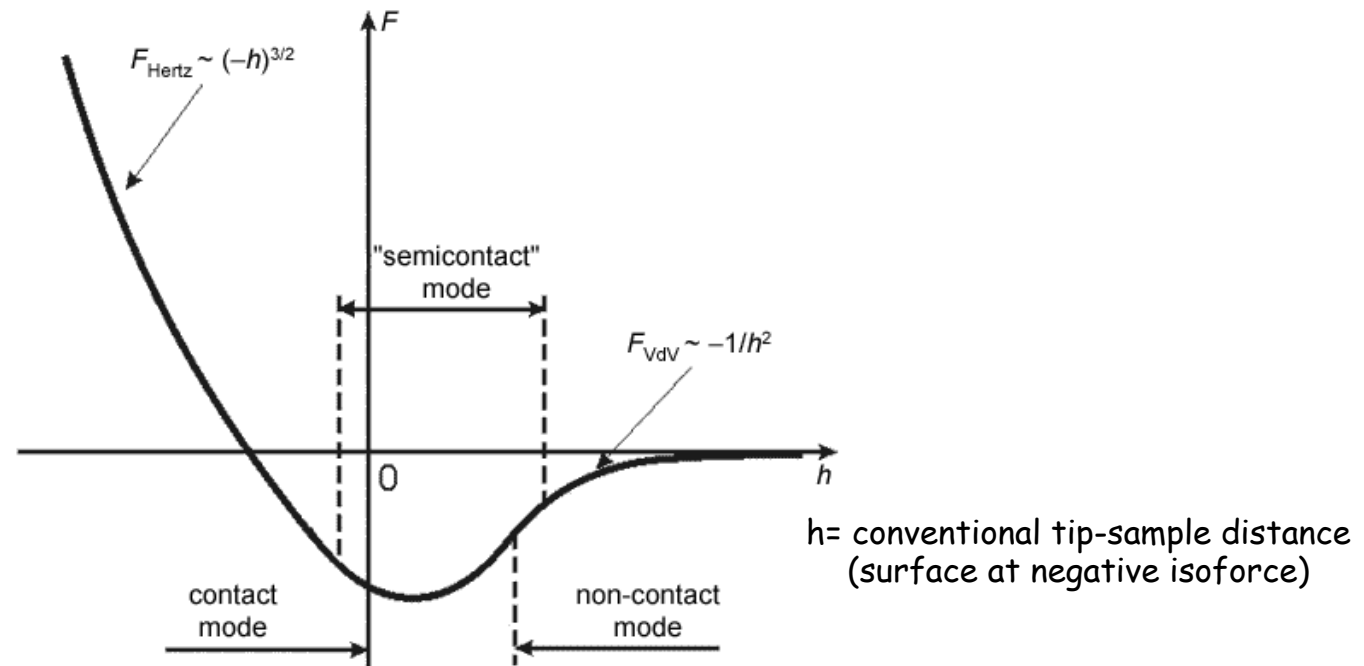
a) Top (2D) view ,   b) Axonometric (3D) view

## Tip-sample interaction: short- and long-range forces

In the Contact Modes (both at constant height and at constant force) we exploit the **steepness** of the  $F(z)$  curve slope in the **repulsive** region of the tip-sample interactive force.

At **short distances** in fact prevails the "hard sphere" repulsion due to the Pauli exclusion principle, that forbids the overlap of the electron wave functions of the outer atomic orbitals.

At **large distances** (some nm from the sample surface) the van der Waals polarization prevails and the force becomes **attractive**, with a much **smaller gradient**.



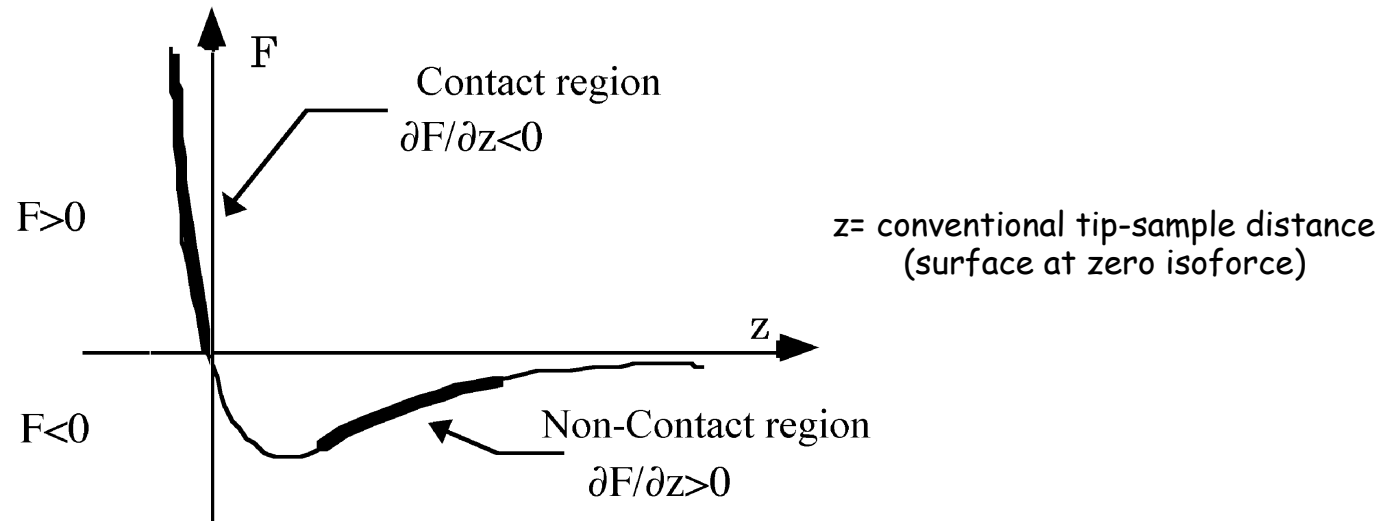
## Contact and Non-Contact

The **slope** of  $F(z)$  changes sign at some  $z$  value and goes to zero for  $z \approx \infty$

Also the **force gradient**  $\partial F/\partial z$  changes sign:

it is negative and **large** at short distance (**contact region**)

and positive and **small** at large distance (**non-contact region**).



In Non-Contact (  $F < 0$  e  $\partial F/\partial z > 0$  ) the cantilever *deflects toward* the surface producing the (small) output signal, suitable for a feedback.

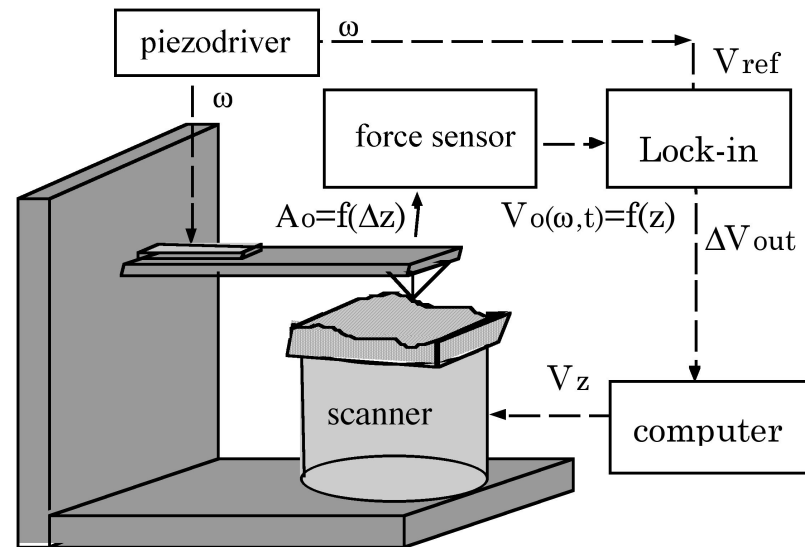
The cantilever **elastic constant** in this case must be chosen **large enough** to avoid *positive* feedback (when the attractive force is larger than the Hooke's restoring force).

This further **decreases** the force probe **sensitivity** in Non-Contact Mode.

## "Non-Contact": working principle

To increase the system sensitivity a great improvement in the signal/noise ratio must be provided: a **lock-in** technique is needed.

The cantilever is **forced into vibration** at its **resonant frequency**  $\omega_0$ , and the changes in oscillation **amplitude**  $A$  due to changes in the **force gradient**, are used as feedback signal.

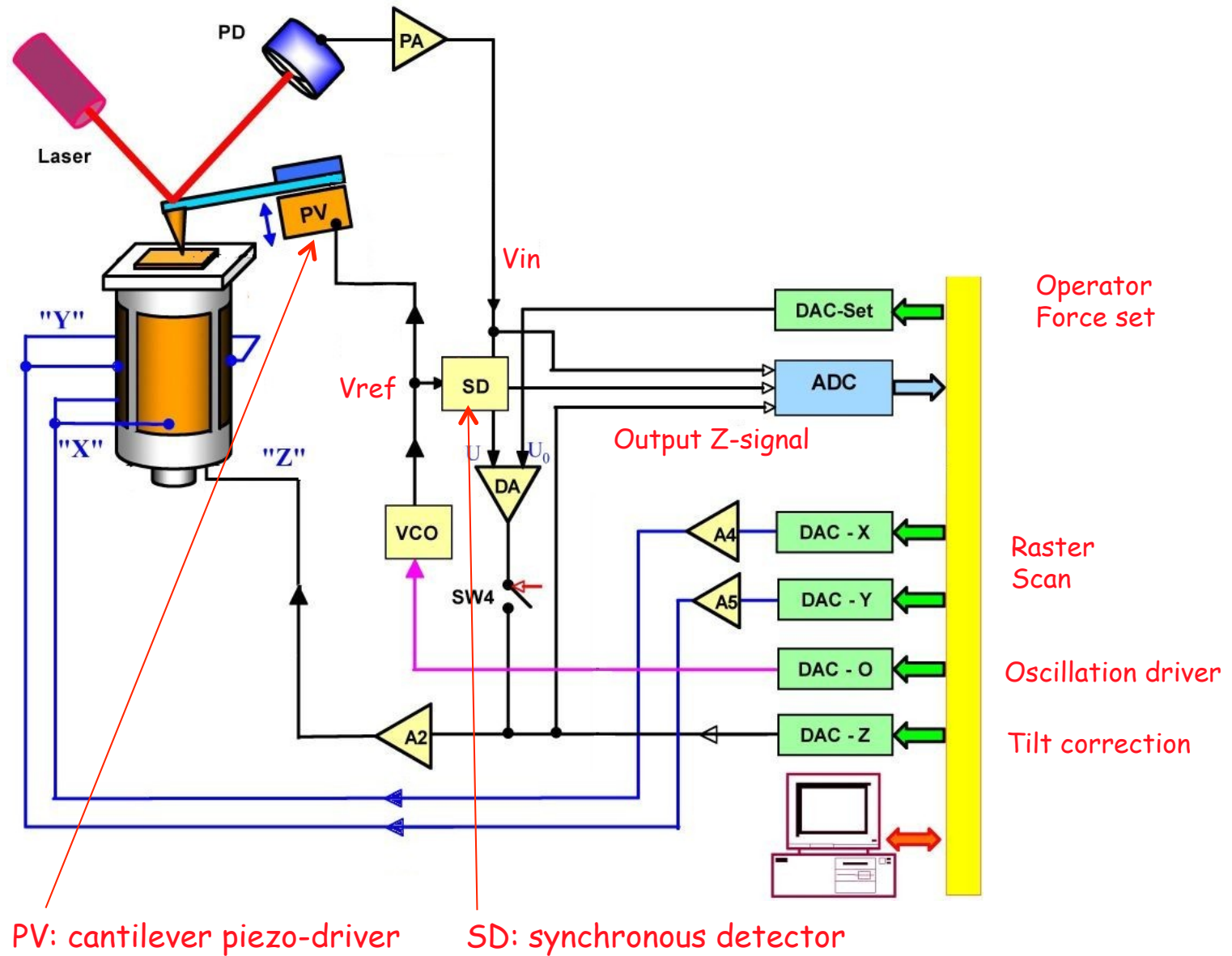


A **synchronous detector** (lock-in), locked to the reference signal, excites the cantilever into oscillation through a **piezo-driver**.

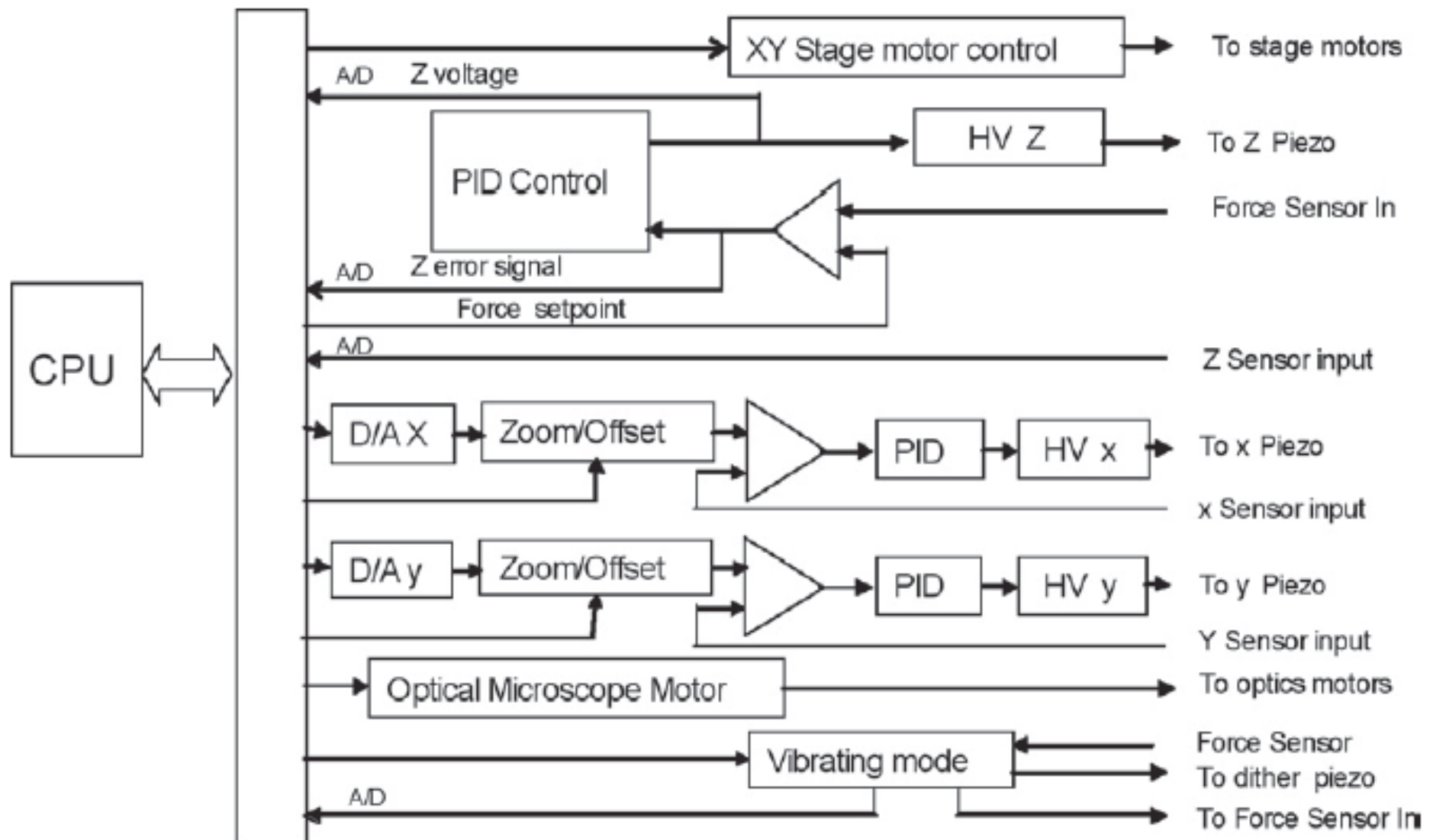
The increased **dissipation** near the sample surface **broadens** the resonance curve and the **force gradient** produces a **shift** of the resonant frequency: both the effects **reduce the oscillation amplitude**.



# Structure of SPM for Non-Contact Mode



## Electronic Blocks for SPM



A/D = analog to digital converter    D/A = digital to analog converter    PID= Proportional, Integral, Derivative filter

## How the force gradient changes the resonance curve

The cantilever may be considered a spring obeying to the Hooke's law :

$$F_0 = -k\Delta z, \text{ where } k \text{ is the elastic constant.}$$

In presence of a force gradient  $\partial F / \partial z$ , in a linear approximation:

$$F \approx F_0 + (\partial F / \partial z) \Delta z = -k\Delta z + (\partial F / \partial z) \Delta z = -(k - \partial F / \partial z) \Delta z = -k' \Delta z.$$

the *effective elastic constant  $k'$  decreases* approaching the surface due to the positive force gradient:

$$k' = k - \partial F / \partial z$$

The *resonant frequency  $\omega_0$*  may be written :  $\omega_0 = \sqrt{k / m}$   
where  $m$  is the effective oscillating mass of the cantilever.

Due to the force gradient the resonant frequency *shifts* (in a linear approximation), to a *lower value  $\omega_0^*$*  :

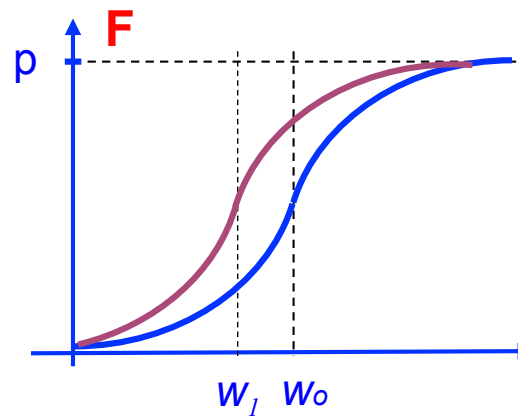
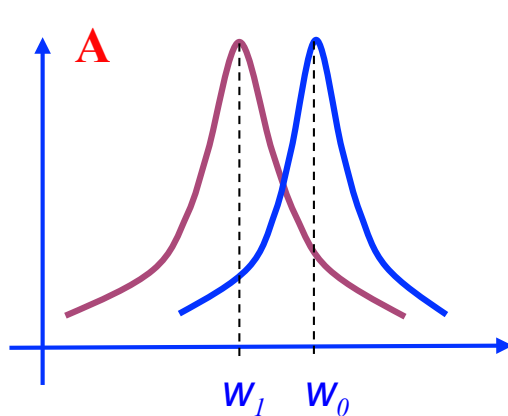
$$\omega_0^* \approx \sqrt{k / m} \left( 1 - \frac{\partial F / \partial z}{2k} \right) = \omega_0 \left( 1 - \frac{\partial F / \partial z}{2k} \right)$$

## Frequency, Amplitude and Phase dependence on the interactive force

For small **frequency** shift:  $\Delta\omega_0/\omega_0 = (\omega'_0 - \omega_0)/\omega_0 \ll 1$ , we get :  
$$\Delta\omega_0/\omega_0 \approx -(\partial F/\partial z)/2k$$

The relative **amplitude** change  $\Delta A/A$  may be evaluated in terms of the **quality factor**  $Q = \omega_0/(\omega_2 - \omega_1)$  :  
$$\Delta A/A \approx Q \Delta\omega_0/\omega_0 = -Q(\partial F/\partial z)/2k$$

A third feedback signal may be taken from the **phase**  $\Phi$  between excitation and response signals.



Blue= large distance  
Violet= small distance

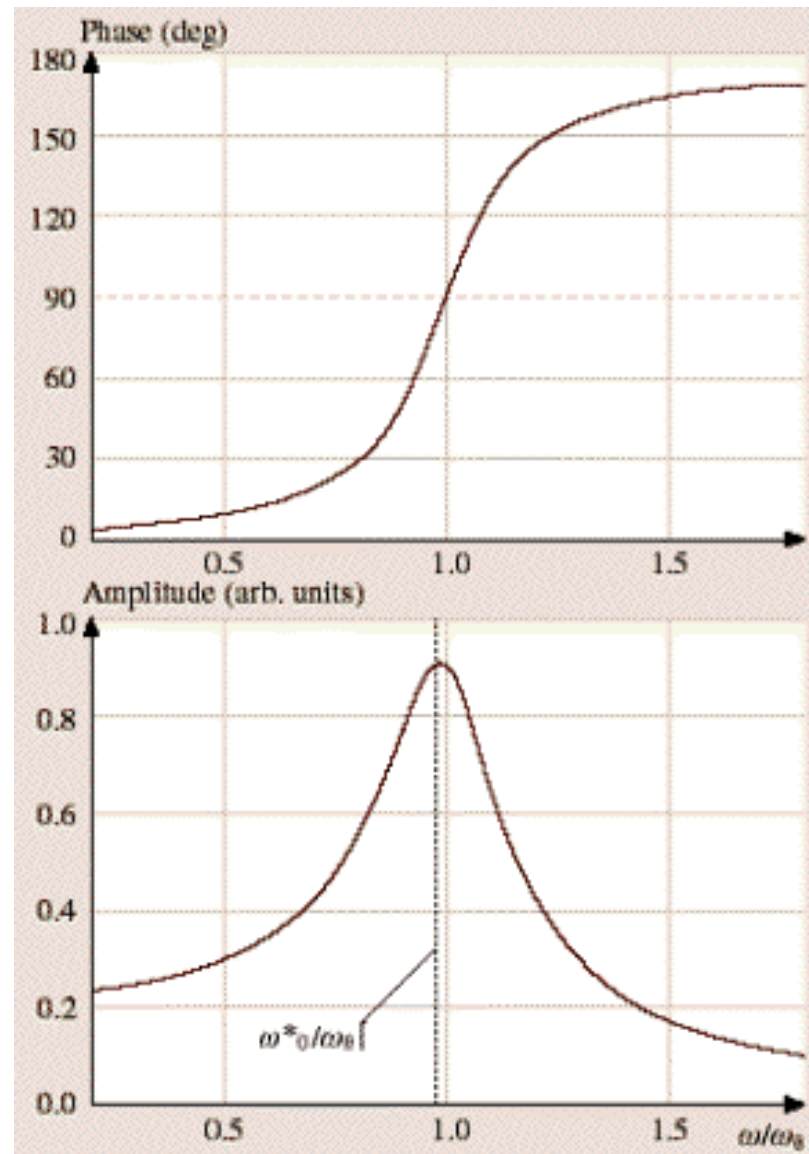
## Phase and Amplitude plots

The phase relation between excitation and response, near the resonant frequency  $\omega_0$ , changes rapidly from  $\sim 0$  to  $\sim 180$  degrees

$$\phi(\omega) = \arctan \left[ \frac{\omega \omega_0}{\left\{ \omega_0^2 - \omega^2 - (\partial F / \partial z) / m \right\}} \right]$$

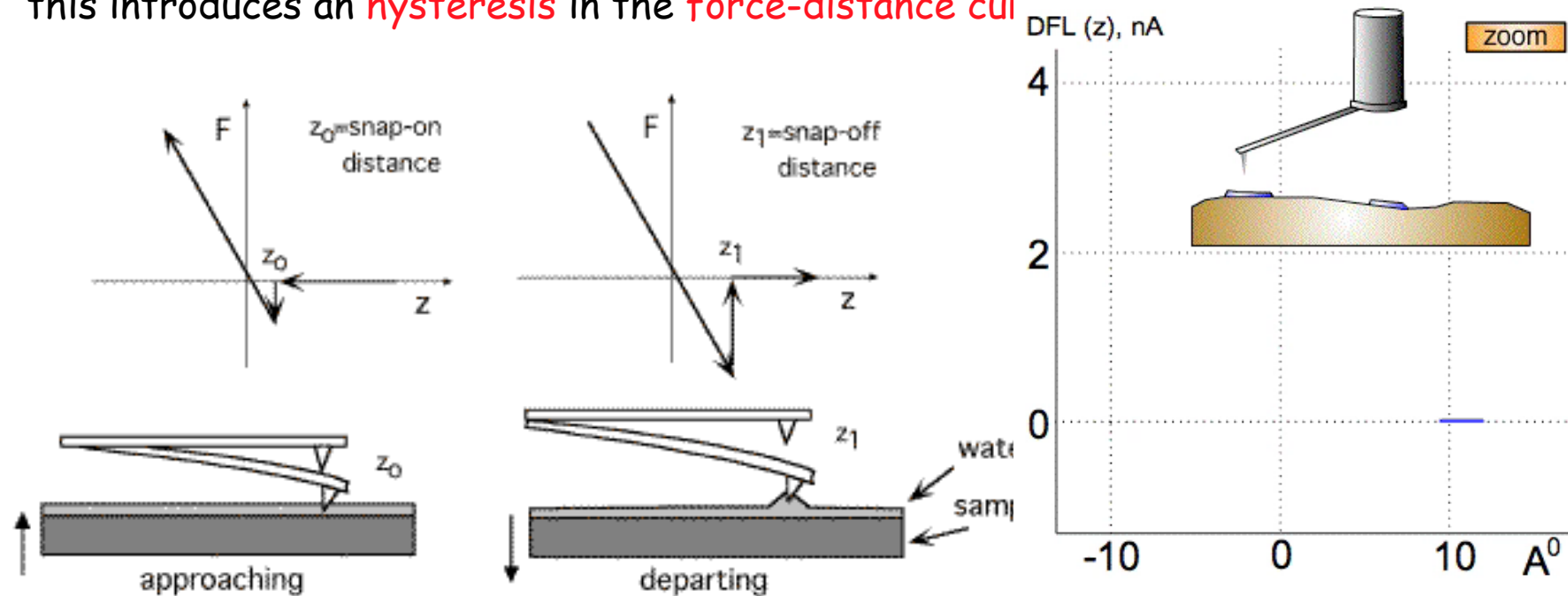
The amplitude changes depend strongly on the quality factor  $Q$

$$A(\omega) = \frac{u_0 \omega_0^2}{\sqrt{\left[ \omega_0^2 - \omega^2 - (\partial F / \partial z) / m \right]^2 + \omega^2 \omega_0^2 / Q^2}}$$



## The water film

Working in air (normal condition for SFM) a **water film** (one or more monolayers) covers the sample producing a capillary force of the order of  $10^{-8}$  N: this introduces an **hysteresis** in the **force-distance curve**



When the tip approaches the surface, the module  $|\partial F / \partial z|$  of the force gradient increases until it becomes greater than the cantilever elastic constant  $k$ .

At this point (**snap-on distance  $z_0$** ) the cantilever increases its deflection until it touches the water film at the surface.

When the scanner retracts the capillarity effect impedes the cantilever detachment until the coordinate  $z$  reaches a larger value ( **$z_1 > z_0$  snap-off distance**).

# Contact vs Non Contact: Advantages and Disadvantages

## Contact Mode

### »Advantages:

- High scan speeds
- “atomic resolution” images
- Easier scans in rough samples with extreme changes in topography

### »Disadvantages:

- Lateral (shear) forces can may give distorted images
- Higher tip-sample interaction
- The combination of lateral forces and high normal forces may reduce spatial resolution and may damage soft samples

## Non Contact Mode

### »Advantages:

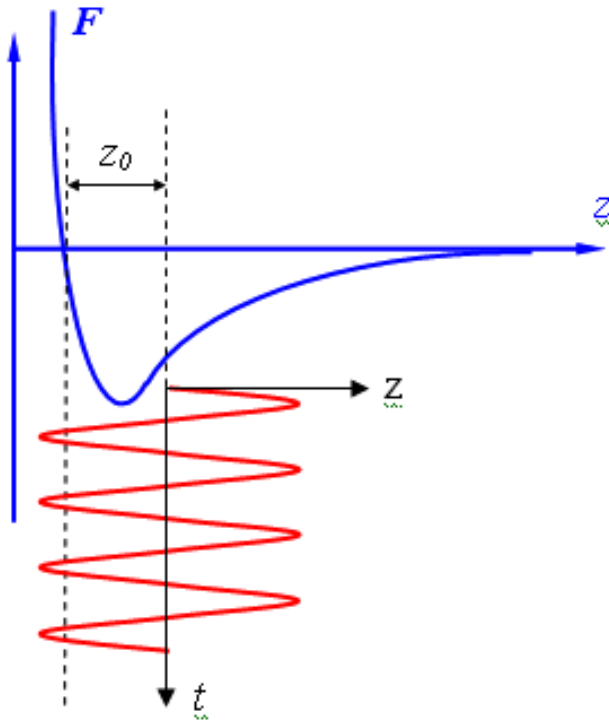
- Allows “Lift Mode” techniques and “Phase Contrast” imaging
- Lower forces and less damage to soft samples

### »Disadvantages:

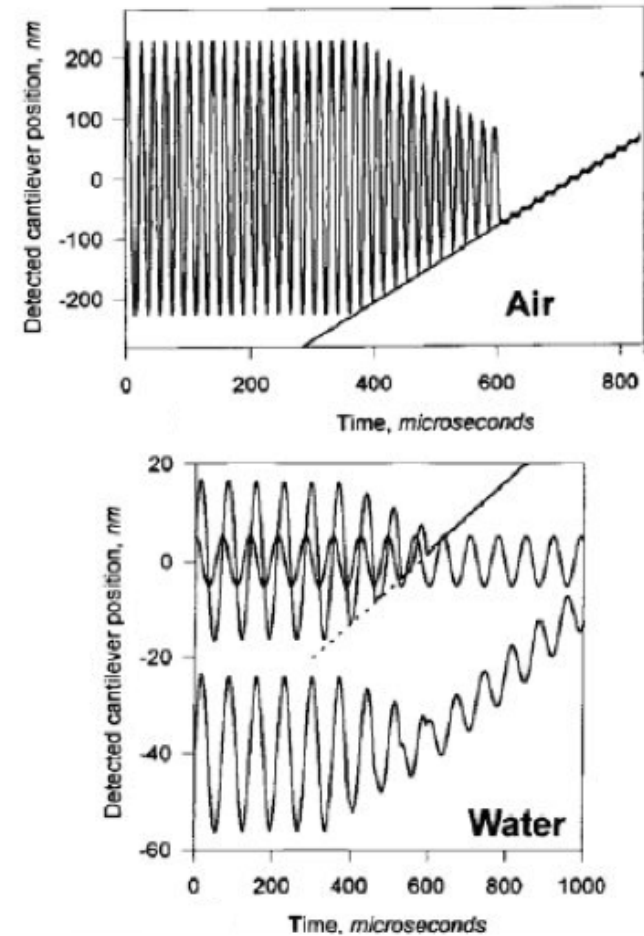
- Slightly lower scan speed

## "Tapping-Mode"

In "**Tapping Mode**" also named "**Periodic Contact Mode**" or "**Semicontact Mode**" or "**Intermittent Contact Mode**" the cantilever oscillates with an amplitude between 20 and 100 nm. In case of measurement in air, this is sufficient to make the tip to enter and exit the liquid water layer at each period.



Tapping mode may also be used while measuring in liquid (the whole cantilever submerged)

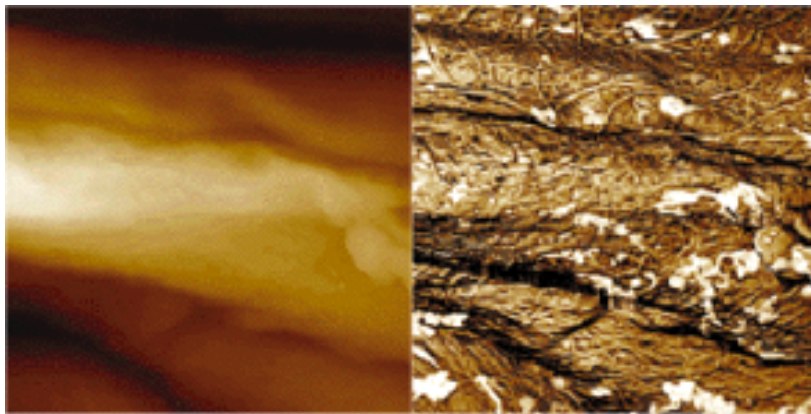
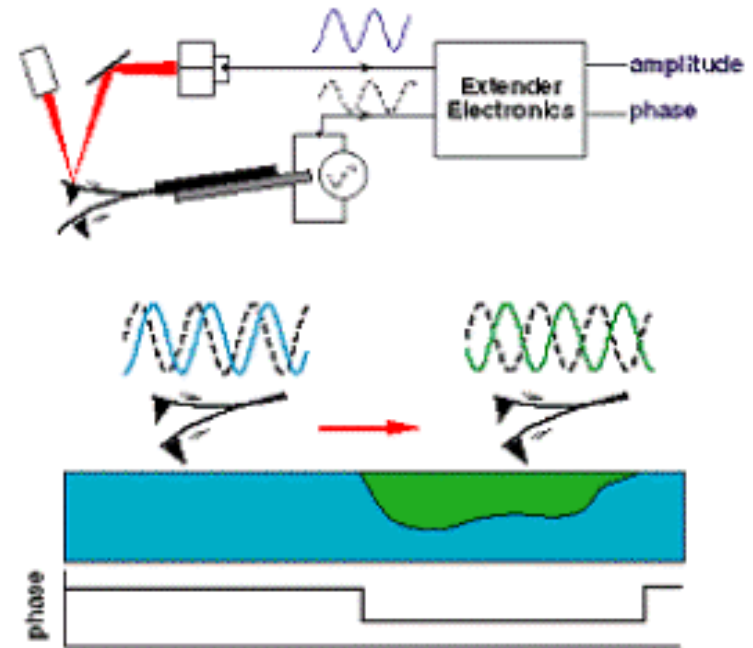


taken from "How does a tip tap?" by N.A. Burnham et al.

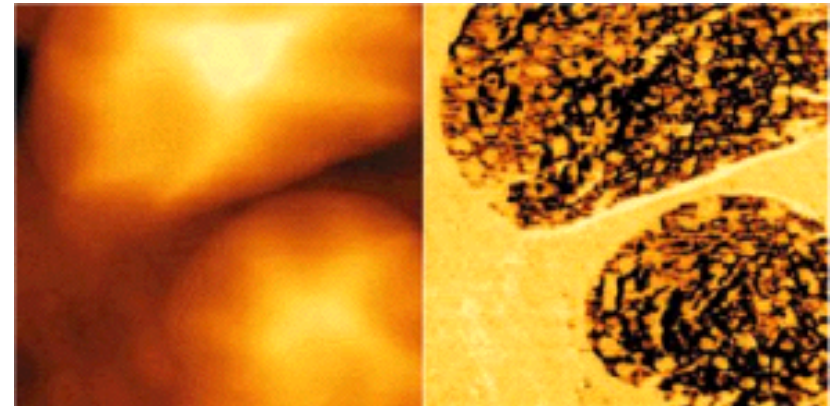


## Phase contrast images

The **phase-image** is a map of the changes of the cantilever oscillation phase that may give information on the surface properties (composition, adhesion, friction).



Topography and Phase-image of a sample of wood: cellulose microfibers appear more sharply defined in the phase image



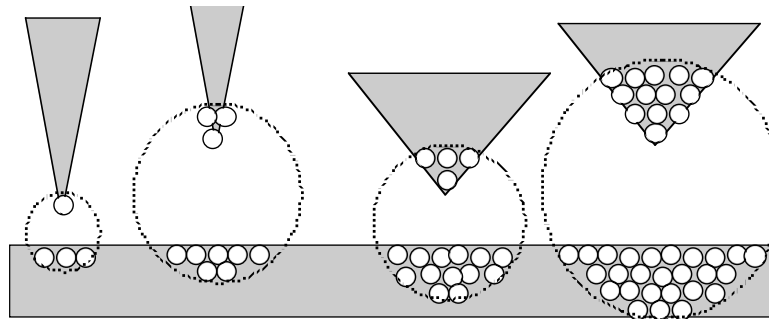
Topography and Phase-Image of a polymer composite

## Non-Contact: more details

The oscillation amplitude is kept very small (of the order of 0.1 nm) while the **tip-sample distance is relatively large** (from 10 to 100 nm).

The larger tip-sample distance corresponds to a **smaller slope  $\partial F/\partial z$**  of the force-distance curve and therefore the probe **sensitivity is smaller**.

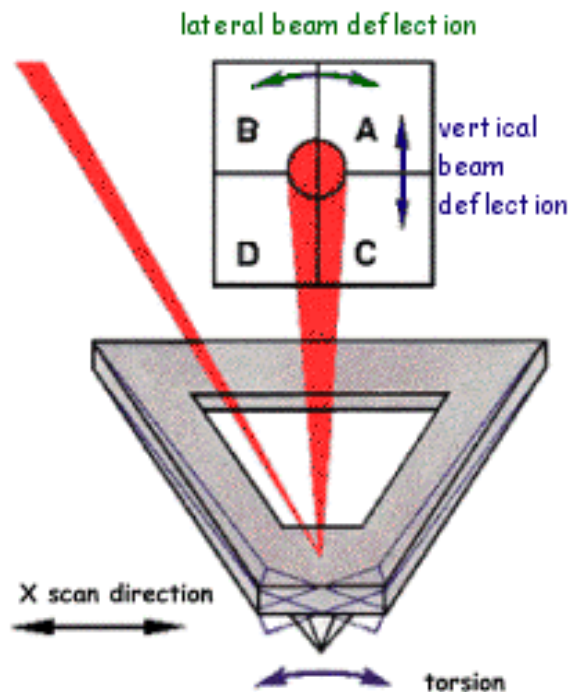
Moreover **at larger distance the interaction involves more atoms** and this may decrease the lateral resolution.



The **lateral resolution** may be increased either by **decreasing the tip-sample distance** or by **decreasing the curvature radius** of the tip apex

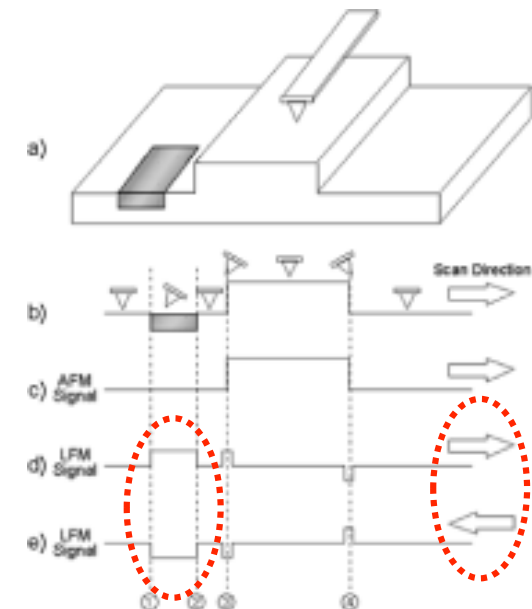
# LFM

The microscopic friction forces may be mapped using the “**Lateral Force Mode**” (LFM). A signal proportional to the lateral force originated during the relative tip-sample movement in contact (due to differences in the local friction coefficient) may be obtained by detecting the **cantilever torsion** that produces a **lateral displacement of the reflected light beam**. The lateral displacement is detected using a **four quadrant** split photodiode by measuring both the difference and the average value in the light intensity in adjacent quadrants). This system allows to resolve lateral forces of the order of  $10^{-11}\text{N}$ .

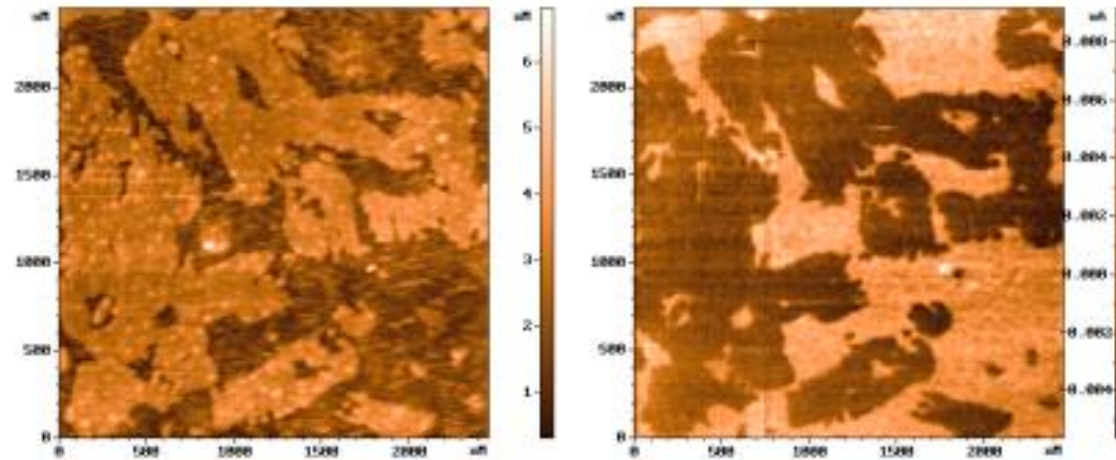
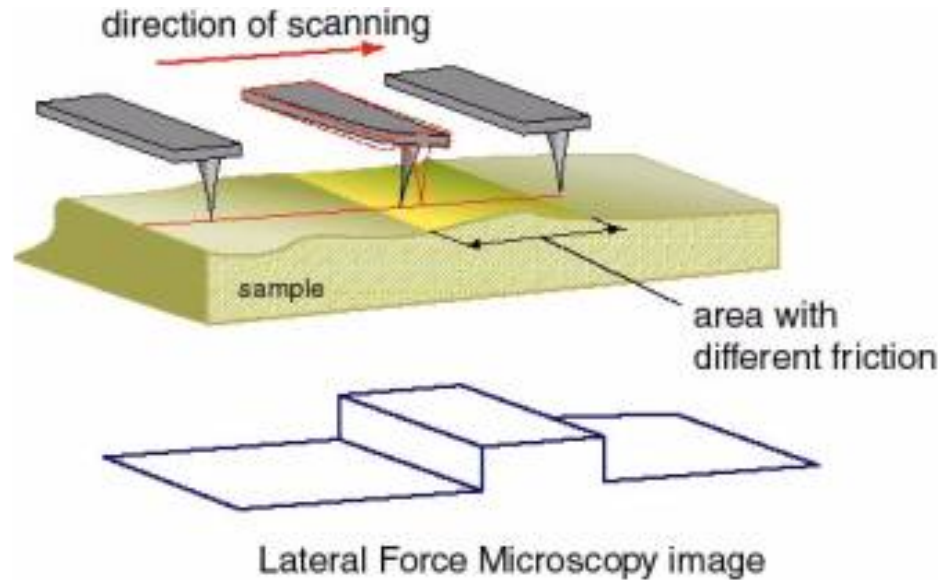


In the geometry shown here, the cantilever moves along X and the **friction** signal is calculated as  $(A + C) - (B + D)$ , while the **topographic** signal is calculated as  $(A + B) - (C + D)$ .

LFM may be useful to **enhance contrast at the edge of relief** or at the boundary of different compounds. **Reversing scan direction**, the LFM signal due to friction change sign.

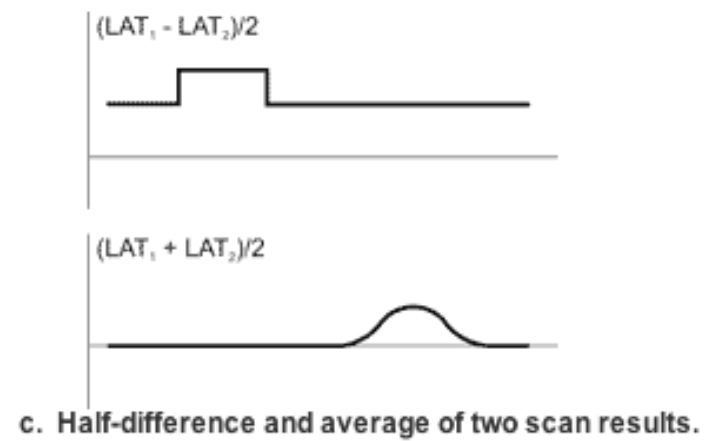
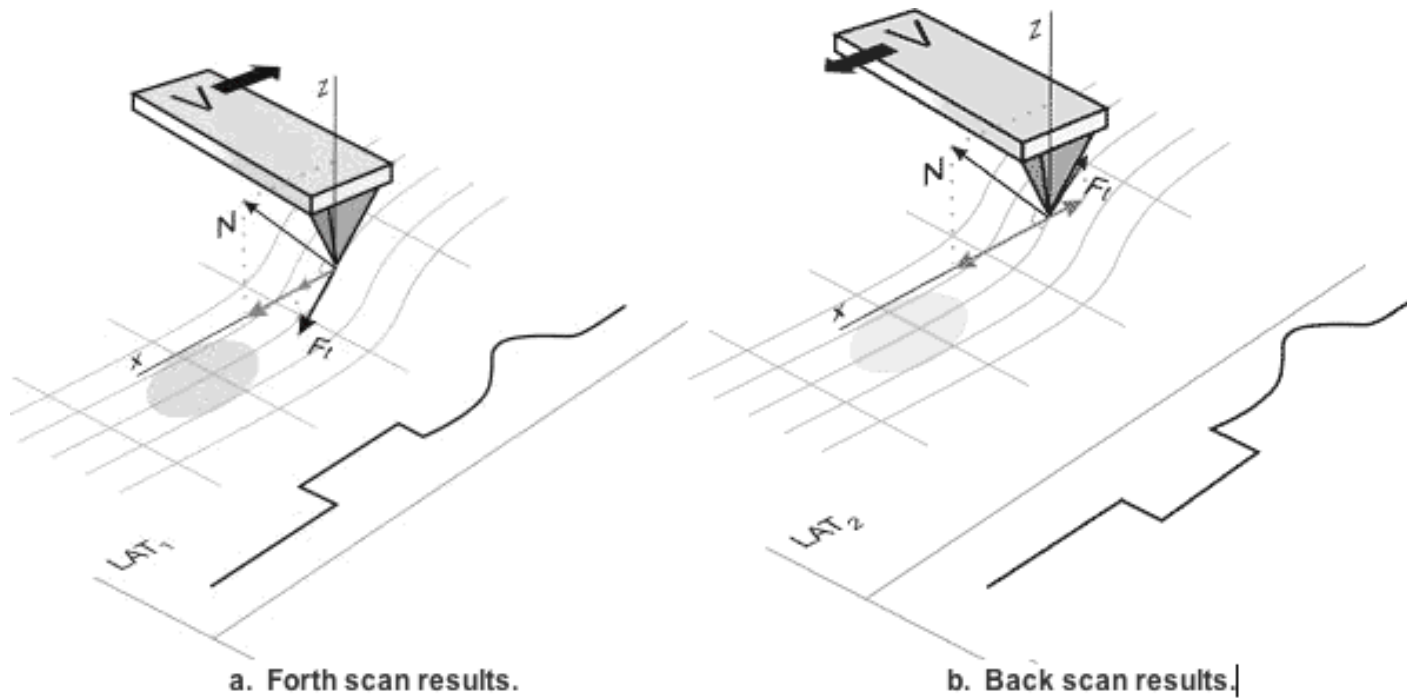


## LFM (2)



The sample is one monolayer Langmuir-Blodgett (LB) film deposited on silicon surface.  
Fast scanning direction: in the image at left  $\rightarrow$  in the image at right :  $\leftarrow$

## LFM (3)



## SFM : which force does it measures ?

The **SFM** measures the tip-sample **interaction force**.

Which force ?

The tip-sample **interaction** may be due to many kinds of **different forces**, depending both on the type of tip and sample **material**, on the value of the tip-sample **separation**, on the possible presence of **electric field** between tip and sample, on the possible presence of **magnetic field** (either produced by the tip or by the sample)....

It is a task of the user to choose the particular force he wants to measure, and consequently to choose the particular technique that best fit his goal.

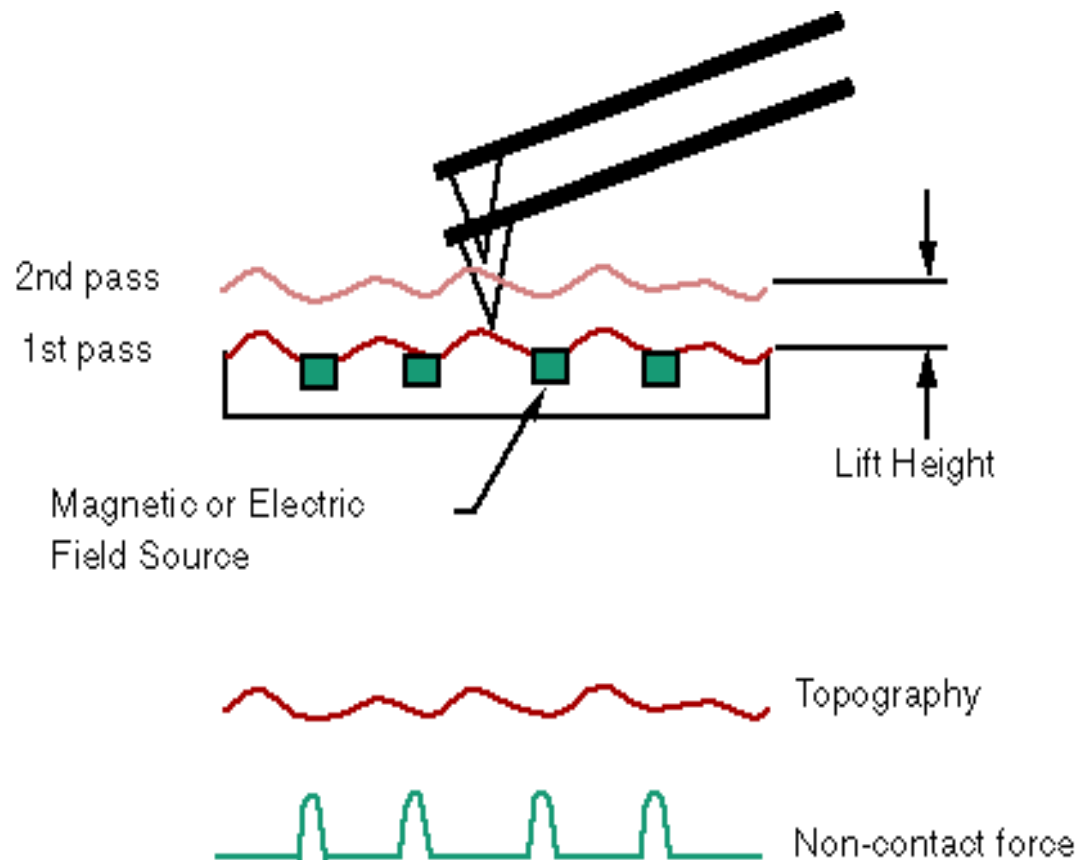
Using different tip-sample separations allows to make negligible either the **short-distance** forces or the **long-distance** forces,

Using a voltage applied to a conductive tip or to a conductive sample allows to make the **electric force** prevailing over other interatomic forces,

Using a magnetized tip allows to investigate the **magnetic force**...



## The two-pass or Lift Mode



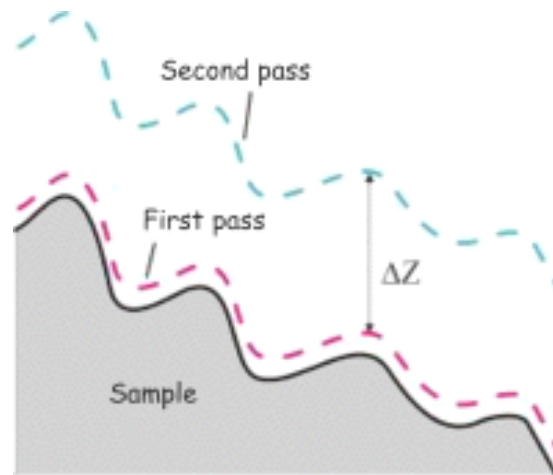
Two passes are made over the sample. The first measures topography while the second measures a material property (magnetic, electric, etc.)

# MFM (magnetic force microscopy)

The **MFM** technique gives a spatial distribution of the parameters that describe the tip-sample **magnetic interaction**.

The cantilever is **coated by a magnetic film** (e.g. cobalt).

The MFM image is obtained by separating the contribution due to magnetic force from that due to the sample topography, e.g. using the **two-pass** method (or **Lift Mode**).



In the **first scan** the topographic profile is recorded in contact (or tapping) mode.

In the **second scan (lifted)** the cantilever is **moved at a preset distance  $\Delta z$**  from the sample surface and the **feedback loop is broken** (the line scan is controlled by the previous recorded profile).

The separation  $\Delta z$  (5-50 nm) must be large enough to make negligible the Van der Waals force, leaving only the magnetic term (that decays at larger distance).



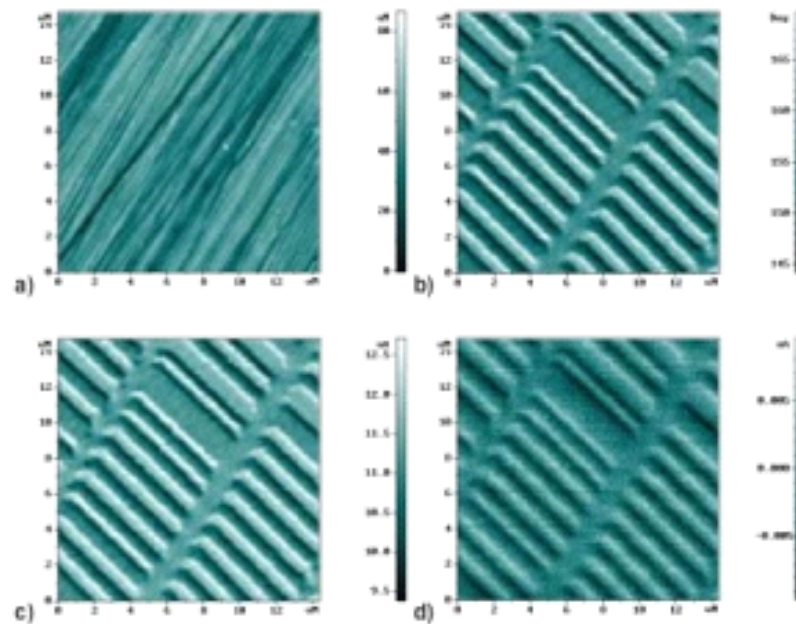
## MFM: various techniques

Different techniques are used in the MFM two-pass method:

1) if the cantilever is not excited into oscillation during the second pass, we get a **DC MFM** image, where the recorded force is between the tip magnetic dipole  $\vec{m}$  and the magnetic field produced by the sample surface

$$F = (\vec{m} \cdot \vec{\nabla}) H$$

2) if the cantilever is excited at its resonant frequency during the second pass two types of images **AC MFM** may be obtained : by recording the **phase shift** or the **amplitude** changes.



Various SPM images on Hard Disk:

a) **Topography**, b) **Phase ACMFM** c) **Amplitude ACMFM**, d) **DC MFM**

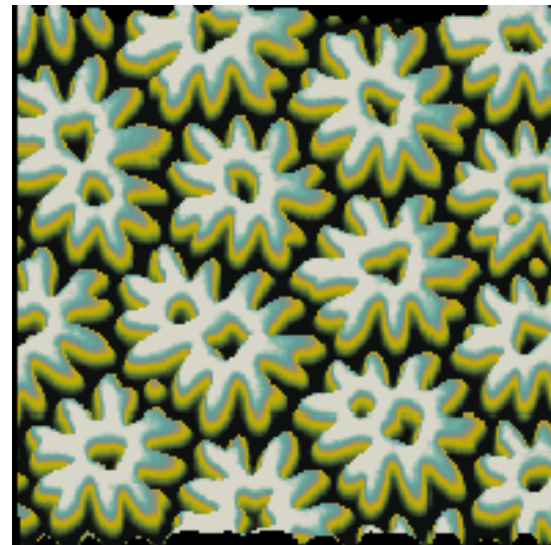
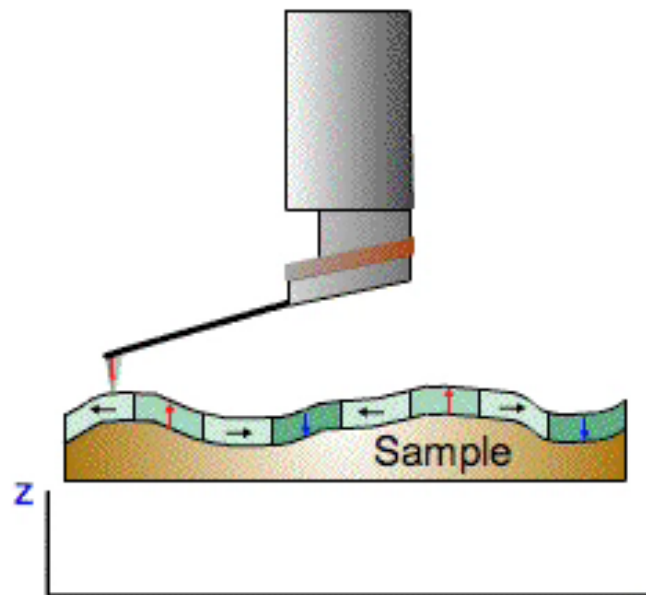
## DC-MFM (Lift Mode)

In the **first pass** the topography is determined in Semicontact mode (Tapping).

In the **second pass** the **magnetized** cantilever is **lifted** to a selected height for each scan line and scanned using the **stored topography** (without feedback);

the tip-sample separation during second pass is therefore kept constant and it is large enough to make negligible the Van der Waals' force so that the cantilever is affected mostly by **long-range magnetic force**.

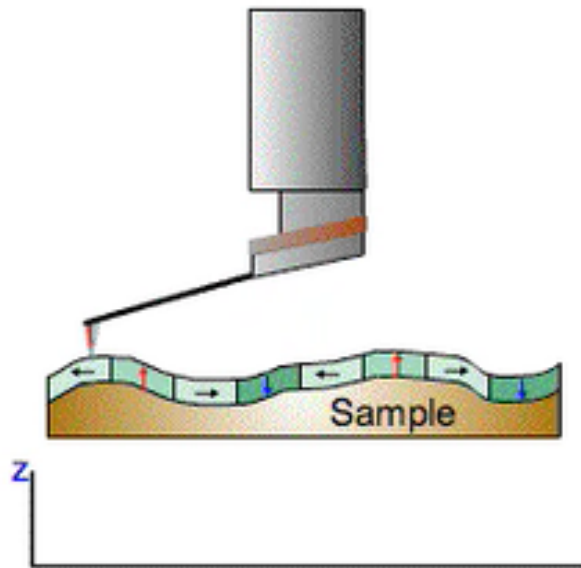
1-st pass. Sample profile acquisition.



Domains in a 80 micron garnet film

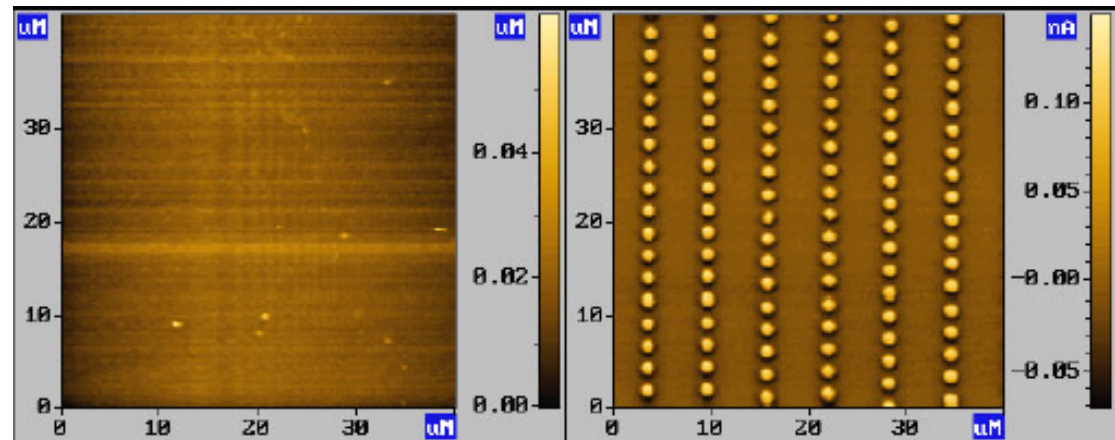
## AC-MFM (Phase Shift Image)

1-st pass. Sample profile acquisition



In the **first pass** the topography is determined in Semicontact mode  
In the **second pass** the cantilever is driven at its **resonant frequency**;  
the **phase shift** are recorded.

Magneto-optical disc



AFM topography

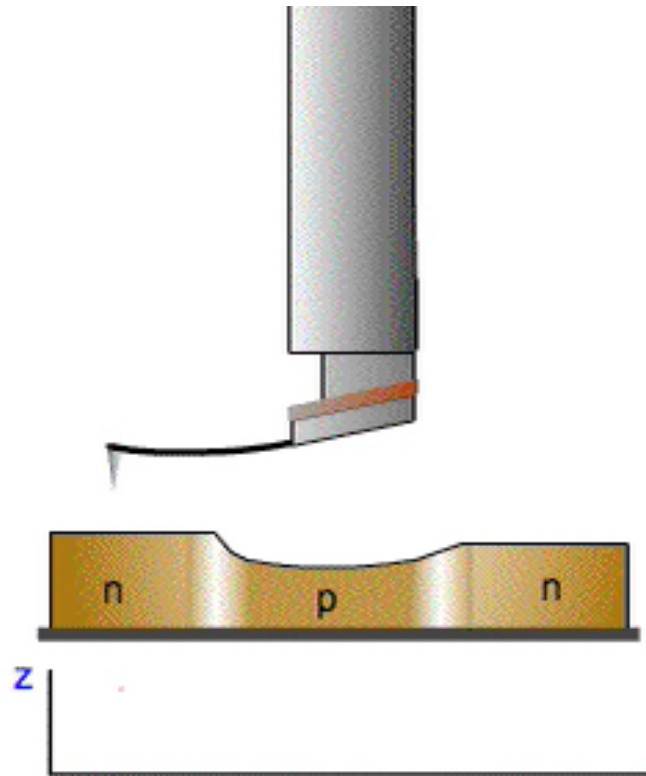
MFM image

## EFM (electric force microscopy)

Also EFM images are obtained using the two-pass method (Lift Mode).

During the second scan the (conducting) cantilever is forced at resonance and biased with a constant voltage.

The tip-sample capacitive induction produces a modulation of the resonant frequency (and consequently changes in the oscillation phase and amplitude).



# Scanning Capacitance Microscopy

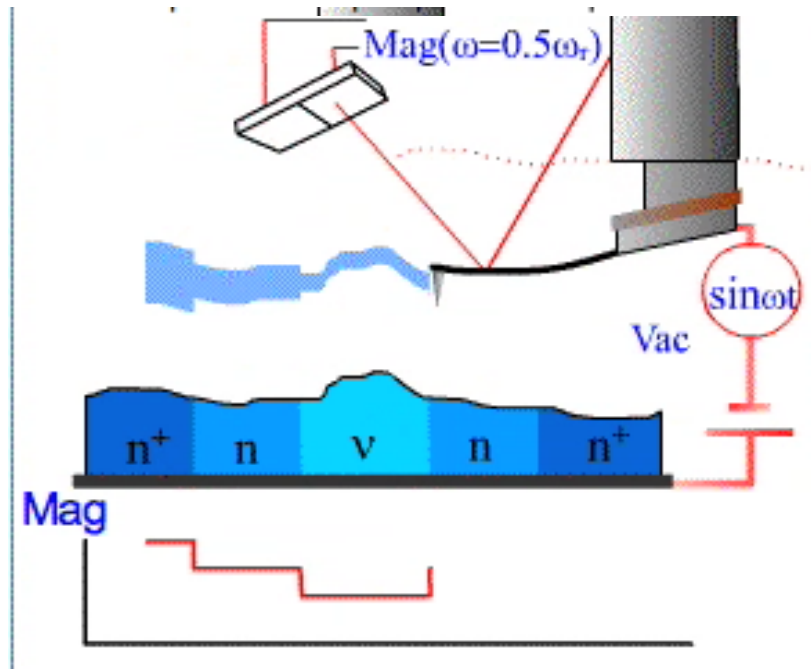
The **SCM** images are a particular kind of **EFM** images

In **SCM** the cantilever is biased with a **modulated** voltage:  $V_{\text{tip}} = V_{\text{dc}} + V_{\text{ac}} \sin(\omega t)$  And the sample is biased at  $V_s$

The tip-sample capacitive **force**  $F_c(z)$  is:

$$F_c(z) = (1/2) (V_{\text{tip}} - V_s)^2 (dC/dz)$$

Where the tip-sample capacity  $C(z)$  depends on the tip and sample geometry and on the distance  $z$ .



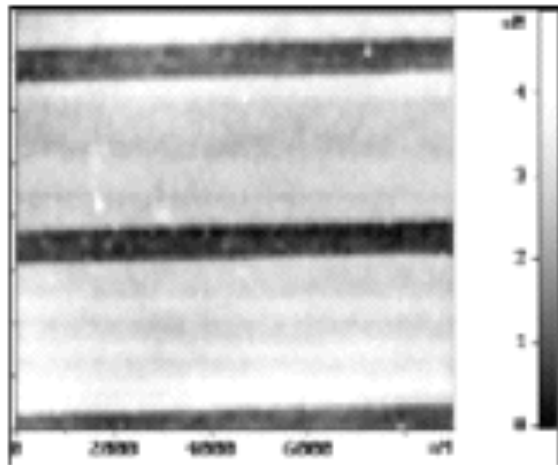
The **second harmonic**  $F_{c2}(z)$  depends **only** on  $(dC/dz)$  and  $V_{\text{ac}}$

$$F_{c2w}(z) = (1/2)(dC/dz) V_{\text{ac}}^2 \sin(2\omega t)$$

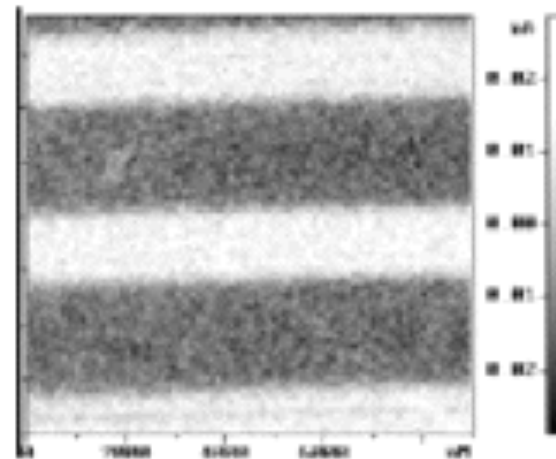
To optimize the second harmonic signal the driving frequency is chosen at half the resonant frequency of the cantilever.

## SCM 2

Scanning Capacitance Microscopy of nonuniformly boron doped silicon. Scan size: 9 x 9  $\mu\text{m}$



topography image of silicon surface,  
strip doping regions are well visible.



SCM image,  
resulting distribution of dopant impurity.



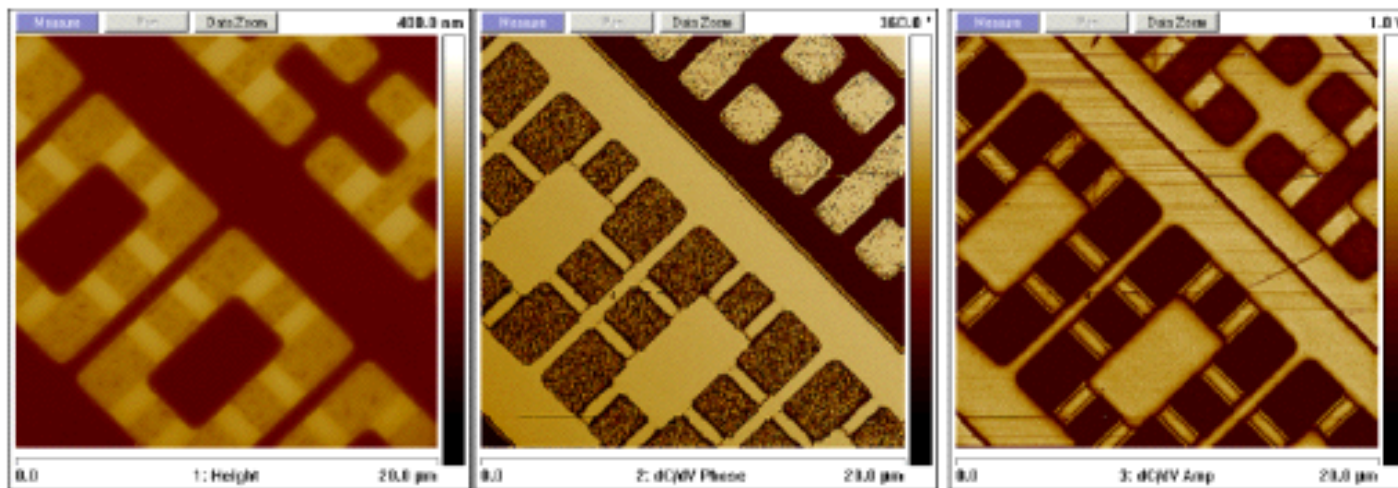
## UHF SCM

The electrical properties in semiconductors (e.g. charge. density) may be modified by doping (without any topographic signature).

To measure the **local distribution of the surface density of the charge carriers** two methods are available: **SKPM** or **UHF SCM**

In **UHF-SCM** a "ultra-high-frequency" resonant capacitive sensor is connected to the (conductive) tip by means of a tuned line. When the tip touches the surface, the sample becomes part of the **resonant circuit**.

The tip-sample capacity loads the line, changing the resonant frequency. The sensitivity may be very high, achieving a resolution of the attofarad ( $10^{-18}$  farads)



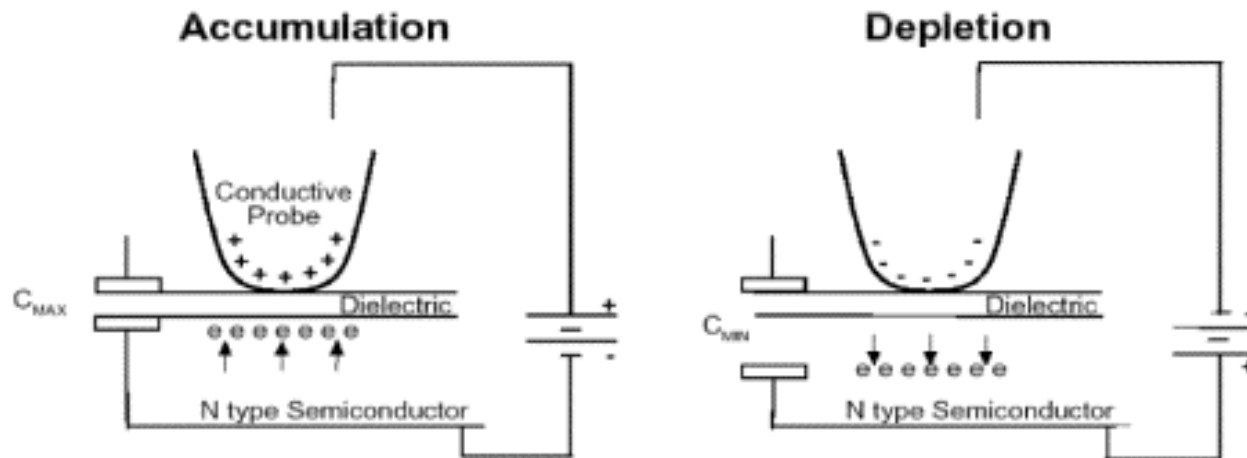
sample: silicon DRAM

## Charge displacement in UHF SCM

By applying a **low-frequency** bias voltage (a few kHz) changes are induced in the capacitor, made of tip and sample separated by the (dielectric) surface oxide film

The free charges in the semiconductor, close to the contact, moves under the applied a.c. voltage and the junction behaves as a **variable capacitor**.

Capacity changes are due to : 1) applied **voltage** amplitude; 2) **thickness** and type of dielectric film; 3) **free charge density**.



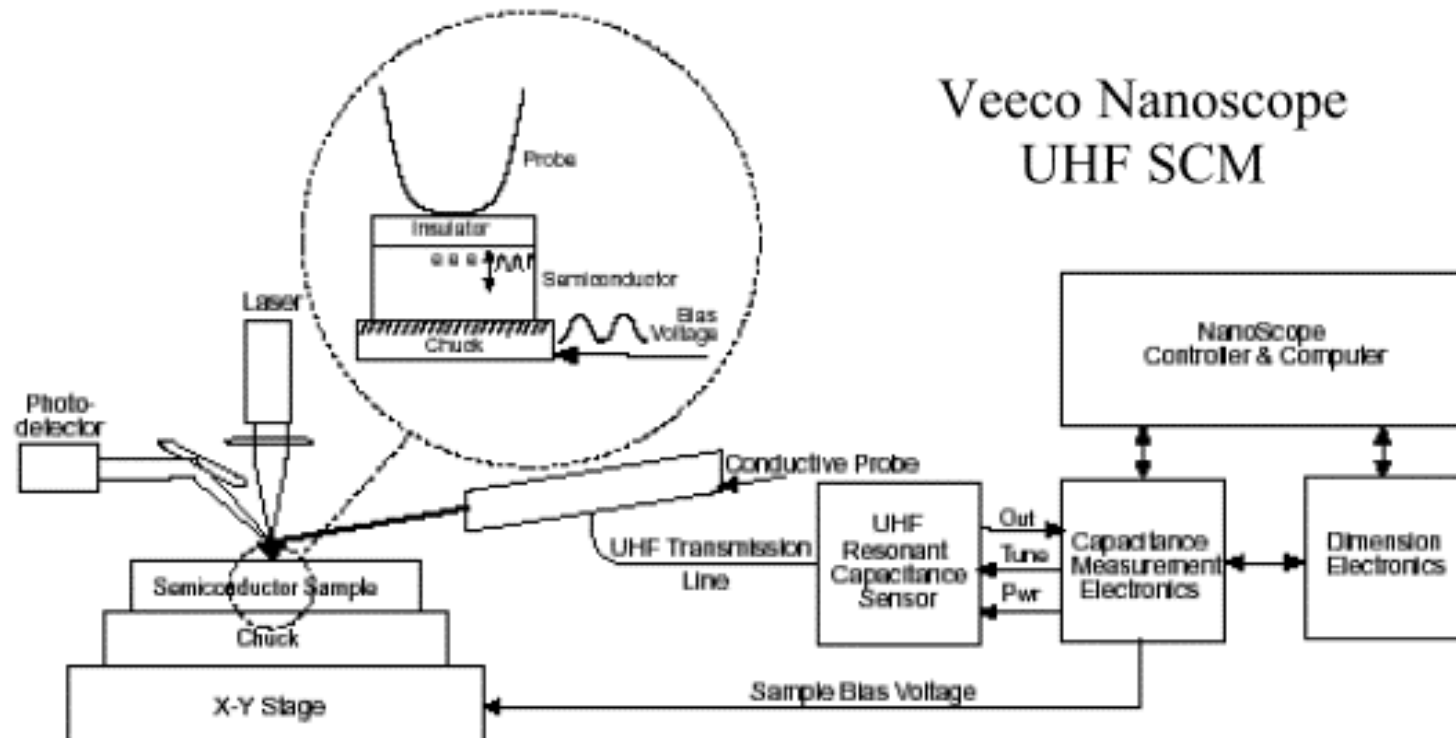
The free charges screen the electric field : the higher is the field (or the **lesser is the charge density**, or the **thinner is the film**) the **deeper is the field penetration** into the semiconductor (= **smaller capacity**).

E.g. in a sample with uniform doping, with **variable oxide thickness**, the fields penetrates deeper in the thinner oxide regions.

In a sample with **variable charge density**, for the same applied voltage, the field penetration is deeper were the charge density is smaller.



## UHF SCM working principle

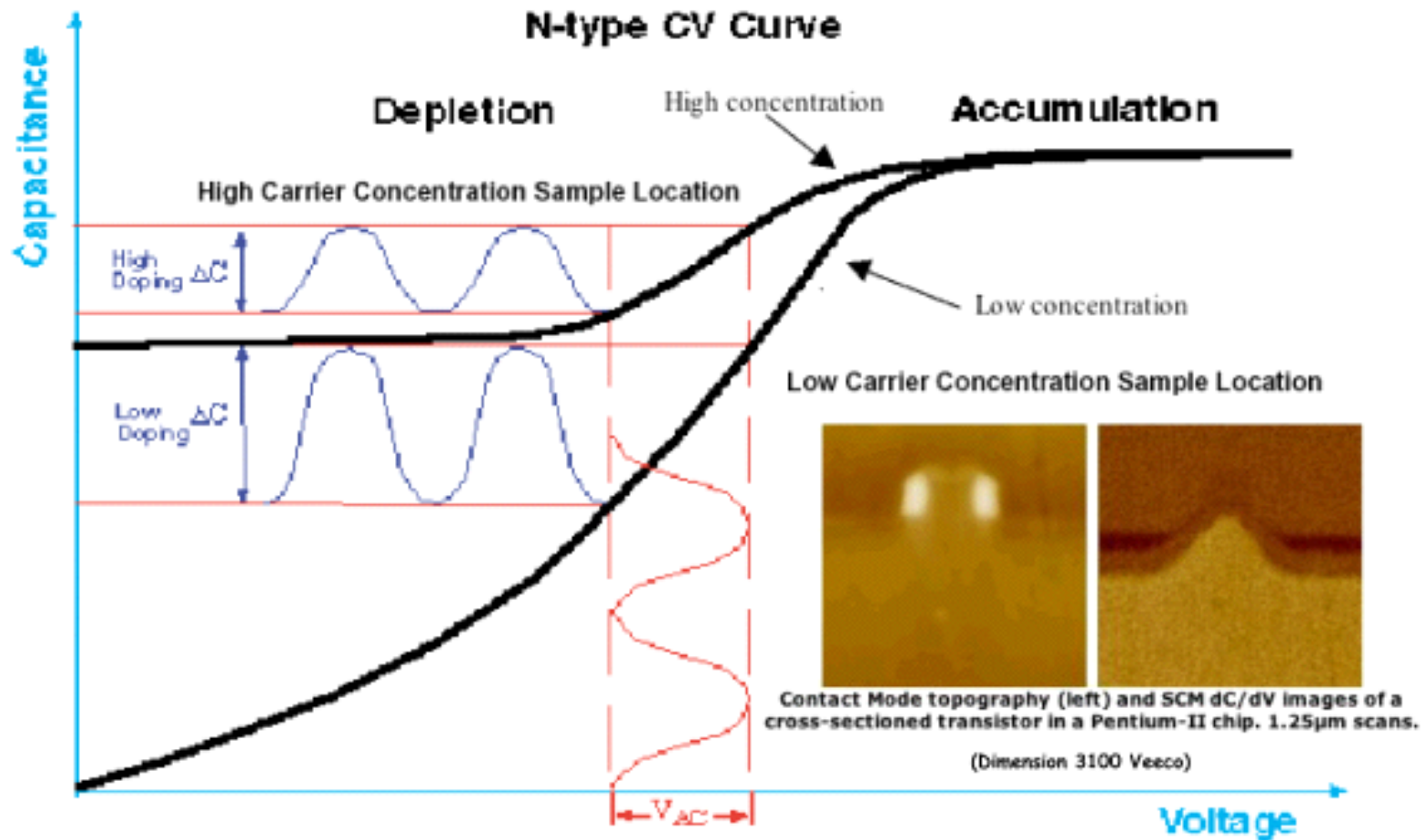


The UHV SCM technique measures the **contact capacity changes** as a function of the **applied field changes**. The quantity  $dC/dV$  is inversely proportional to the free **charge density**, and to the oxide **thickness**.

The signal used to measure  $dC/dV$  is a high frequency constant-amplitude sine wave ( $\approx 900$  MHz), adjusted close to the resonance for the circuit including the tip-sample junction.

A lock-in detects the **amplitude changes produced by the capacity changes**.

## $dV/dC$ in UHF SCM



A DC voltage may be added to the AC signal, to adjust the working point.

# SKPM (Kelvin Mode of Scanning Probe Microscopy)

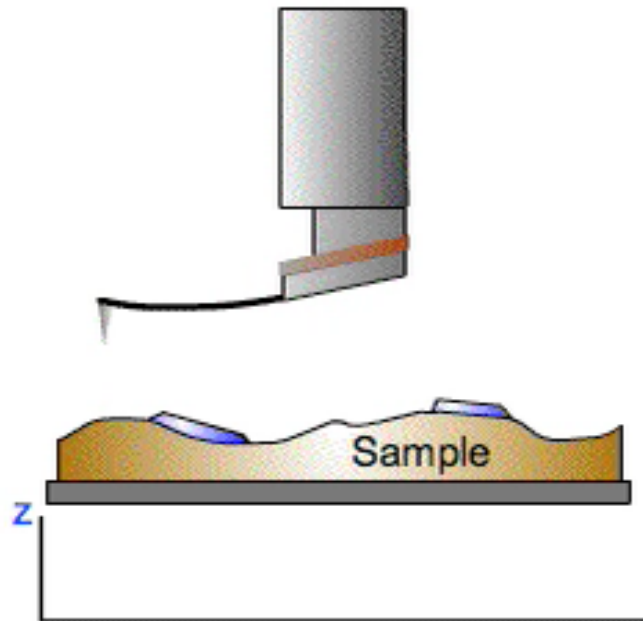
SKPM images offer a mapping of the tip-sample work function  $F(x)$ .

The first pass records the line-profile.

The second pass is made (in Non-Contact) with the cantilever retracted and excited by a voltage  $V_{tip}$  with a.c. and d.c. components :

$$V_{tip} = V_{dc} + V_{ac} \sin(\omega t).$$

1-st pass. Sample profile acquisition.



The electric force due to the tip-sample capacitive induction  $F_{cap}$  is:

$$F_{cap} = (1/2) (V_{tip} - F(x))^2 (dC/dz)$$

whose first harmonic

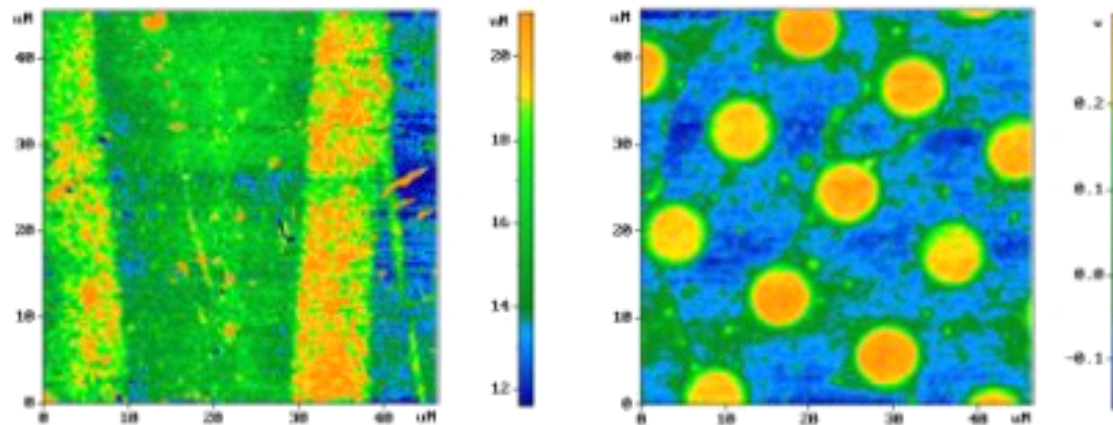
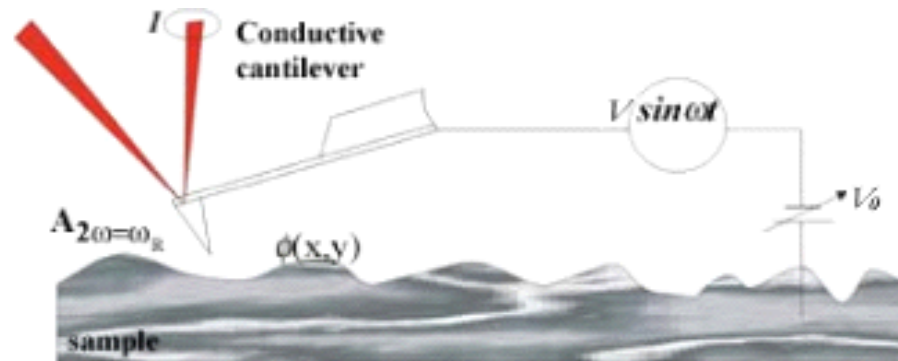
$$F_{cap}(\omega t) = (V_{dc} - F(x)) (dC/dz) V_{ac} \sin(\omega t)$$

drives the oscillation.

The feedback system controls the voltage  $V_{dc}$  in order to bring to zero the oscillation amplitude, letting  $V_{dc}(x,y) = F(x,y)$ .

The SKPM image is the matrix  $V_{dc}(x,y)$

## SKPM (2)



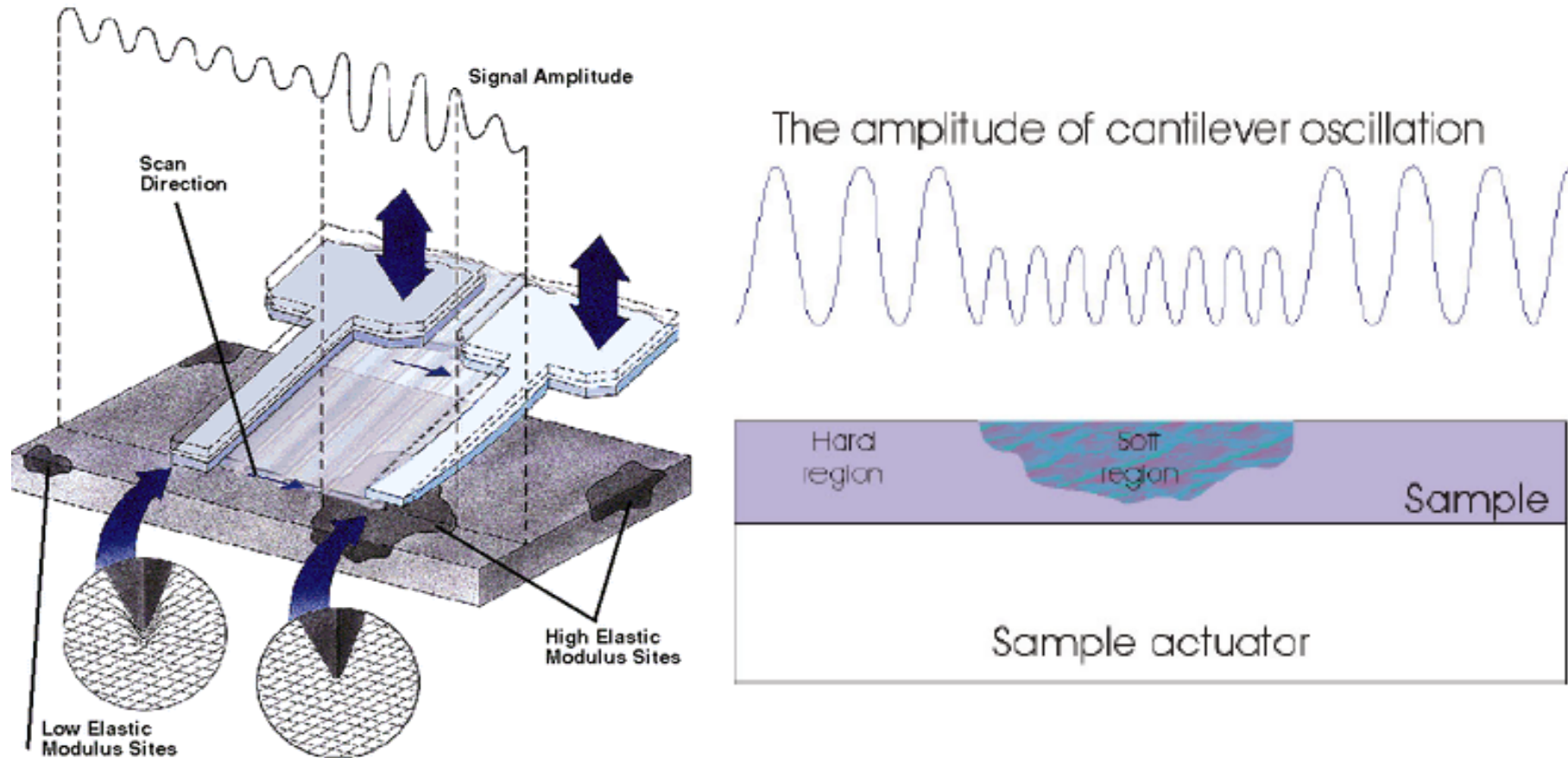
(SolverPro NT-MDT)

Self assembled monolayer of azobenzene containing thiols. The regions with higher potential (round spots) are dodecanethiol(A). Surrounding monolayer is 4-trifluoromethyl-4'-(10-mercapto-decyloxy) azobenzene(B). The SKPM contrast is provided by strong dipole moment of the molecules of B whereas the dipole moment of A is low. Sample courtesy of Dr. P. Karageorgiev and Dr. B. Stiller (University of Potsdam, Germany)

## FFM (Force Modulation Microscopy)

Vibrating the scanner which holds the sample and measuring the amplitude response of the cantilever maps the differences in surface stiffness or elasticity.

Force modulation technique is useful for detecting soft and stiff areas on substrates which exhibit overall uniform topography.

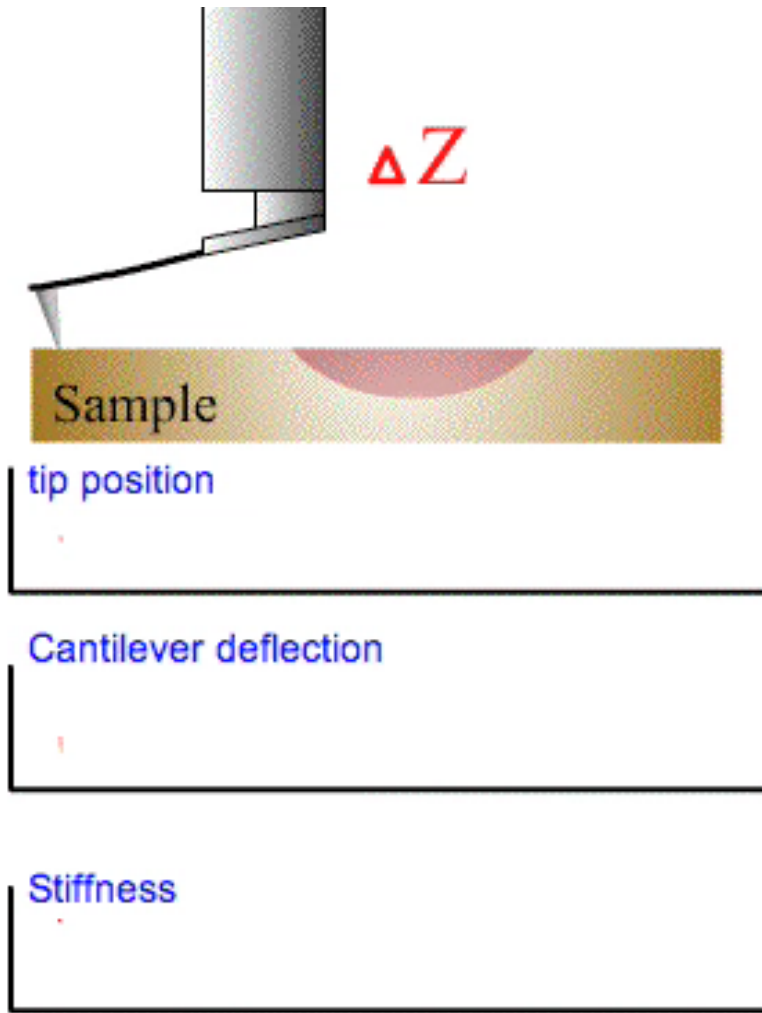




## FMM (2)

In **FMM** the sample is scanned in Contact and the cantilever is **periodically pushed** (by an auxiliary piezo) against the sample-

The **indenting depth** produced by the tip depends on the **local stiffness** of the sample.



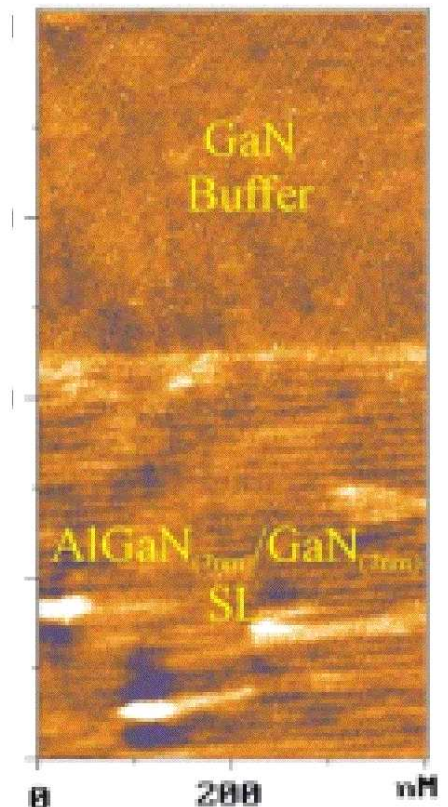
On the stiffer regions the cantilever deflection is larger than in the softer regions .

The opposite holds for the **indenting depth D**.

If **Dz** is the scanner displacement, the vertical cantilever deflection is **Dz-D**.

Once known the cantilever elastic constant **k<sub>c</sub>**, the local elastic constant **k<sub>s</sub>** of the sample is obtained by the relation:

$$k_s = k_c \cdot (Dz/D - 1)$$



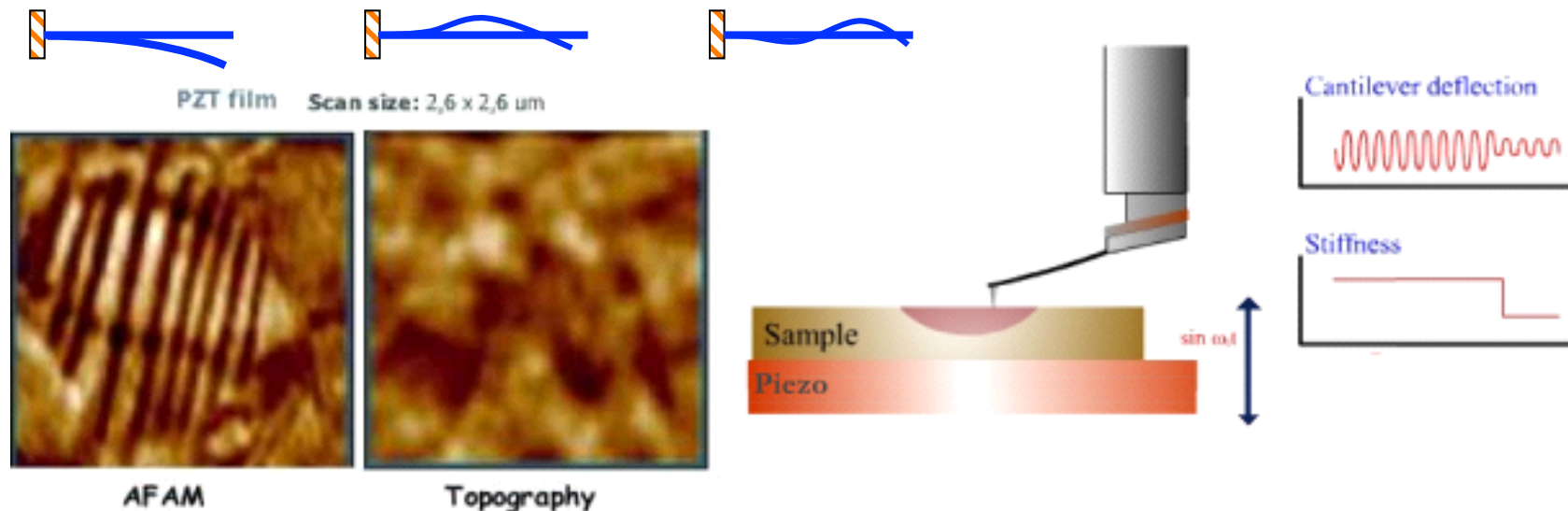
# AFAM (Atomic Force Acoustic Microscopy)

The AFAM images map the cantilever oscillation amplitude by exciting the sample through an auxiliary piezo.

The acoustic wave produced by the piezo-actuator drives the sample surface into vibration and couple with the cantilever through the tip in contact.

The cantilever **vibration modes** (frequencies) depend on the stiffness of the tip-sample contact on the contact area size, (both functions of the Young module of tip  $E_t$  and sample  $E_s$ , of the tip curvature radius  $R$ , on the effective load  $F_n$ , and on the surface topography) .

The **AFAM spectroscopy** is performed by sweeping the piezo-actuator frequency

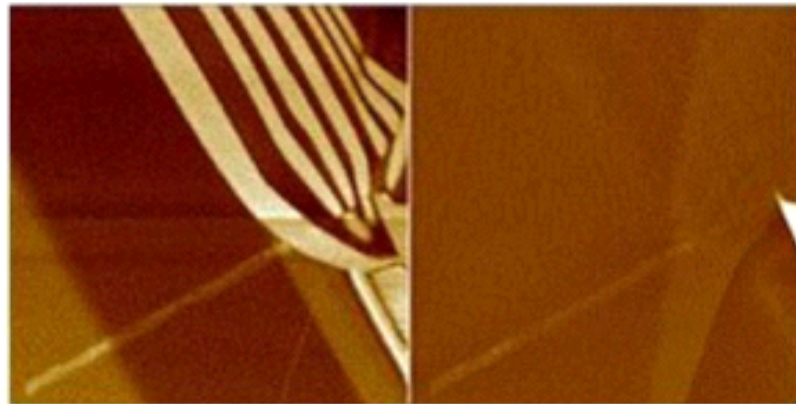


Stripe ferroelectric domain structure are made visible by the difference in local Young's moduli of domains of different polarization. (Sample courtesy of Prof. W. Arnold, Fraunhofer Institute for Nondestructive Testing, Saarbruecken, Germany)

## SSRM (Scanning Spreading Resistance Microscopy)

The SSRM images map the **local surface resistance** by using a **conducting** tip and a **logarithmic current amplifier** (dynamic range from 100mV A to 10 pA).

The sample is scanned in Contact with a biased tip: the resistance is calculated as the ratio between the applied voltage **V** and the measured current **I**



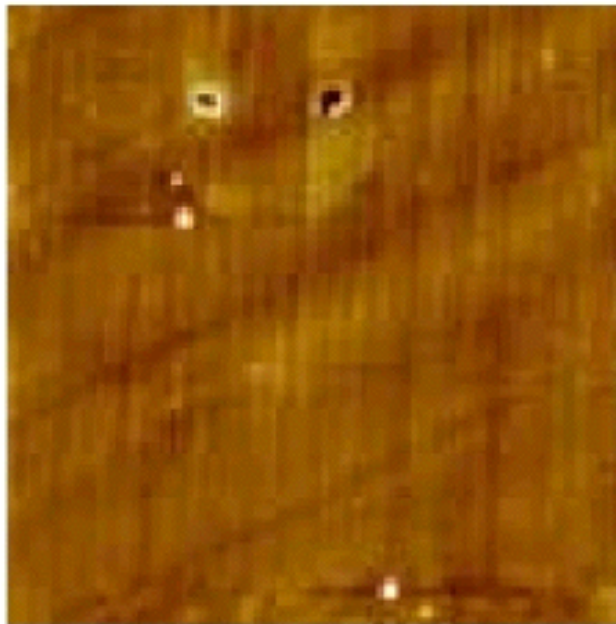
SSRM (left) and contact mode topography (right) scans of an InP-based heterostructure. 7mm scans. Sample courtesy Lucent Technologies. The contrast in the SSRM image shows the different regions of the heterostructure: alternating Zn-doped p-type and S-doped n-type layers.

(Veeco Dimension 3100)

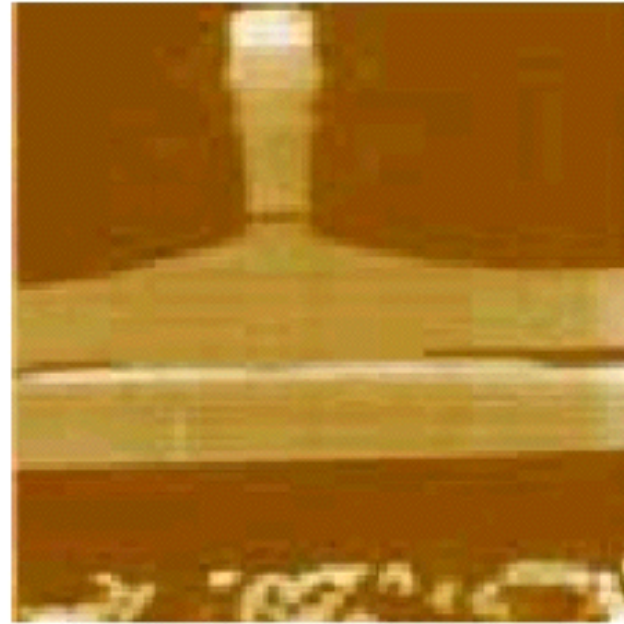


## TUNA (Tunneling AFM)

An extension of **SSRM** technique to samples covered by a thin insulating oxide film is the **TUNA** an STM were very small current are measured (from 100 pA down to 100fA).



topography

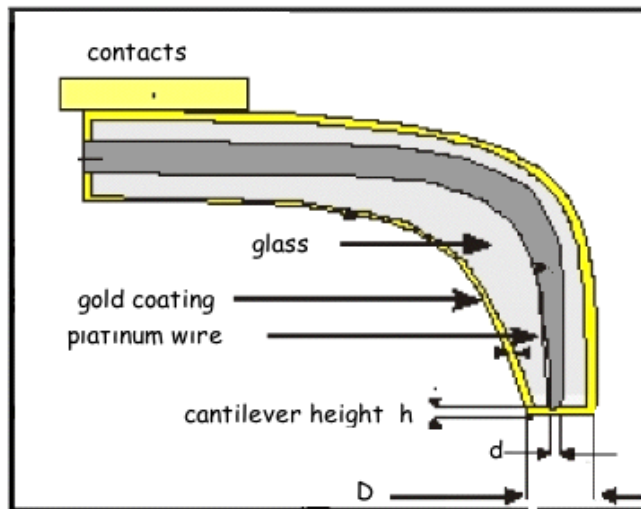
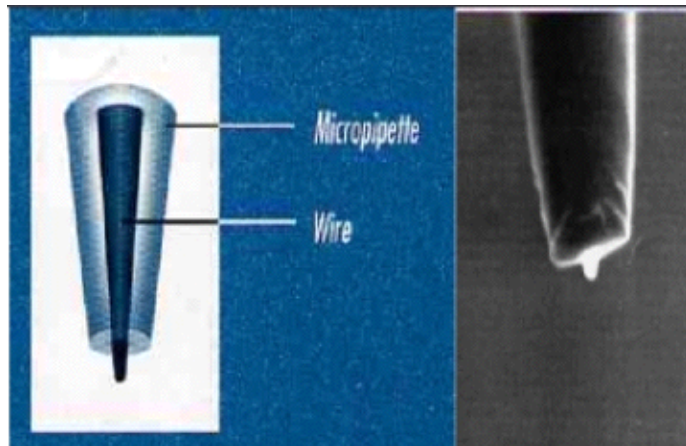


TUNA

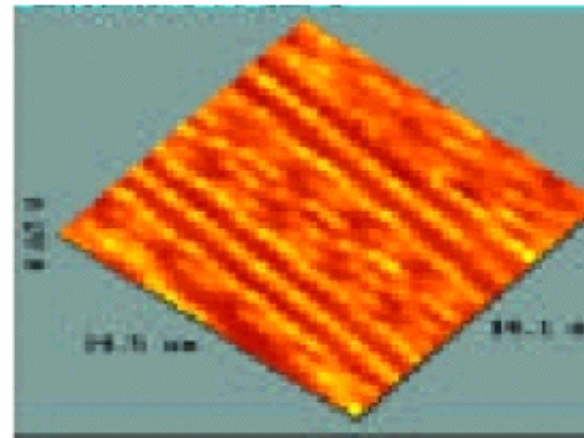
Magnetic recorder head : scan size 12  $\mu\text{m}$

# SThM (Scanning Thermal Microscopy)

SThM images map the local thermal conductivity of the sample surface. It requires special tips (**micro-thermocouples**).



Diagrammatic representation of a single channel thermal cantilevered glass probe.



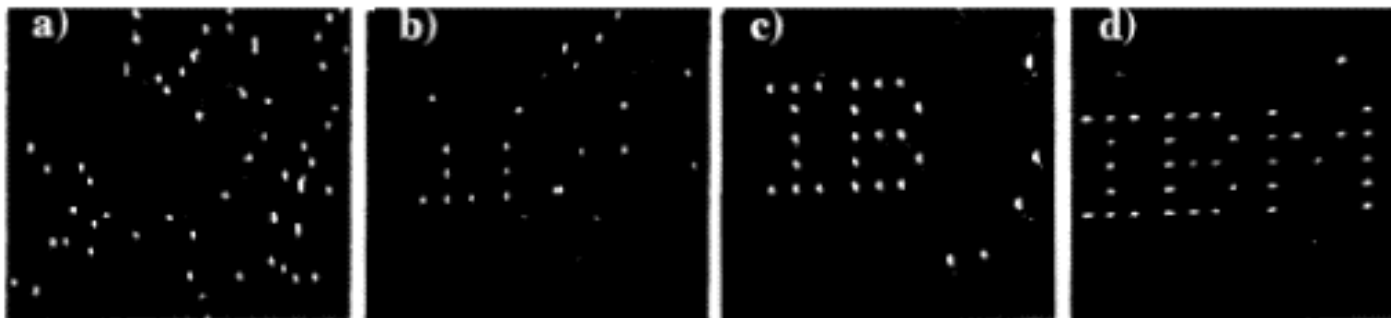
Thermal conductivity image

**Micro-thermocouples** may be obtained as gold coated micropipettes with metallic core

# SPM-Lithography types

Depending on the operating mode, lithography can be done in different ways:  
by applying voltage pulses between the probe and the sample when working in STM mode  
or with conductive cantilevers in AFM mode;  
or by "scratching" , or "engraving" the surface with the probe when working in SFM mode;  
or by using the probe (and applied voltage) to displace atoms on a smooth sample surface.

- STM lithography
- AFM anodic-oxidation lithography
- SFM force lithography



An example of STM nanomanipulation. IBM company name is composed of Xenon atoms precipitated on the nickel surface (picked-up by applying voltage, then shaken-off after positioning).

# Anodic Lithography

Anodic AFM lithography consists in a local modification of the **metallic** sample surface by a **voltage** applied through a **conductive tip**

E.g. a thin Titanium layer on a Silicon substrate may be oxidized even during a **non-contact** scan: the **water film** adsorbed onto the sample provides the electric contact by **capillarity**. The negative biased tip behaves as a cathode and on the sample surface anodic oxidation occurs.

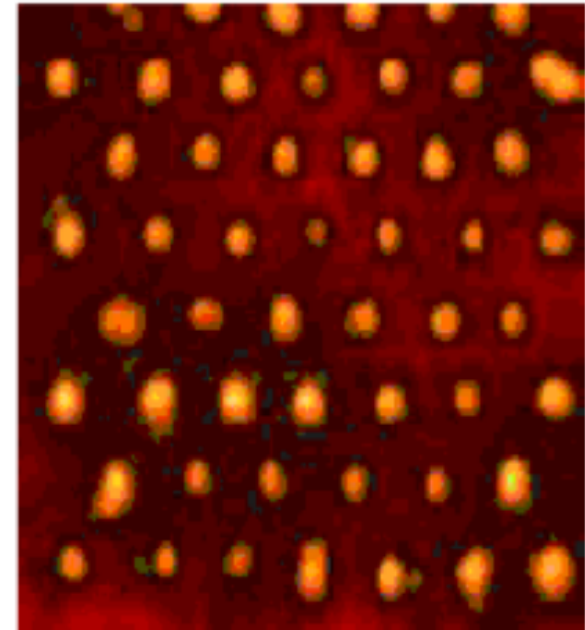
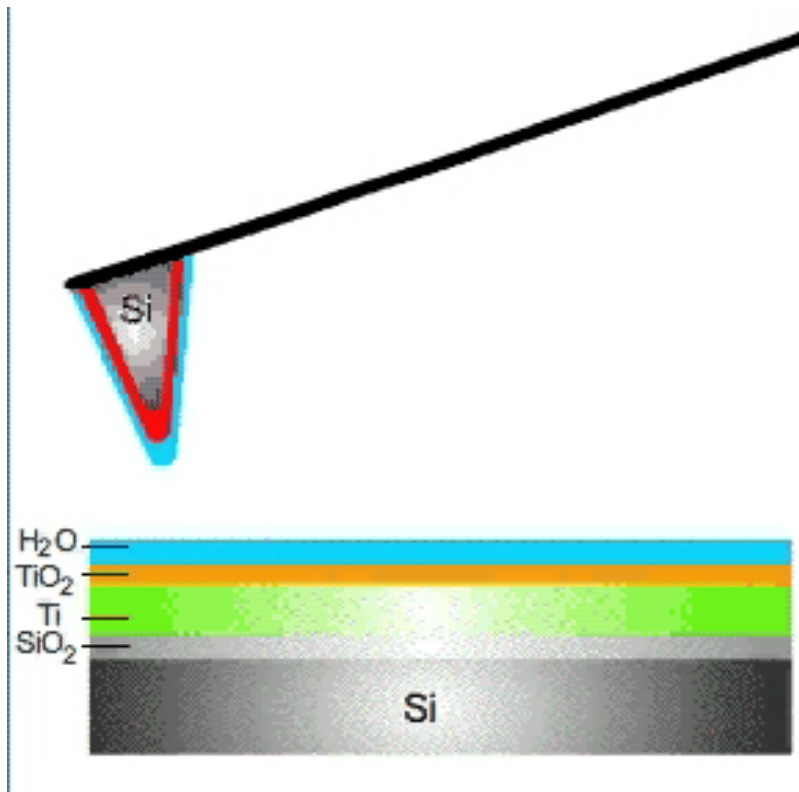
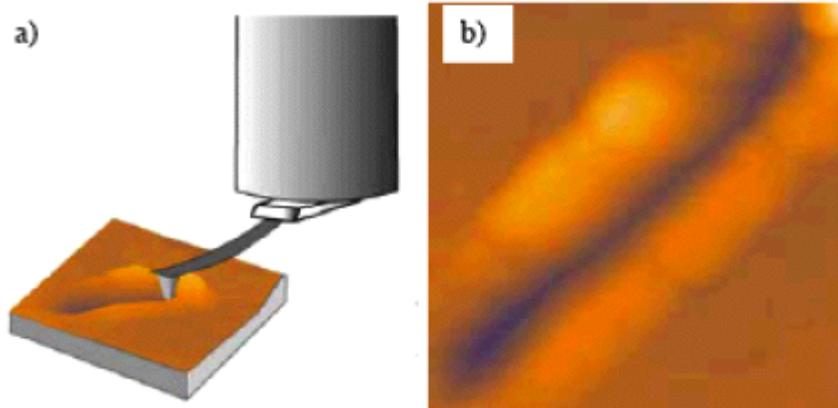
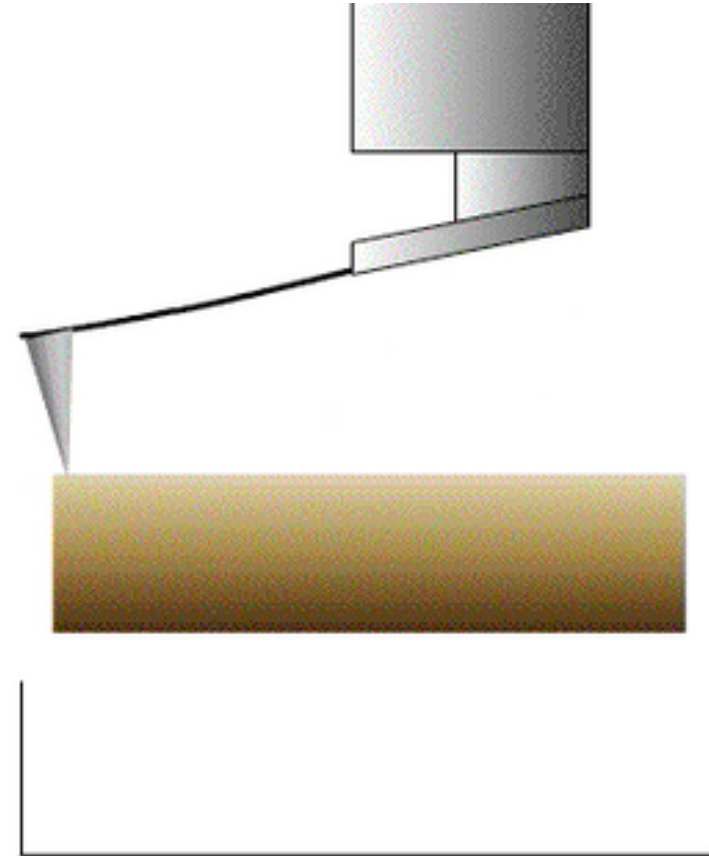


Image (size 200x200 nm<sup>2</sup>) of titanium film on silicon surface, oxidized in the preset points

# Force lithography

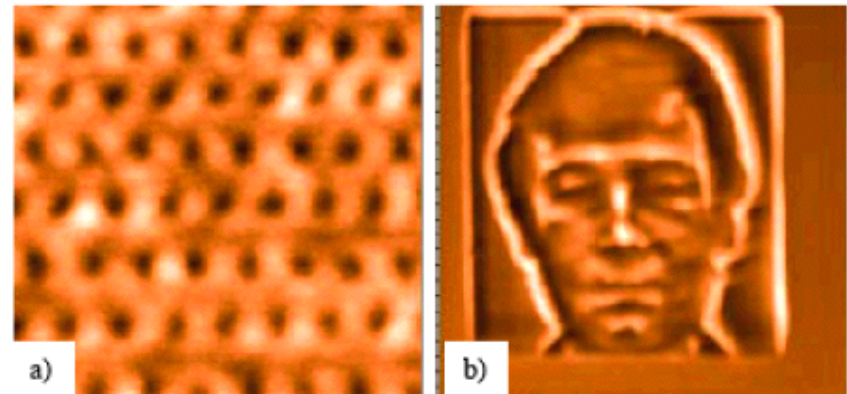


(a) Schematic diagram of **static** force lithography  
 (b) image of Al surface ( $1,6 \times 1,6 \text{ } \mu\text{m}^2$ ) with a scratch



In vector **dynamic** force lithography (nanoembossing) the surface is modified due to indentations formed by oscillating tip in semicontact mode:

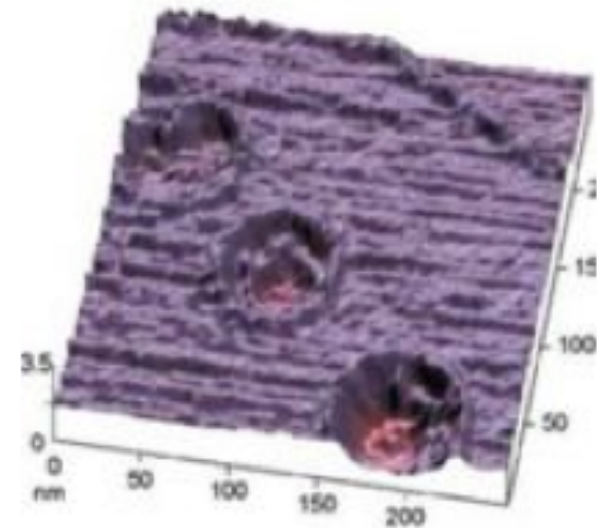
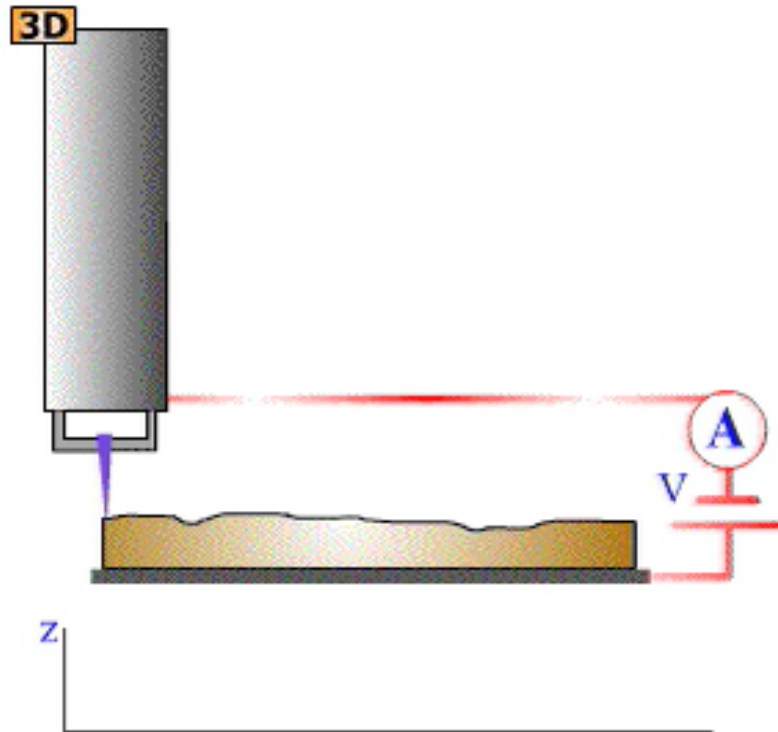
- (a) regular array of pits ( $220 \times 220 \text{ nm}^2$ )
- (b) raster lithography ( $2,5 \times 2,6 \text{ } \mu\text{m}^2$ )





# STM Lithography

Using a current pulse the sample surface under the tip can be melted.



STM Lithography on LB film.

three monolayers of conducting LB film  
after exposure to three electric pulses.

## Cantilevers

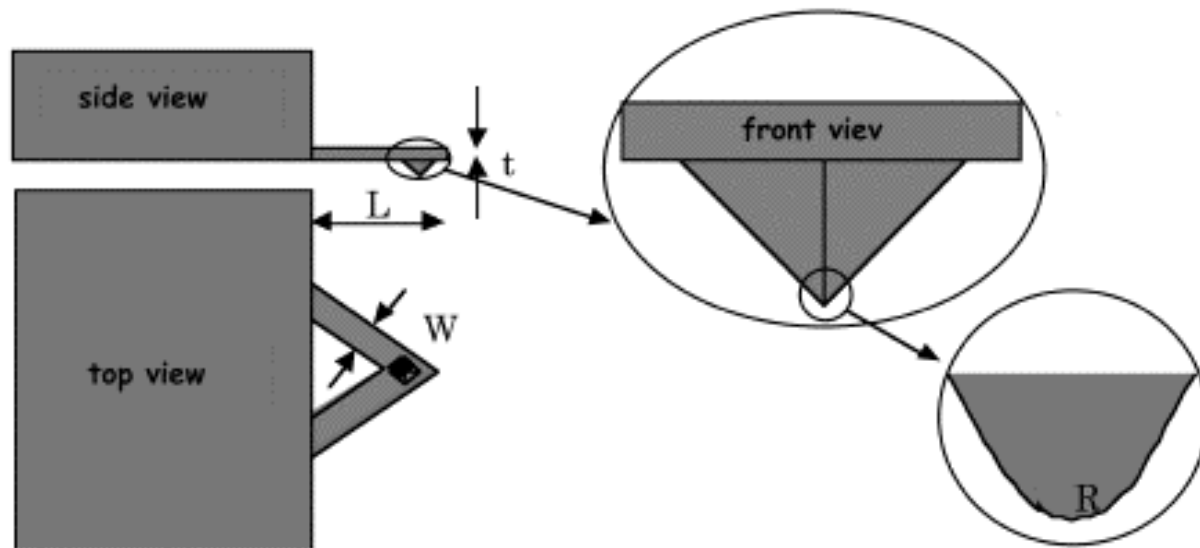
The cantilever **elastic constant**  $k$  must allow not-negligible deflection under forces of the order of  $10^{-8} \div 10^{-11}$  N: typical values are in the range  $k \approx 0.1 \div 100$  N/m.

For a rectangular bar (width =  $W$ , length =  $L$ , thickness =  $t$ ), with a Young modulus  $E$  we have  $k = E(t/L)^3 W/4$ .

Assuming  $E \approx 10^{11}$  N/m<sup>2</sup> (Silicon or Silicon Nitride), we get  $k \approx 0.5$  N/m with  $W \approx 20$   $\mu\text{m}$ ,  $L \approx 100$   $\mu\text{m}$ , and  $t \approx 1$   $\mu\text{m}$ .

The most flexible cantilevers (used for Contact Mode) are obtained in a **rectangular** geometry that offers high sensitivity to "lateral force"

More stiff cantilever (e.g. for Non-Contact Modes) are "**V**"shaped and insensitive to "lateral force"



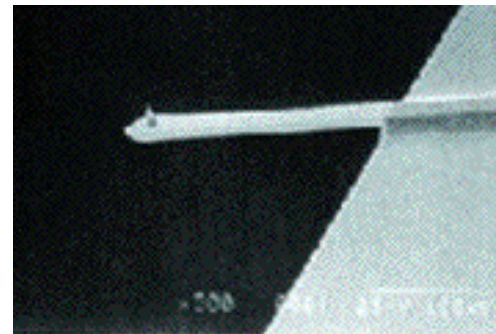
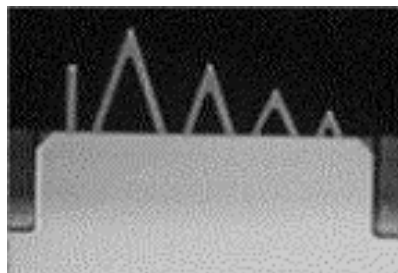
## Cantilevers (2)

The mechanical resonant frequency  $f_r$  of a cantilever with one end blocked is proportional to  $\sqrt{(E/\rho)/L^2}$ , where  $\rho$  is the density and  $E$  the Young modulus.

To increase the frequency  $f_r$  while keeping constant the stiffness  $k$ , the cantilever must be compact.

High resonant frequency allows faster scans : typically the maximum scan rate  $f_s$  ( $=1/T_s$ , where  $T_s$  is the time interval between two signal acquisitions) is chosen  $f_s = f_r/100$ .

Commercial cantilevers offer  $f_r$  ranging from a few kHz to fraction of MHz.

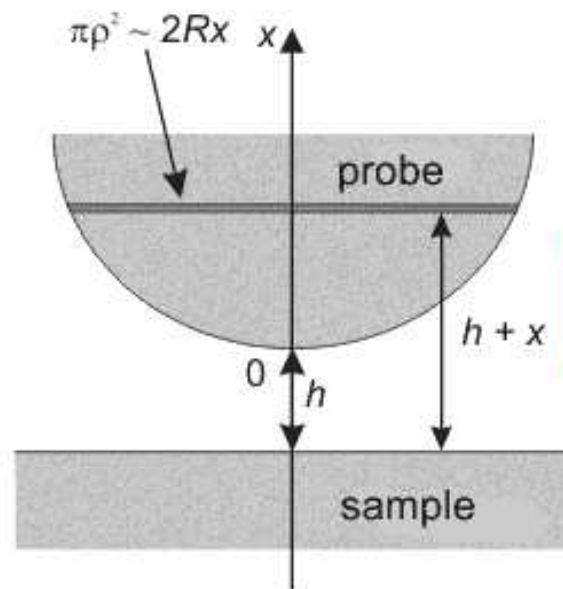




# Tip-Sample interaction

Dependence on tip shape and on tip-sample distance

1. Parabolic or spherical probe.



$$F = \frac{\pi^2 n_1 n_2 A_3 R}{6 h^2}$$

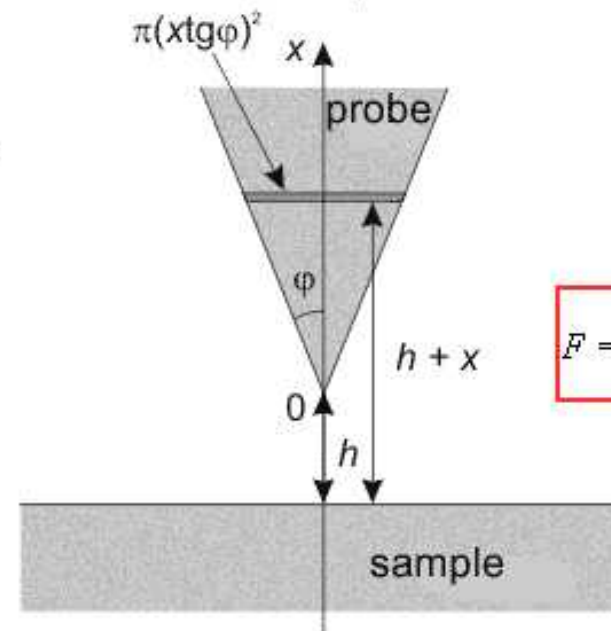
$$A_3 \approx 10^{-78} \text{ J} \cdot \text{m}^6$$

probes with a spherical tip at small tip-sample separations  $R \gg h$ .

The same result is obtained generally for the parabolic tip.

at  $R = 10 \text{ nm}$ ,  $h = 0.1 \text{ nm}$ ,  $F \approx 3.3 \cdot 10^{-9} \text{ N}$

2. Conical probe.



$$F = \frac{\pi^2 n_1 n_2 A_3 \text{tg}^2 \varphi}{6 h}$$

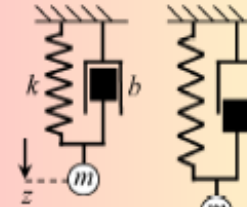
when tip curvature radius can be neglected ( $R \ll h$ ).

at  $h = 100 \text{ nm}$ ,  $\varphi = 11^\circ$ ,  $F \approx 1.3 \cdot 10^{-15} \text{ N}$

# Cantilevers Formulas (from Asylum Research)

## The Physics of Atomic Force Microscopy

### Simple Harmonic Oscillator



$$F = -kz$$

$$\omega_0 = 2\pi f_0 = \sqrt{\frac{k}{m}}$$

$$T = \frac{2\pi}{\omega_0}$$

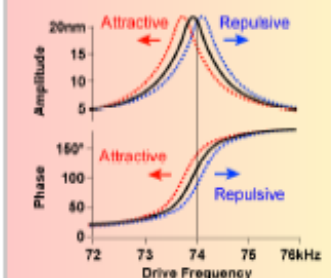
$$Q = \frac{k}{\omega_0 b} = \frac{A_{\max}}{A_{\text{drive}}} \equiv \frac{\omega_0}{\Delta\omega}$$

$$m \frac{d^2 z}{dt^2} = F_{\text{drive}} - b \frac{dz}{dt} - kz + F_{\text{ext}}$$

$$F_{\text{drive}} = k A_{\text{drive}} \cos \omega t$$

$$A = \frac{A_{\text{drive}} \omega_0^2}{\sqrt{(\omega_0^2 - \omega^2)^2 + (\omega \omega_0 / Q)^2}}$$

$$\tan \theta = \frac{\omega \omega_0 / Q}{\omega_0^2 - \omega^2}$$



$$\delta A_{(\text{max slope})} = \frac{2QA_0}{3\sqrt{3}(k - F')} F'$$

$$\delta \omega_0 \approx -\frac{\omega_0 F'}{2k} \quad \delta \theta_{(\text{res})} = \frac{Q}{k} F'$$

$$\bar{P}_{\text{sp}} = \frac{1}{2} \frac{kA^2 \omega}{Q} \left[ \frac{QA_{\text{drive}} \sin \theta}{A} - \frac{\omega}{\omega_0} \right]$$

### Cantilever Beam Theory

$$k = 3 \frac{EI}{l^3} \quad f_0 = \frac{C}{2\pi} \sqrt{\frac{k}{m_i + 0.24m_c}} \quad m_c = \rho A l$$

$$C = 1 \quad I = \frac{\pi d^4}{64}$$

$$C = 6.25 \quad I = \frac{\pi}{64} (d_o^4 - d_i^4)$$

$$C = 17.5 \quad I_z = \frac{wt^3}{12}$$

$$C = 34.4 \quad I_z = \frac{w_o t_o^3 - w_i t_i^3}{12}$$

### Cantilever Shapes

$$h_{\text{end}}(x) = \frac{3Lx^2 - x^3}{2L^3}$$

$$h_{\text{dist}}(x) = G(\cosh \kappa x - \cos \kappa x) + H(\sinh \kappa x - \sin \kappa x)$$

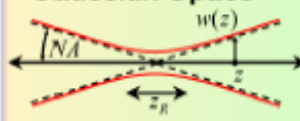
### Added Mass Correction

$$m_i = m_w \left( \frac{L - \Delta L}{L} \right)^3$$

### Reference Spring

$$k = k_{\text{ref}} \left( \frac{\Delta z_{\text{ref}}}{\Delta z} - 1 \right)$$

### Gaussian Optics



$$w(z) = w_0 \sqrt{1 + \left( \frac{\lambda z}{\pi w_0^2} \right)^2}$$

$$z_R = \frac{\pi w_0^2}{\lambda} \quad N.A. = \frac{\lambda}{\pi w_0}$$

### Energies

$$k_B T = 4 \text{ pNnm}$$

ATP hydrolysis  
12-21  $k_B T$   
Hydrogen Bond  
4-18  $k_B T$   
Covalent Bond  
100-200  $k_B T$   
Protein Stability  
6-20  $k_B T$

### Forces

Covalent Bonds  
2-5 nN  
Unzipping DNA  
20 pN (GC)/10 pN (AT)  
1 mW of light reflecting  
off of a surface  
7 pN

### Distances

Covalent Bonds  
0.1 nm  
Hydrogen Bond  
0.25 nm  
Tip Radius of Curvature  
2-50 nm  
DNA diameter  
2 nm

Stiffness  
Covalent Bond  
10 N/m  
Cantilevers  
0.01 - 100 N/m

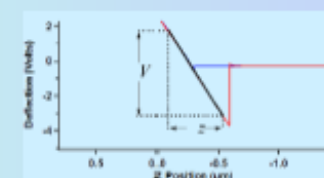
### Coherence

$$\text{Length} \quad \Delta l = c \Delta t \approx \frac{\lambda_0^2}{\Delta \lambda_0}$$

$$\text{Thin Lens} \quad \frac{1}{s} + \frac{1}{s'} = \frac{1}{f}$$

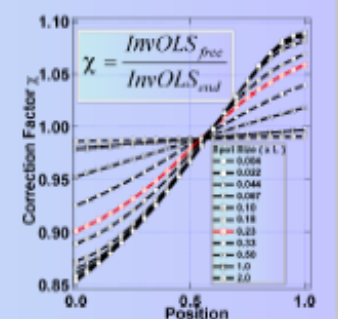
|           | Young's Modulus<br>E (GPa) | Density<br>$\rho$ (kg/m <sup>3</sup> ) | Speed of Sound<br>(m/s) | Thermal Expansion<br>( $\mu\text{m/mK}$ ) | Thermal Conductivity<br>$\lambda$ (W/mK) | Heat Capacity<br>$c_p$ (J/gK) |
|-----------|----------------------------|--|-------------------------|---|--|-------------------------------|
| Stainless | 200                        | 7760                                   | 5100                    | 10-13                                     | 12-25                                    | .5                            |
| Steel     | 210                        | 7850                                   | 5200                    | 11  | 35                                       | .46                           |
| Ti        | 116                        | 4500                                   | 5100                    | 8.9                                       | 17                                       | .528                          |
| Al        | 70                         | 2700                                   | 5100                    | 24  | 190                                      | .88                           |
| Invar     | 148                        | 8050                                   | 4300                    | 1.3                                       | 10.15                                    | .515                          |
| SiN       | 260-320                    | 3100                                   | ~9800                   | 3   | 30                                       | .71                           |
| Si        | 179                        | 2330                                   | 8800                    | 2.6                                       | 150                                      | .7                            |
| Cu        | 117                        | 8900                                   | 3600                    | 17  | 383-391                                  | .385                          |
| W         | 400                        | 19300                                  | 4500                    | 4.4                                       | 163                                      | .134                          |
| Granite   | 20-60                      | 2500-2700                              | ~5000                   | 3.7-11                                    | 1.4-4.2                                  | .21-.35                       |
| Pyrex     | 61                         | 2250                                   | 5500                    | 4.4                                       | 163                                      | .134                          |

### Thermal Method



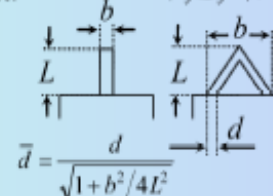
$$\text{InvOLS}_{\text{end}} = \Delta z / \Delta V (\text{nm/volt})$$

$$k = \frac{k_B T}{\langle \delta V^2 \rangle \chi^2 \text{InvOLS}^2}$$



### Sader Method

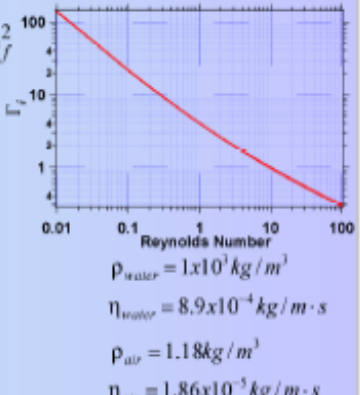
$$k_{\text{rect}} = 0.1906 b L^2 \rho_f Q_f \Gamma_1(\text{Re}) \omega_f^2$$



$$\bar{d} = \frac{d}{\sqrt{1 + b^2/4L^2}}$$

$$D_0 = k_{\text{rect}} \frac{4L^3}{b} \quad \text{Re} = \frac{\rho \omega b^2}{4\eta}$$

$$k_{\text{oi}} = \frac{D_0 \bar{d}}{2L^3} \left( 1 + \frac{4\bar{d}^3}{b^3} \right)^{-1}$$



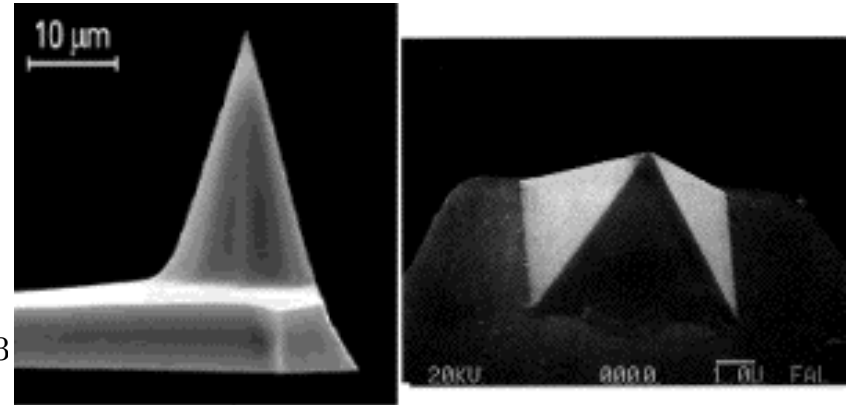
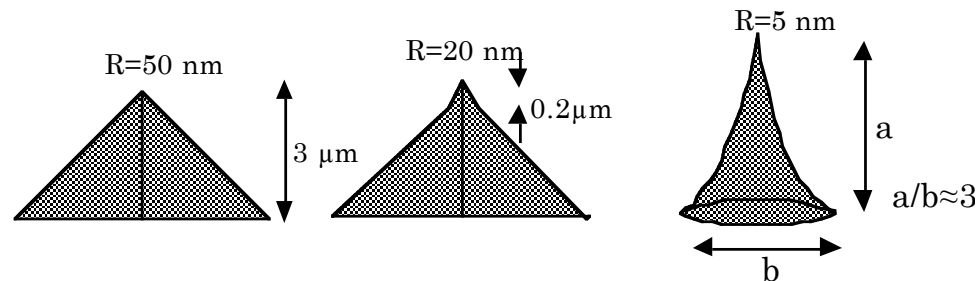
## Tips

Different commercial tips are available with different values of the **apex curvature radius  $R$**  : typically

**Pyramidal**  $R \approx 500 \text{ \AA}$

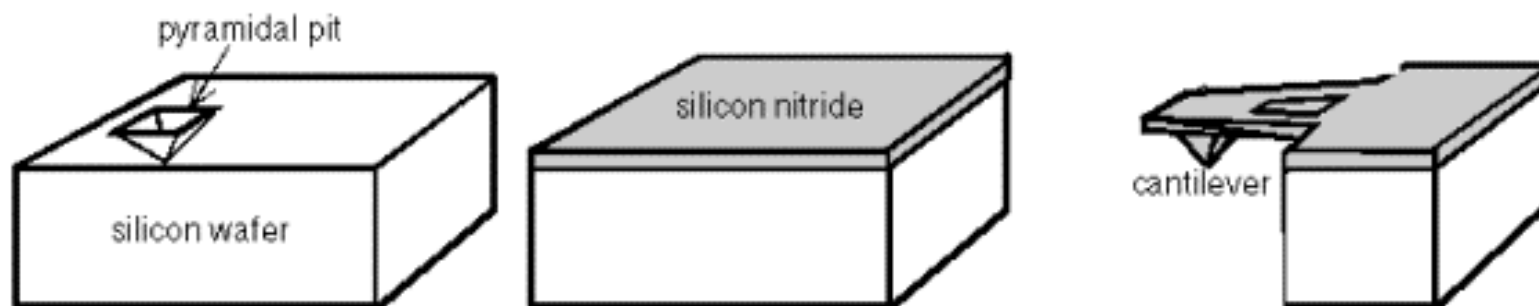
**Sharpened pyramidal**  $R \approx 200 \text{ \AA}$

**Conical** (*ultratip*)  $R \approx 50\div 100 \text{ \AA}$



**Pyramidal** tips are obtained by **photolithography**: through a squared hole in a mask evaporated onto a silicon wafer, a pyramidal pit is produced by **anisotropic etching** of [001] plane; then a Silicon Nitride film is deposited and glued onto a glass plate. By chemical etching the silicon is removed leaving the Silicon Nitride cantilever with pyramidal tip.

**Conical** tip are grown by **SEM deposition** in "dirty" atmosphere, or **ion-milling** (**FIB** Focused Ion Beam)



## Modified Tips

Special tips may be functionalized through physical or chemical modifications

Chemical or biological coatings can be applied to particle probes or off-the-shelf tipped AFM cantilevers.

Gold, Platinum, Diamond, Cobalt coatings are available



Chemically & Biologically Coated AFM Tips

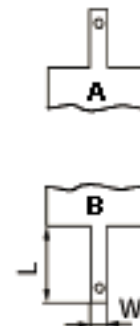
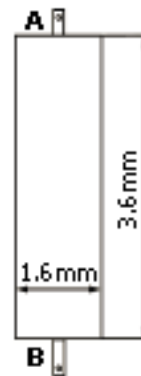


Particle AFM Probes



Custom AFM Probe Modifications

|                           |                 |
|---------------------------|-----------------|
| Chip thickness            | 0.4mm           |
| Reflective side           | Au              |
| Spring number             | 2               |
| Aspect ratio              | 3:1             |
| Cone angle $\phi$         | $\leq 22^\circ$ |
| Curvature radius of a tip | typical 10nm    |



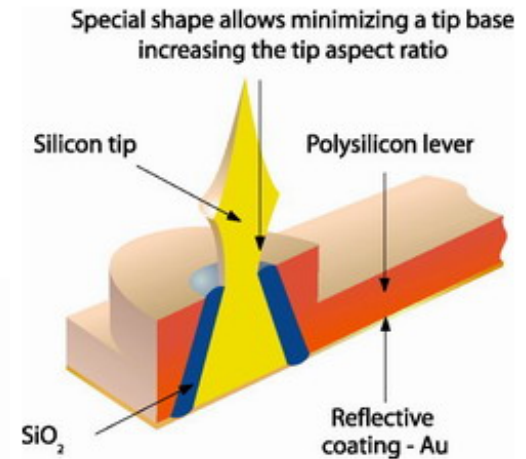
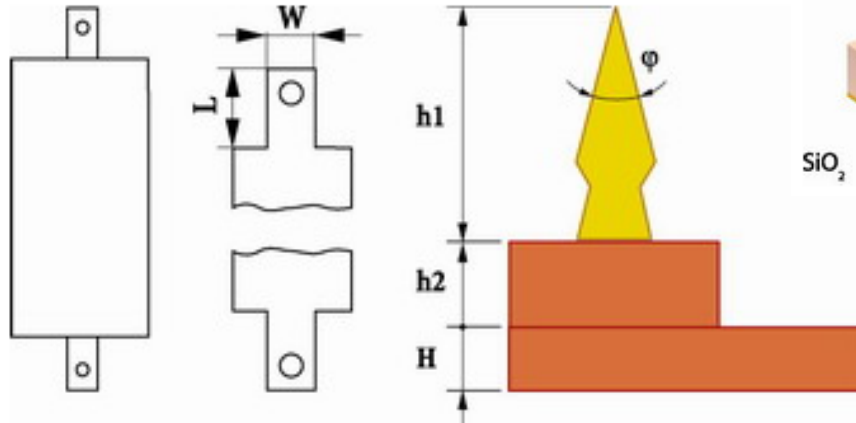
| Available Cantilever series | Spring | Cantilever length, L $\pm 5\mu\text{m}$ | Cantilever width, W $\pm 3\mu\text{m}$ | Cantilever thickness, $\mu\text{m}$ |         |     | Resonant frequency, kHz |         |     | Force constant, N/m |         |      |
|-----------------------------|--------|---|--|-------------------------------------|---------|-----|-------------------------|---------|-----|---------------------|---------|------|
|                             |        |   |  | min                                 | typical | max | min                     | typical | max | min                 | typical | max  |
| DCP11                       | A      | 100                                     | 35                                     | 1.7                                 | 2.0     | 2.3 | 190                     | 255     | 325 | 5.5                 | 11.5    | 22.5 |
|                             | B      | 130                                     | 35                                     | 1.7                                 | 2.0     | 2.3 | 115                     | 150     | 190 | 2.5                 | 5.5     | 10   |

# Etalon Tips

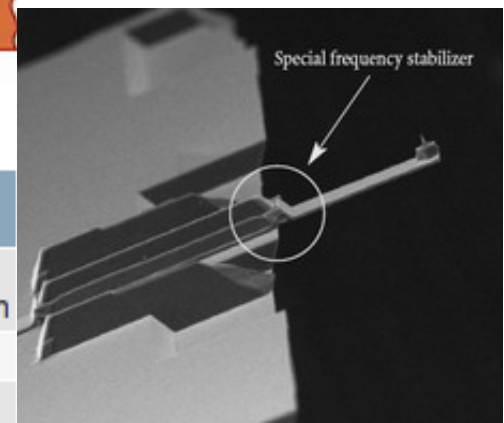
polysilicon levers with silicon high resolution tips  
 reproducible parameters (typical dispersion  $\pm 10\%$  /  $\pm 20\%$ )  
 high aspect ratio (cone angle  $22^\circ$ )  
 typical curvature radius of 10nm.

Specification for HA\_NC probes

|                           |                    |
|---------------------------|--------------------|
| Chip thickness            | 0.45mm             |
| Reflective side           | Au                 |
| Spring number             | 2                  |
| Tip height h1             | 5-10 $\mu\text{m}$ |
| Tip base height h2        | 4-6 $\mu\text{m}$  |
| Ratio h1/h2               | >1                 |
| Tip aspect ratio          | 5:1                |
| Cone angle $\alpha$       | $\leq 22^\circ$    |
| Curvature radius of a tip | typical 10nm       |



| Cantilever series | Spring | Cantilever lenght, L $\pm 2\mu\text{m}$ | Cantilever width, W $\pm 3\mu\text{m}$ | Cantilever thickness, $\mu\text{m}$ |         |     | Resonant frequency, kHz |                    | Force constant, N/m |                    |
|-------------------|--------|---|--|-------------------------------------|---------|-----|-------------------------|--------------------|---------------------|--------------------|
|                   |        |   |  | min                                 | typical | max | Nominal                 | Typical dispersion | Nominal             | Typical dispersion |
| HA_NC             | A      | 87                                      | 32                                     | 1.7                                 | 1.75    | 1.8 | 200                     | $\pm 10\%$         | 5.8                 | $\pm 20\%$         |
|                   | B      | 117                                     | 32                                     | 1.7                                 | 1.75    | 1.8 | 120                     | $\pm 10\%$         | 3.4                 | $\pm 20\%$         |

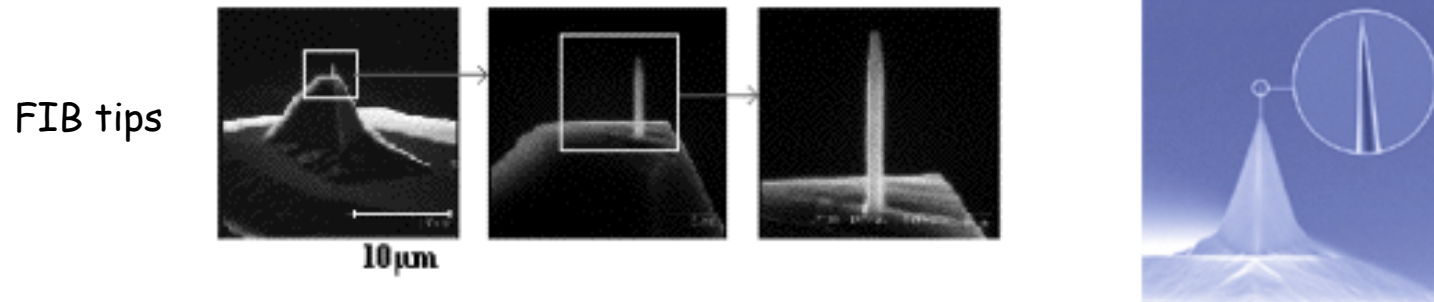




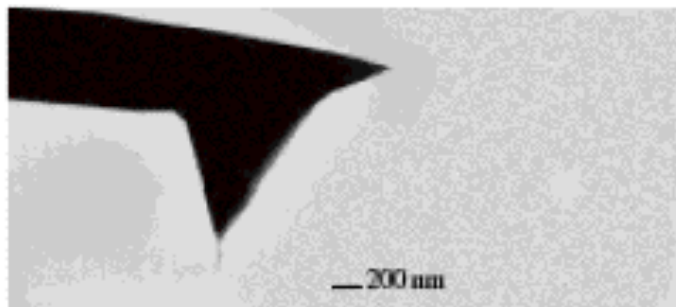
## Aspect Ratio and Curvature Radius

An important parameter is the **aspect ratio** (ratio between tip height and base)  
The larger is the aspect ratio the better is resolved the SPM image.

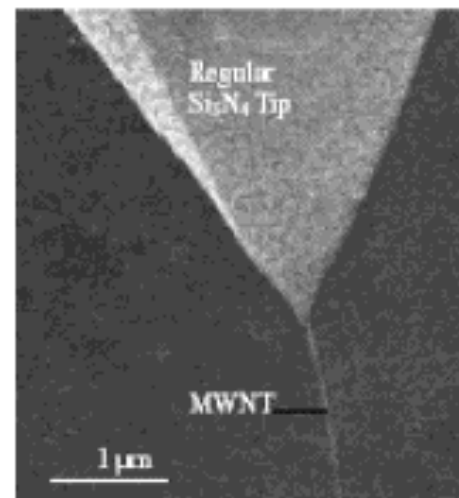
Alternatively the tip quality is defined by the **sidewall angle**, that for a pyramidal tip is  $45^\circ$  or  $27.5^\circ$  (edge or face of the tetrahedron ) and for conical tips varies from base to apex reaching a minimum of about  $22^\circ$ .



Very high Aspect Ratio tips may be obtained from **nanotubes**

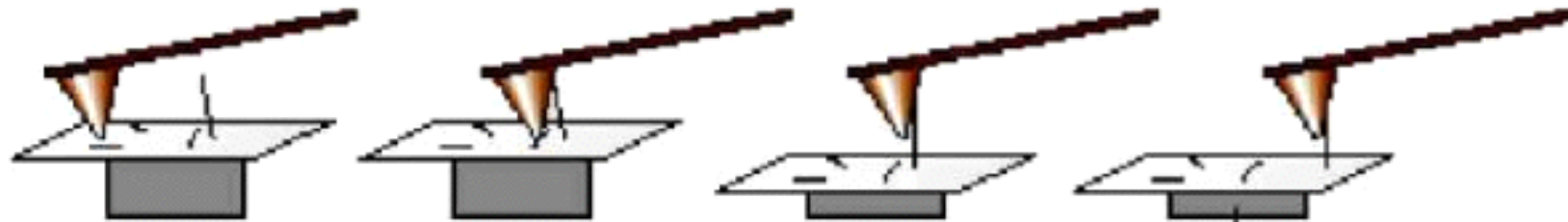


**SEM** micrograph of a multi-walled carbon nanotube (MWNT) tip physically attached on the single-crystal silicon, square-pyramidal tip (Courtesy Piezomax Technologies, Inc.)

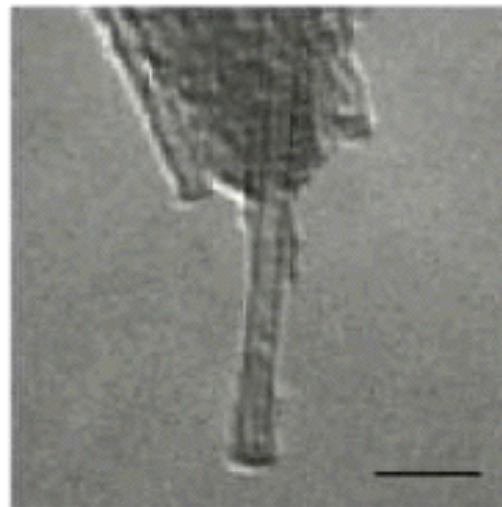
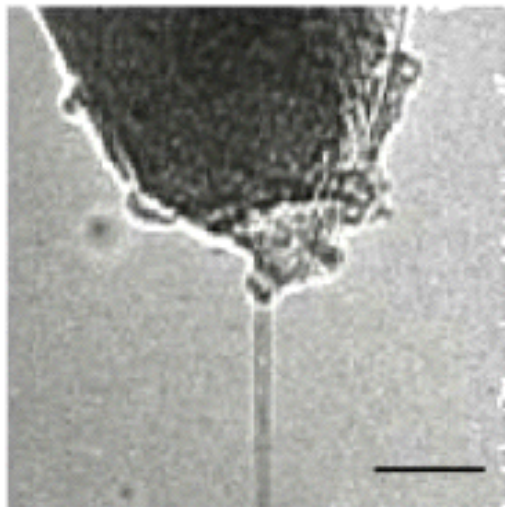


Scanning electron microscopy image of a carbon nanotube (MWNT) mounted onto a regular ceramic tip as a probe for atomic force microscopy

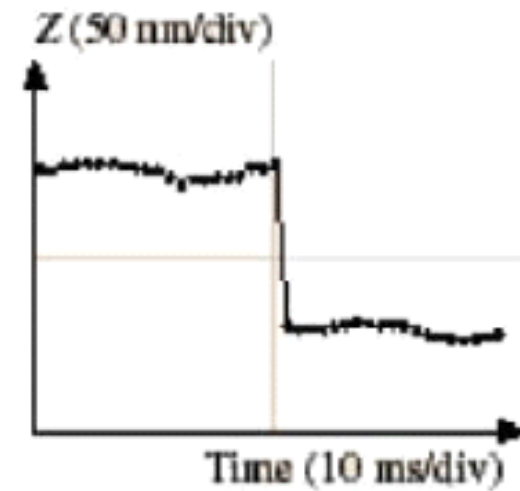
## Nanotube tips: high aspect ratio



Pick-up tip assembly of nanotube probes.

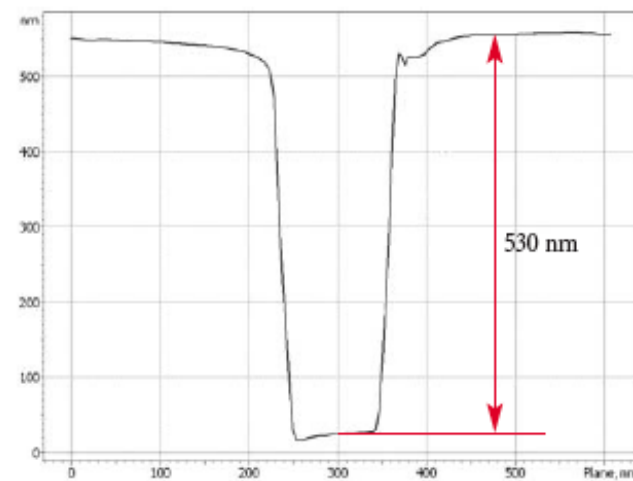
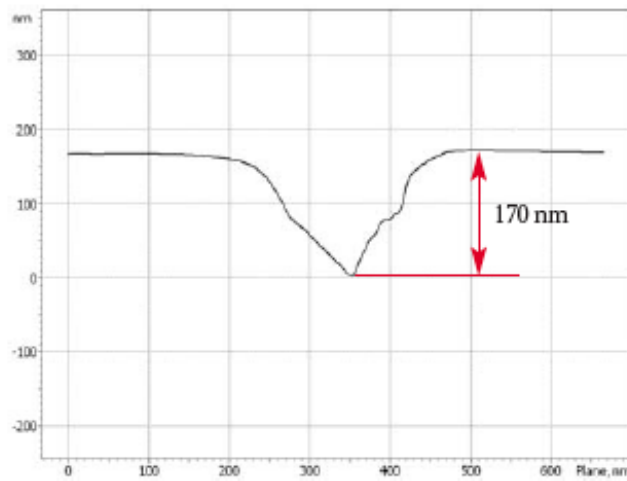
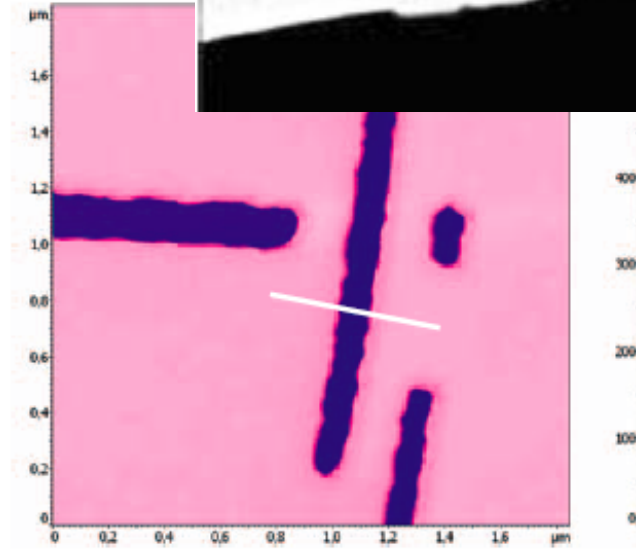
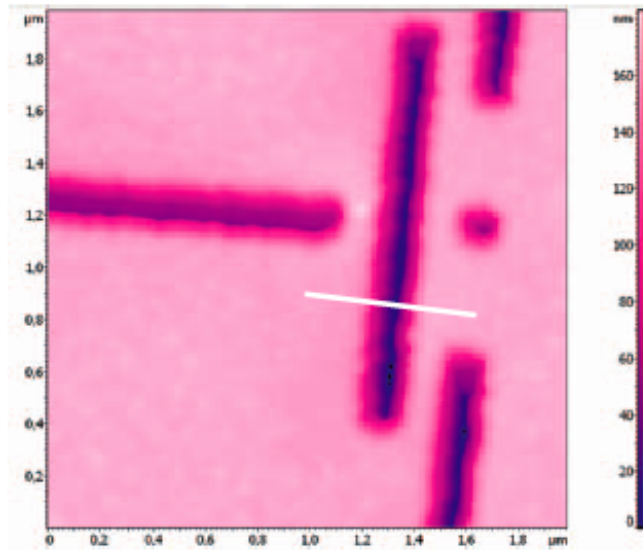


(diameters 0.9 nm and 2.8 nm)



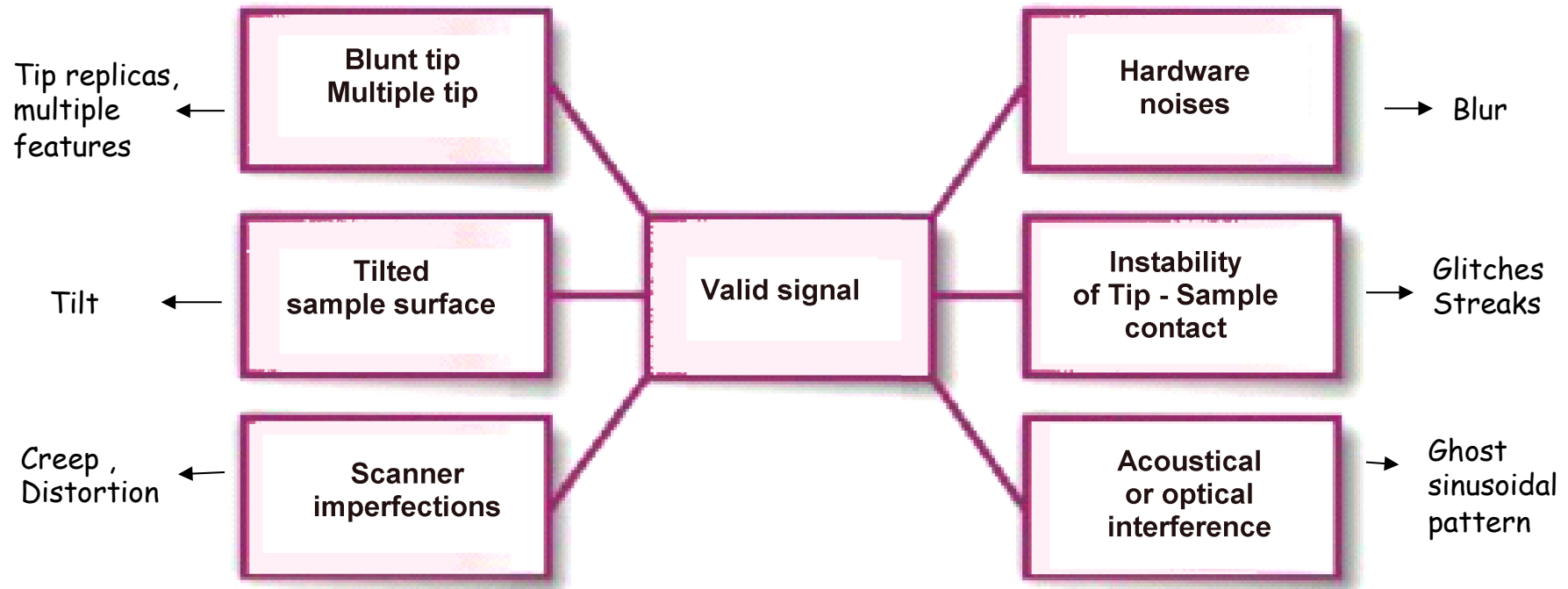
trace of the Z-position during a pick-up event.

## Whisker tips: high aspect ratio





## Sources of Image artifacts



Z offset - Tilt - Non-linearity & Drift - Blur - Glitches

## Scanner non-ideality

Typical scanner imperfections are:

Non-linearity

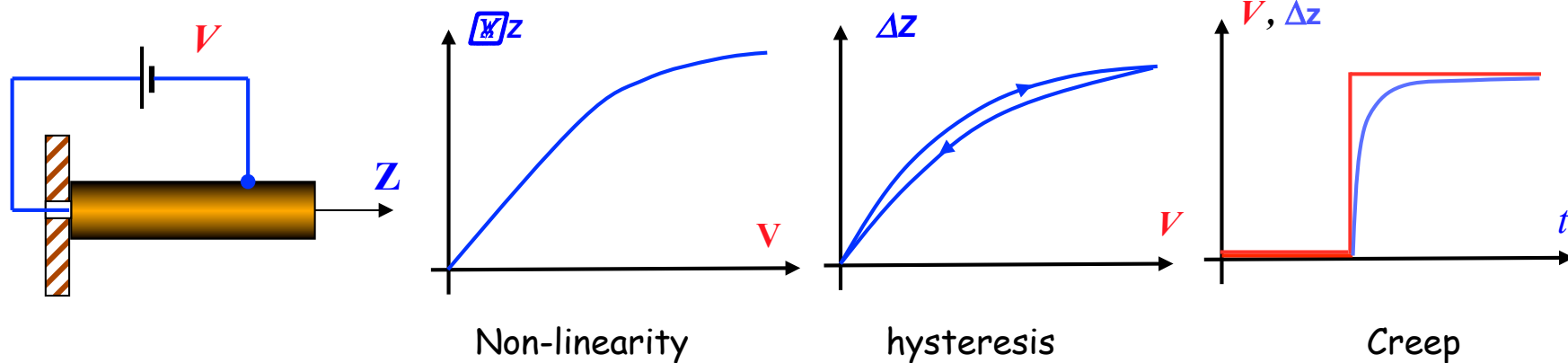
Creep

Hysteresis

Aging

Thermal drift

Cross-coupling among x-y-z displacements



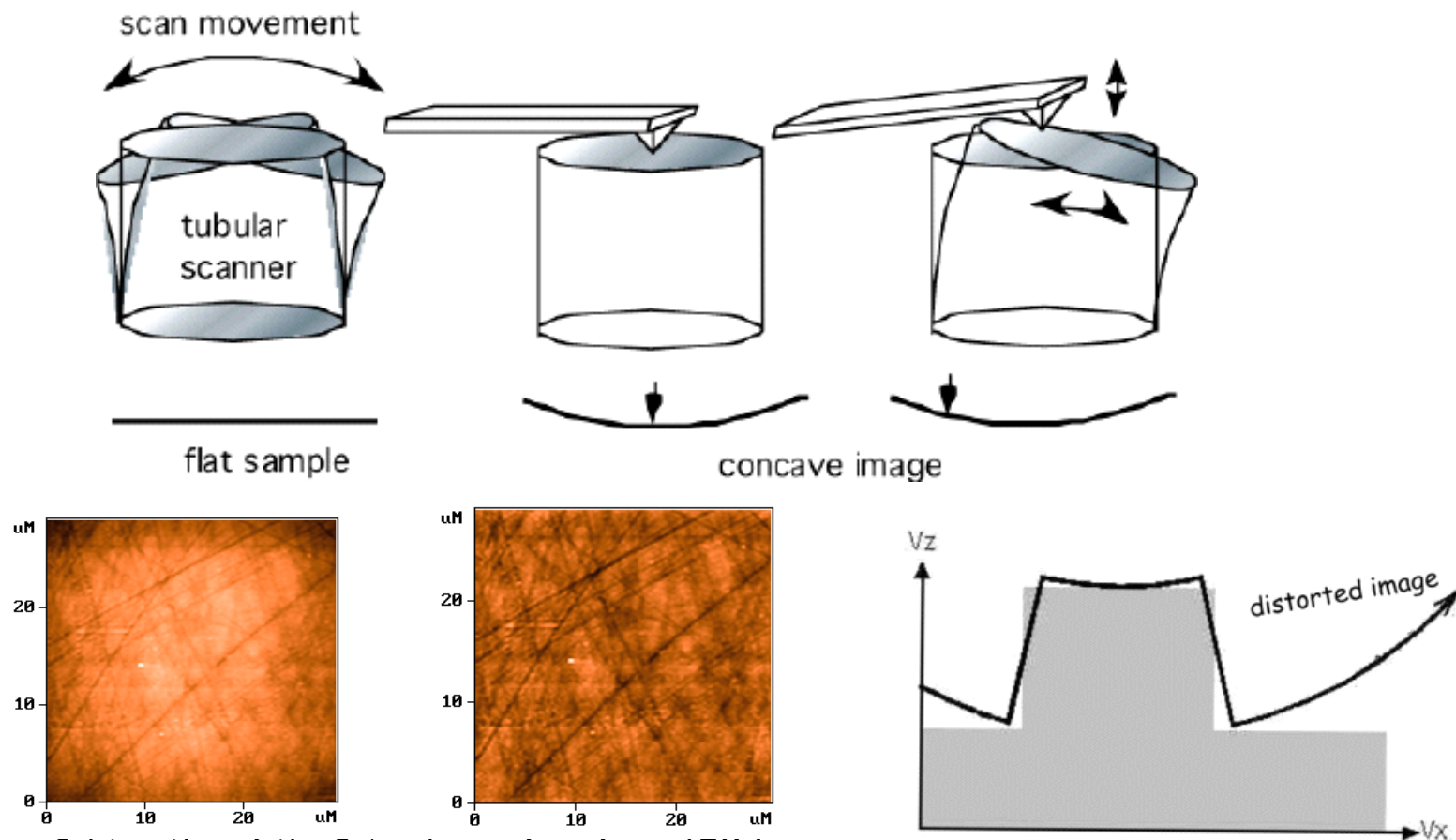
Scanner non-linearity introduces image distortions:

to improve linearity **secondary position detectors** (optical, capacitive...) may be used, or a correction through non-linear transfer function (**LUT = Look-Up-Table**) may be calculated through scanner calibration, measuring the applied voltages ( $V_x, V_y, V_z$ ) corresponding to known values of displacements ( $x, y, z$ ) on a **standard calibration grating**.

## X-Y-Z cross coupling

In tubular scanners the sample makes a rotation during x-y scan due to *cross-coupling* among horizontal and vertical displacements.

As a result the tip-sample contact moves on a *spherical* surface (whose curvature radius is the scanner length) introducing in to the image a *concave distortion*,



Subtraction of the 2<sup>nd</sup> order surface from AFM image

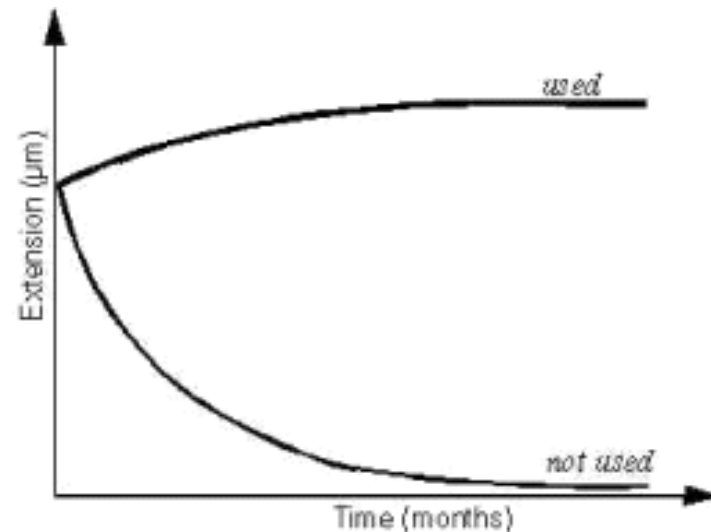
## Scanner aging

The piezoceramics is a polycrystalline material obtained by powder sintering from crystal ferroelectrics.

The ceramic is heated above its Curie temperature  $T_c (>200^\circ\text{C})$ , and then it is slowly cooled in a strong electric field (about 3 kV/cm).

After cooling below  $T_c$ , piezoceramic retains the induced polarization and gets the ability to change its sizes under an applied electric field).

At room temperature the number of dipoles losing alignment increases in time due to thermal energy, (scanner aging): the scanner must be periodically polarized. Using the scanner help keeping the polarization



# Creep

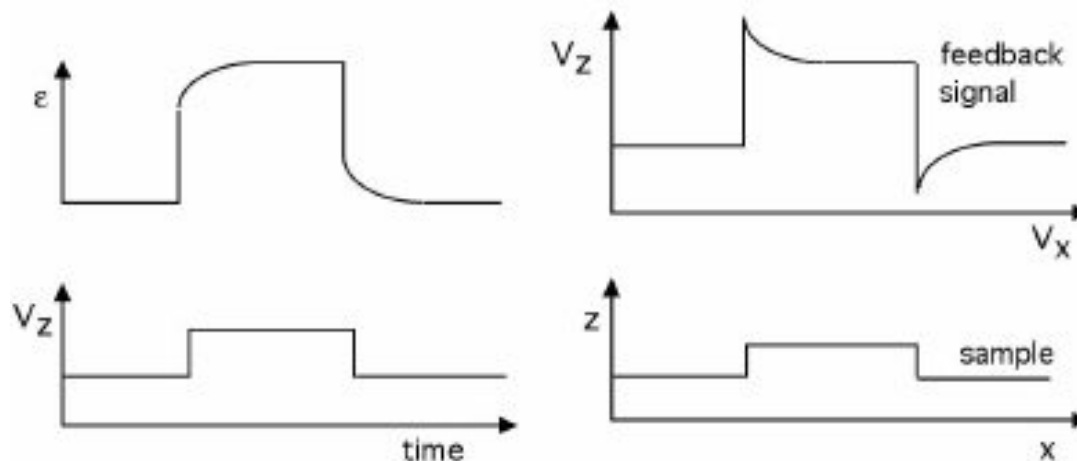
The creep is due to the *finite response time of the piezo-transducer*.

A step voltage applied to a piezo produces a deformation in a finite time interval.

Most of the deformation is achieved in a short time (a few  $\mu\text{s}$ ), the full deformation is achieved after a long time (from 10 to 100 seconds).

Typical creep values : 1% -20%.

Creep introduces not negligible image artifacts when the sample topography has *large and steep relief* or when the investigated sample area is suddenly changed.

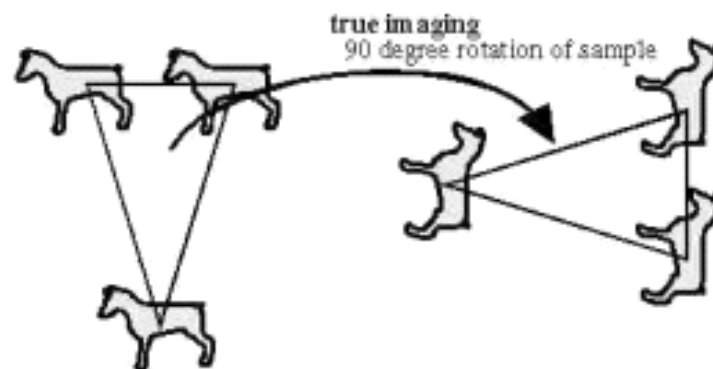
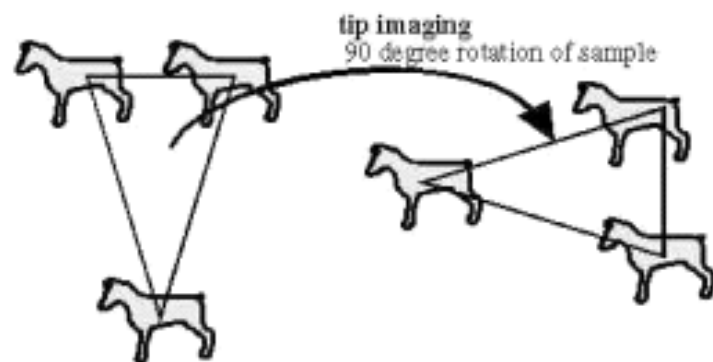


## Tip replicas

False images may be obtained using blunt tips.

A test for such effect may be made by **rotating** the sample: microscopic features should rotate correspondingly.

If not they are inverted replicas of a blunted tip.

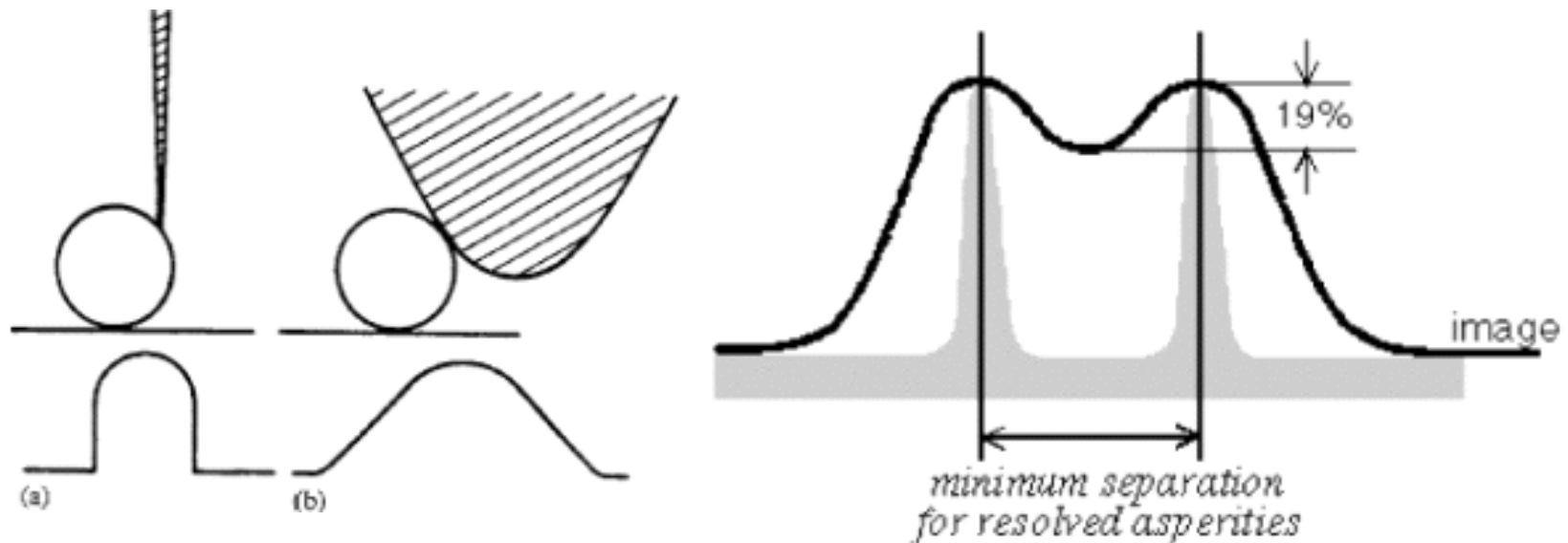


## Lateral resolution

The force measured by the cantilever is the sum of the interactions among all the atoms of the tip apex and of the sample in front of it .

Therefore the image is a **convolution** of the **tip shape** and of the **sample topography**. The **sharper** is the tip (and the **shorter** is the tip-sample **distance**), the **smaller** is the **number of interacting atoms** , and the more accurate is the resulting image.

The best commercial tips (conical) give a lateral resolution of about 10-20 Å, taken as **Rayleigh criterion** for adjacent peaks separation (19% valley between peaks)

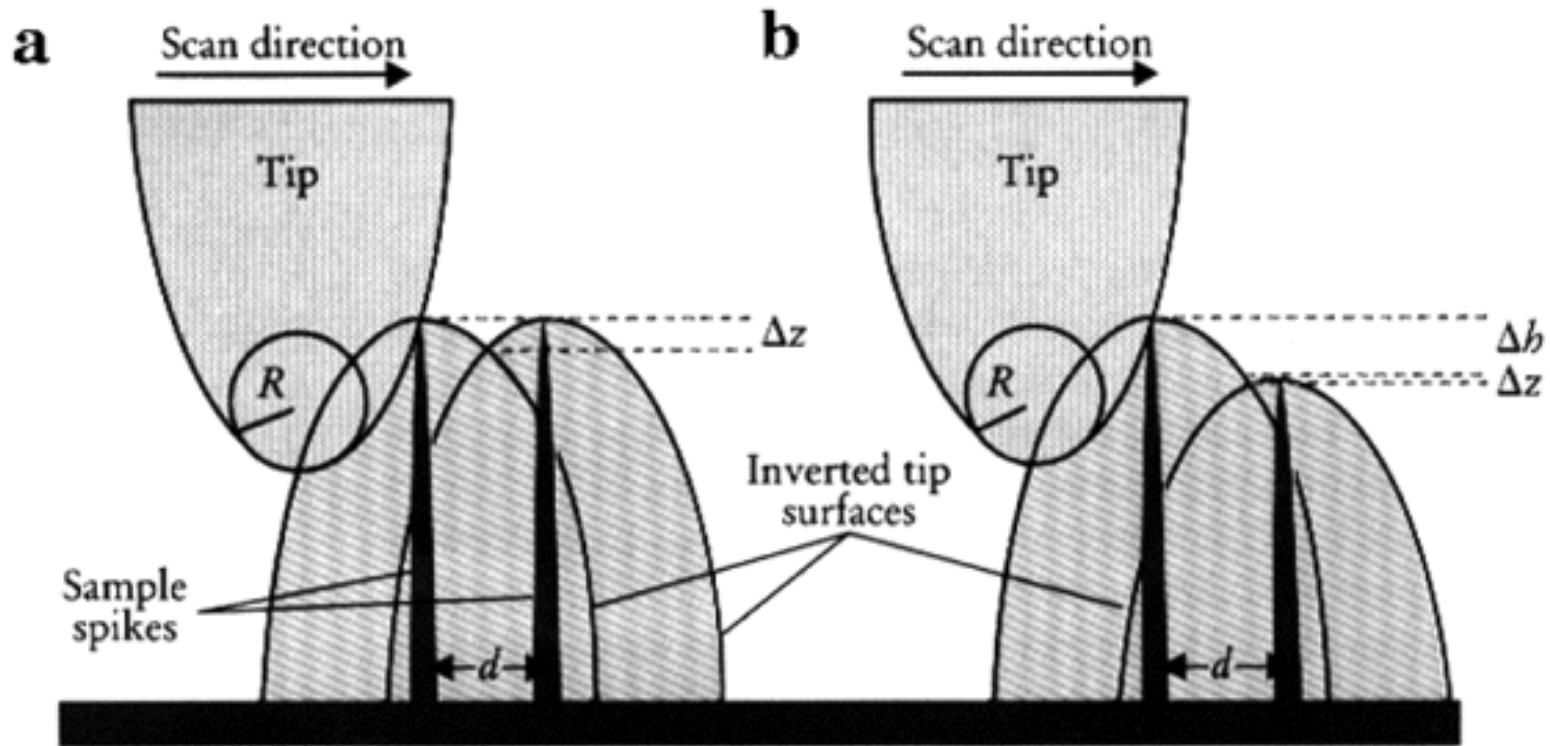


Only in **STM** this limit is exceeded because **only the closest atom** is responsible of the current **tunneling**.

As a comparison: in SEM the maximum resolution is about 100 nm.



## Lateral resolution (2)

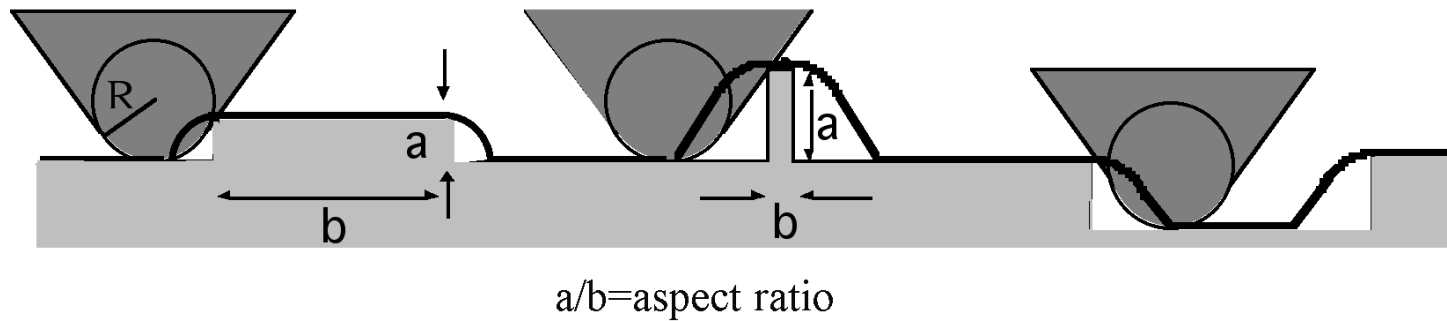


Minimum resolved distance between two spikes as a function of curvature radius  $R$ , peak-valley difference  $\Delta z$  and spike-height difference  $\Delta h$

$$d = \sqrt{2R} \cdot \left( \sqrt{\Delta z} + \sqrt{\Delta z + \Delta h} \right)$$

## Tip convolution effects

The relevance of tip convolution effect increases with the **aspect ratio** of the **sample reliefs** and decreases with the **aspect ratio of the tip**.

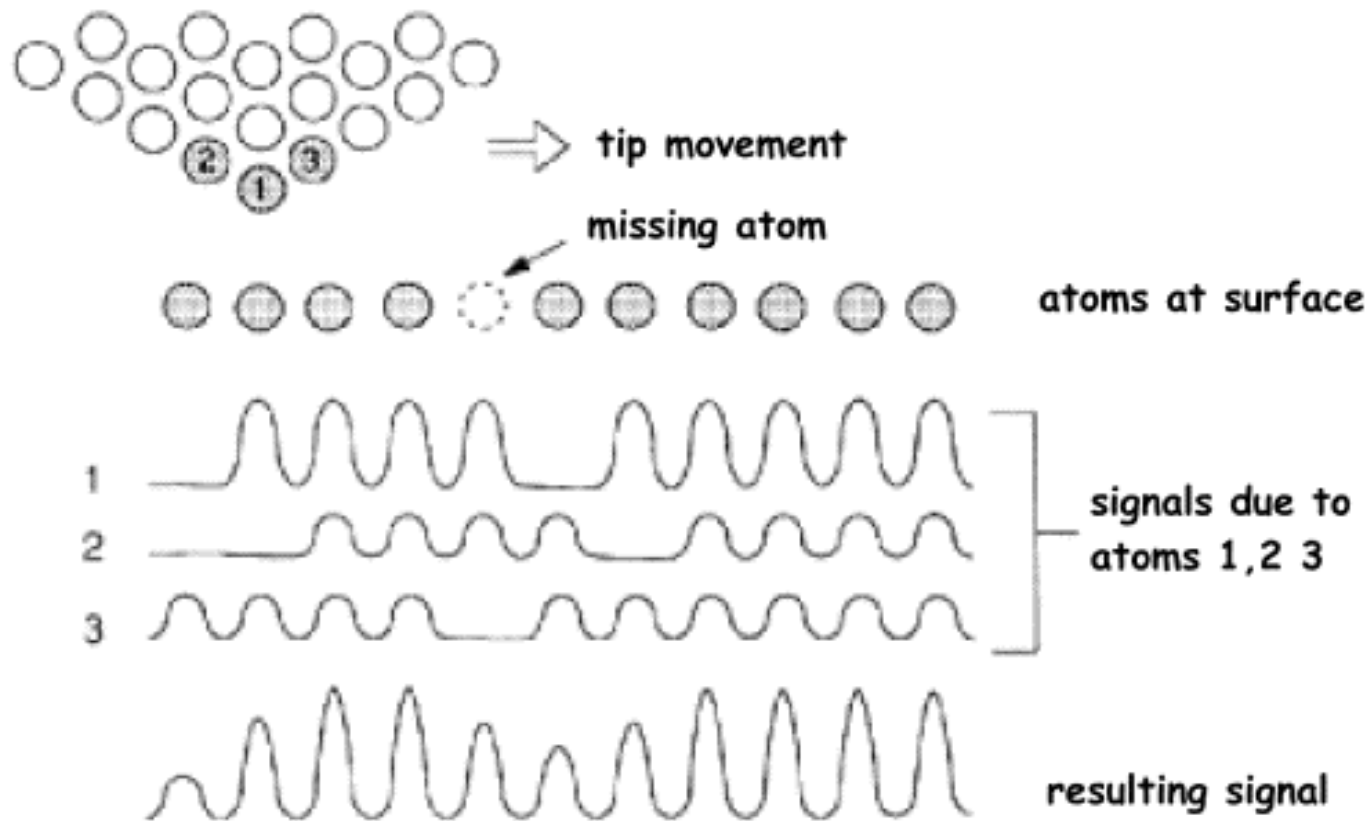


The size of the recorded image of a **relief** is in **excess**.

If the sample surface has **holes** or **cracks**, the size of the deformed image is in **defect**.

## Atomic resolution

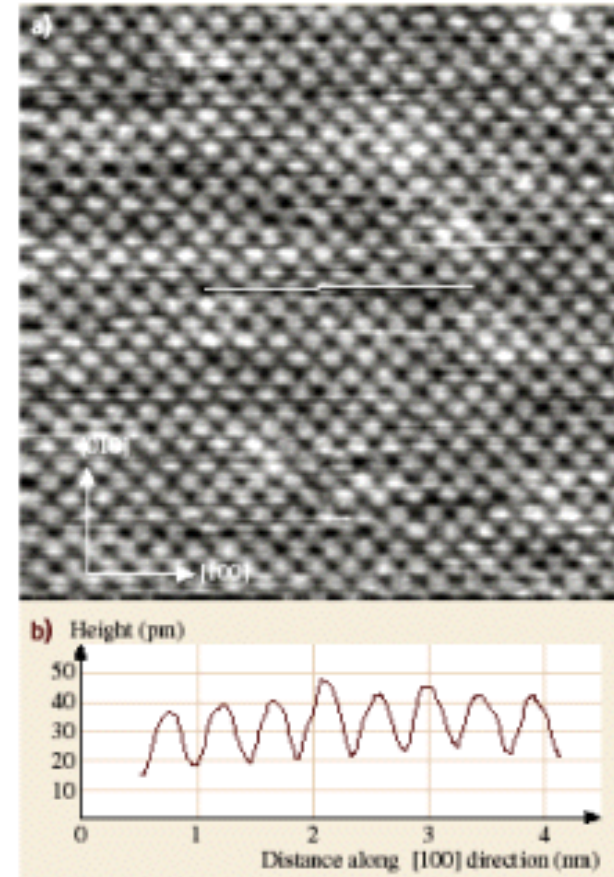
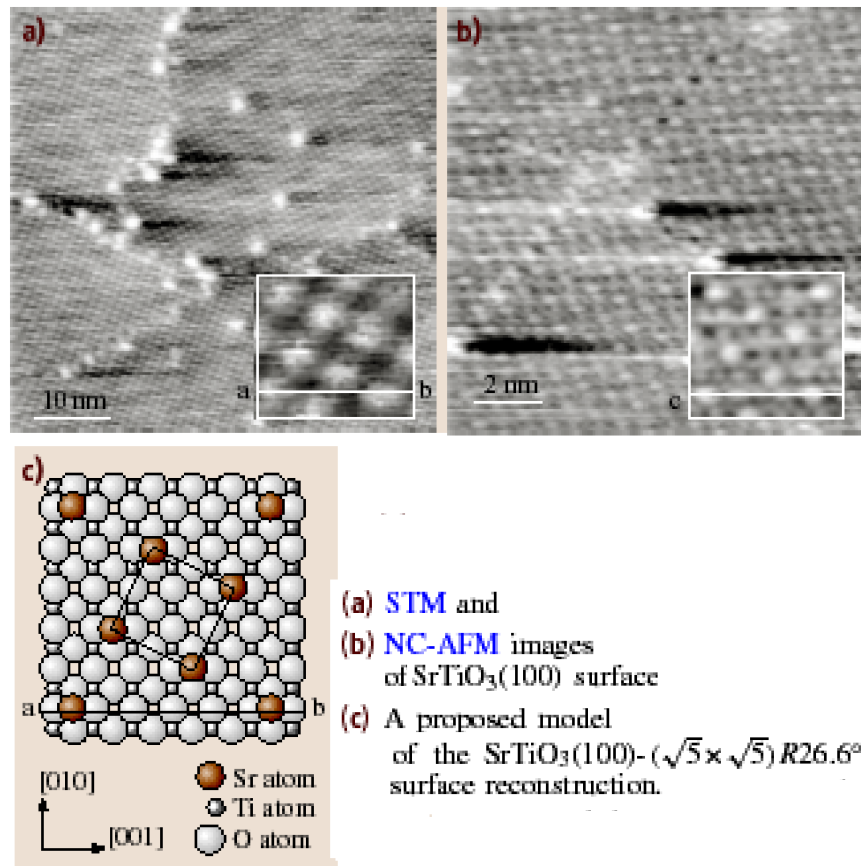
The typical SFM lateral resolution of 10 - 20 Å seems to contradict the suggestion given by images with atomic resolution published by SFM producers. We must distinguish between real **atomic resolution** and images **at atomic scale of periodical structures**



AFM may well reproduce the **periodicity** of a lattice even **without real atomic resolution**.

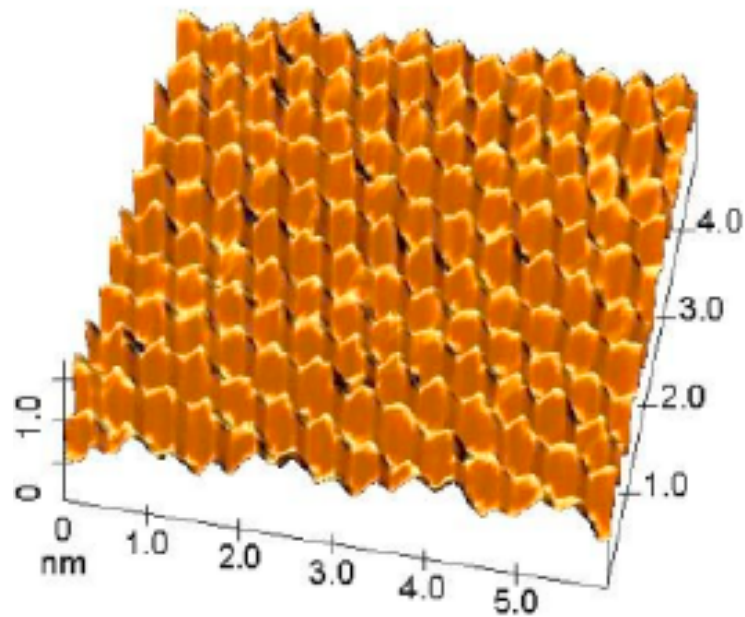
## Atomic resolution (2)

Examples of AFM images with atomic resolution



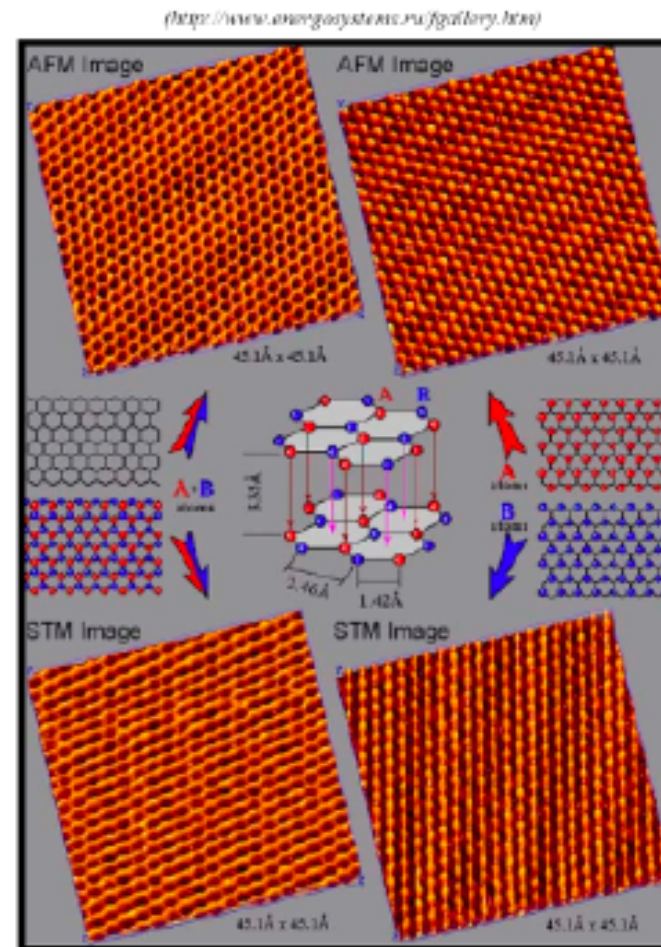
an atomically resolved image of a NiO(001) surface with a ferromagnetic Fe-coated tip

## Atomic resolution (3)



AFM High-Resolution Contact Mode Image  
of Mica

from A.Belyayev, State Research Institute of  
Physical Problems & NT-MDT, Moscow, Russia.



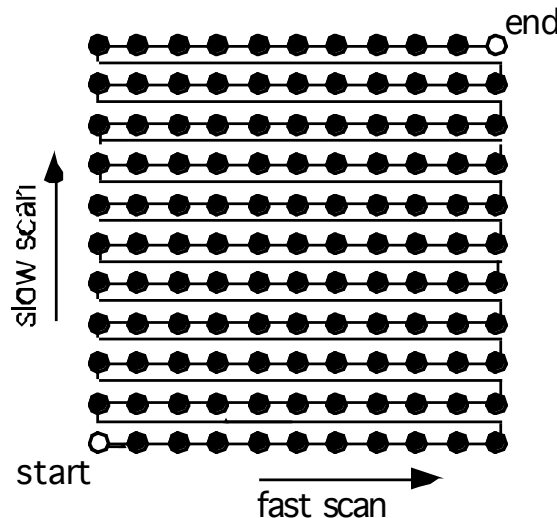
High-Resolution Images of HOPG



## Resolution of mapping

Besides the **lateral** resolution (defined by the tip radius) and the **vertical** resolution (defined by signal/noise ratio and feedback gain), also the **mapping resolution** must be accounted for.

This is defined by the distance between the closest recorded points.



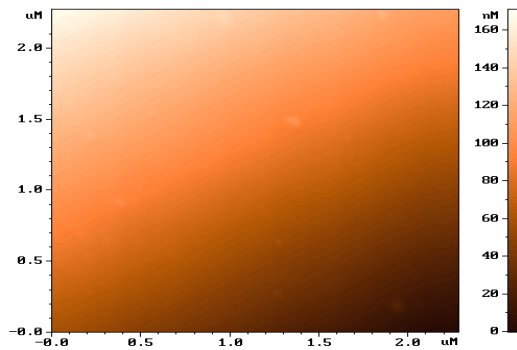
A typical SPM image with  $(512 \times 512)$  pixel covering an area  $(1\mu\text{m} \times 1\mu\text{m})$  should allow a **max theoretical resolution of  $20\text{\AA}$**  ( $1\mu\text{m} / 512$ ).

The best commercial tips have curvature radius of  $50\text{\AA}$ , giving a **lateral resolution of 10 -  $20\text{\AA}$** .

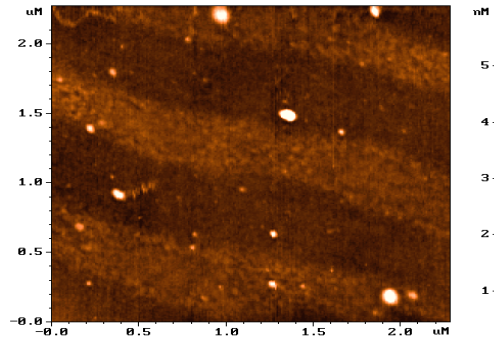
However images covering **larger** areas have a **resolution** that is **limited by the number of pixel**. (e.g.  $25\mu\text{m} \times 25\mu\text{m}$  image taken with  $256 \times 256$  pixels has a resolution of about  **$100\text{ nm}$** )

Larger matrix requires more computer memory and **longer acquisition time** (to give an order of magnitude: with  $256 \times 256$  pixel, 1 line/s, one image requires a few minutes).

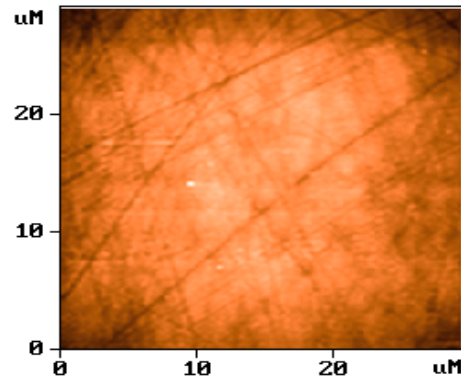
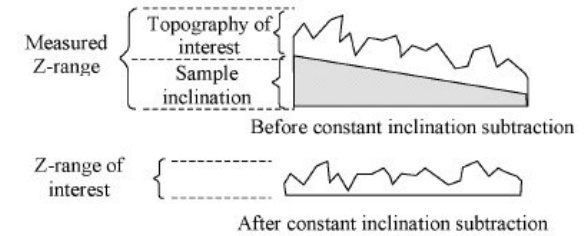
# Image Post-processing



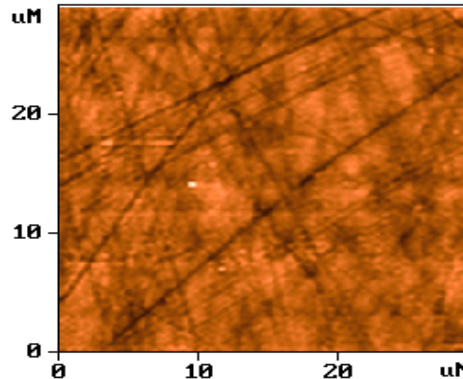
->



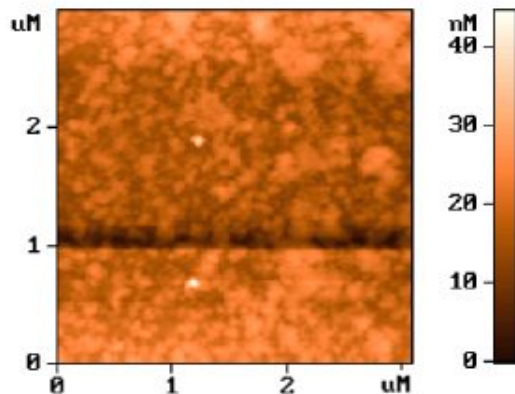
## Tilt correction



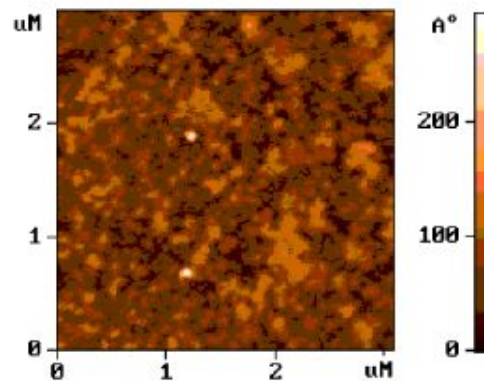
->



## Second-order surface subtraction



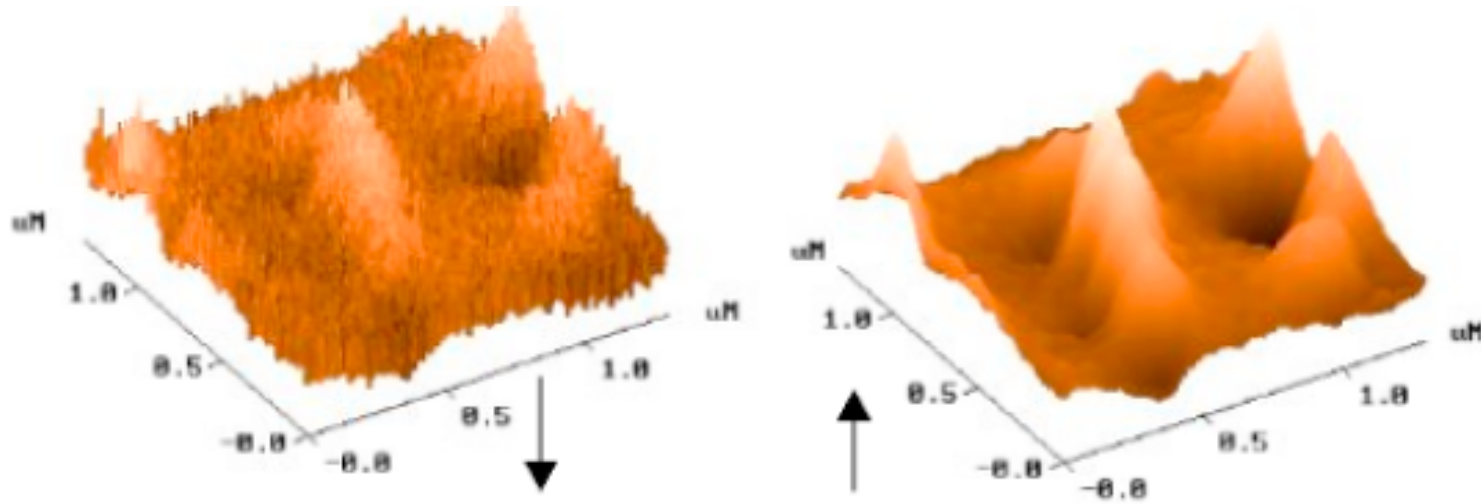
->



## Line averaging

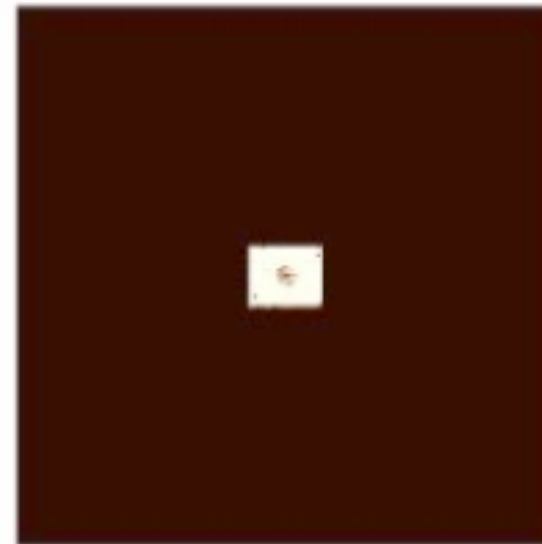
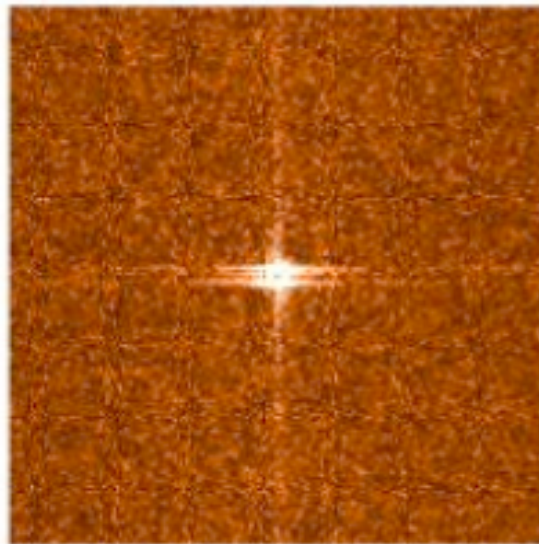


# Spatial filtering: Discrete Fourier Transform



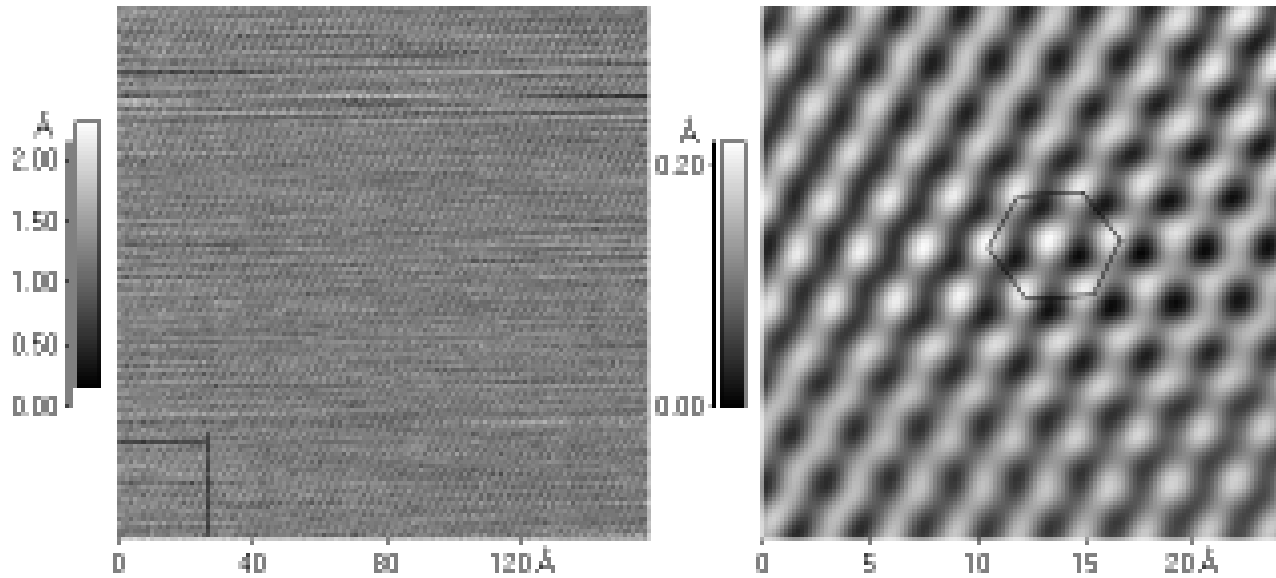
$$F_{\alpha\beta} = \frac{1}{N^2} \sum_{ij} Z_{ij} \exp \left[ 2\pi v \left( \frac{\alpha \cdot i}{N} + \frac{\beta \cdot j}{N} \right) \right]$$

$$Z_{ij} = \sum_{\alpha\beta} F_{\alpha\beta} \exp \left[ -2\pi v \left( \frac{\alpha \cdot i}{N} + \frac{\beta \cdot j}{N} \right) \right]$$



$$F'_{\alpha\beta} = F_{\alpha\beta} \cdot H_{\alpha\beta}$$

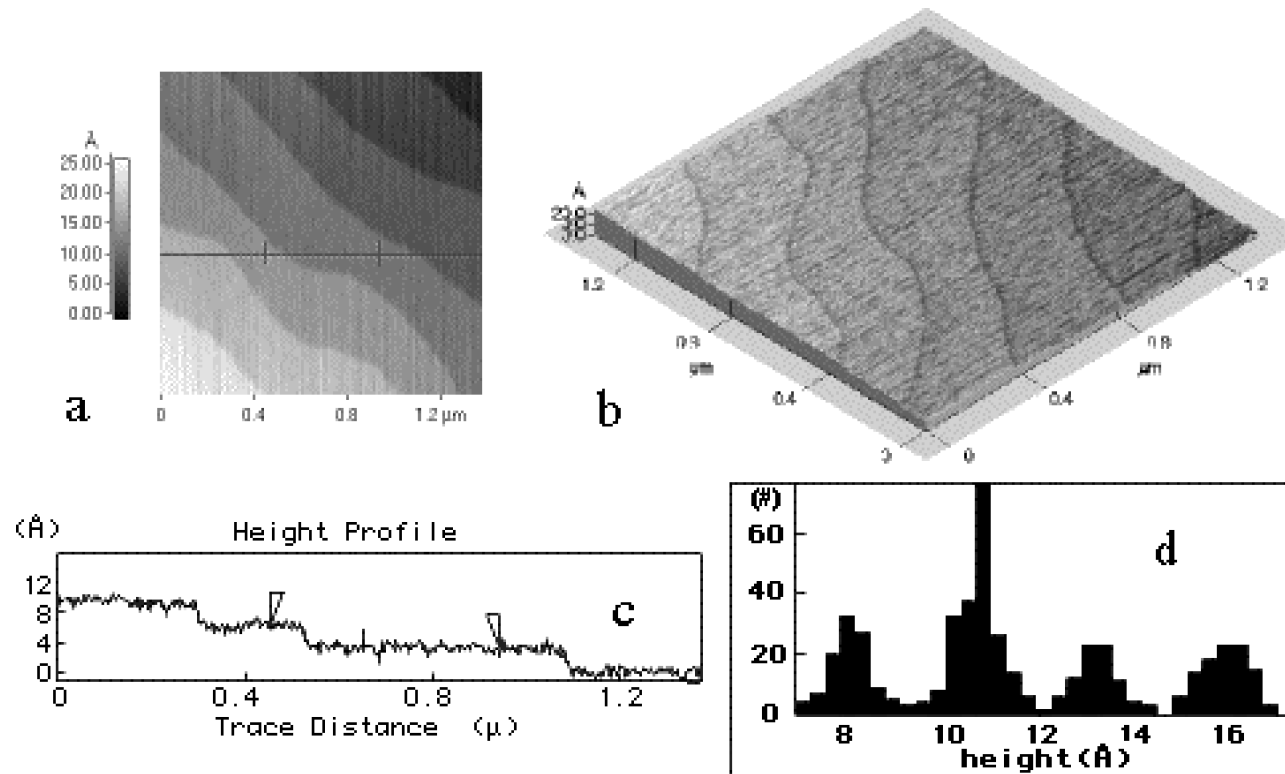
## DFT Filtering example



HOPG (Highly Oriented Pyrolytic Graphite)  
AFM original image (left) and filtered (right)

The DFT filtered image is taken from the square region marked in the lower-left corner.  
(Image taken in contact mode with Park CP - INFM, Padova)

## Atomic layers

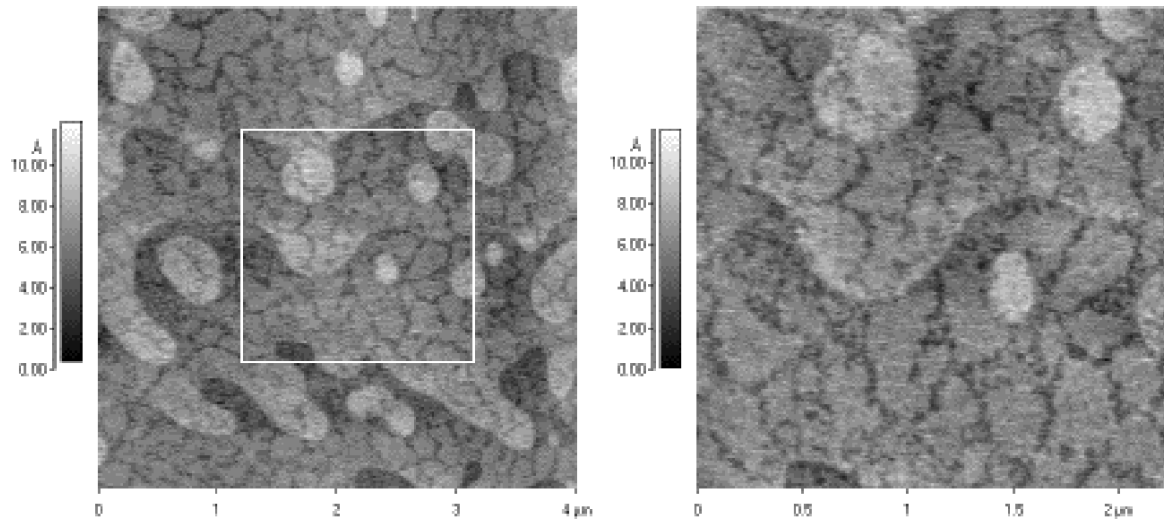


Gallium Arsenide <001>. a) "top view", b) 3D view, c) line profile, d) histogram of height.

The steps ( $\Delta z \approx 0.29 \text{ nm}$ ) between planes are half lattice spacing

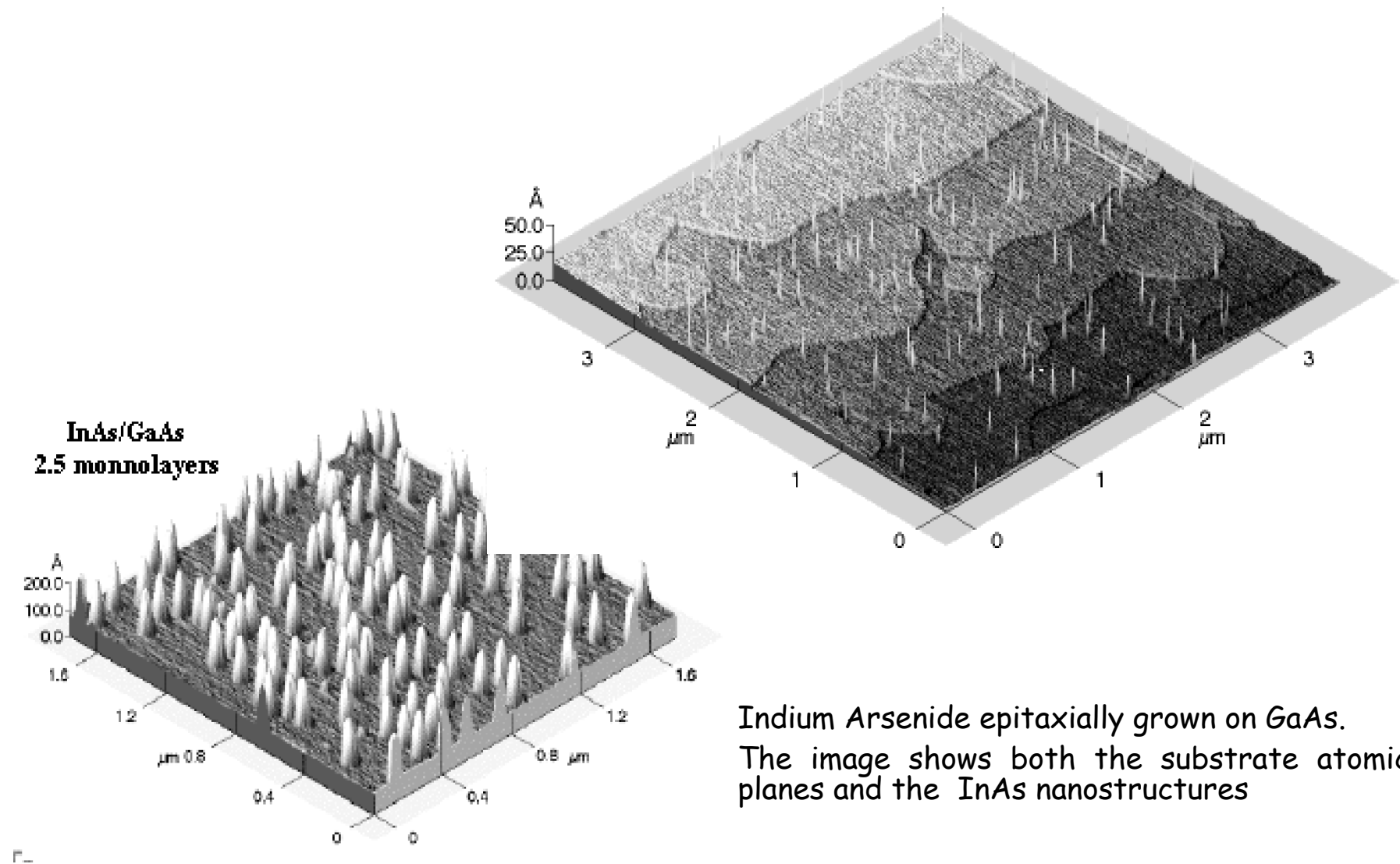
(Image taken in contact mode with Park CP - INFM, Padova)

## Sub monolayer film

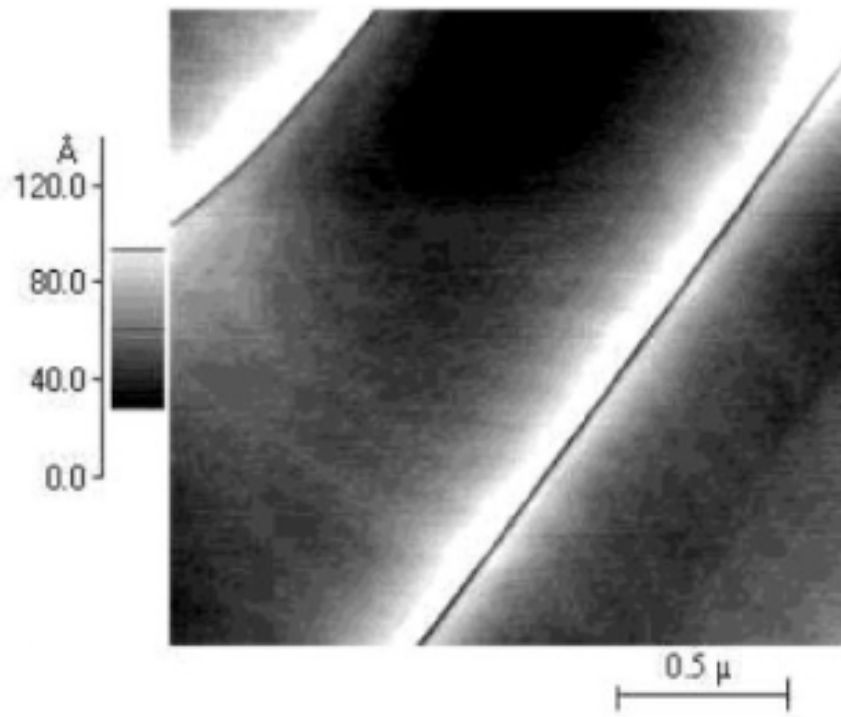


1.7 Monolayer of InP on GaAs. The film, grown layer-by-layer does not complete the first atomic layer before starting the next

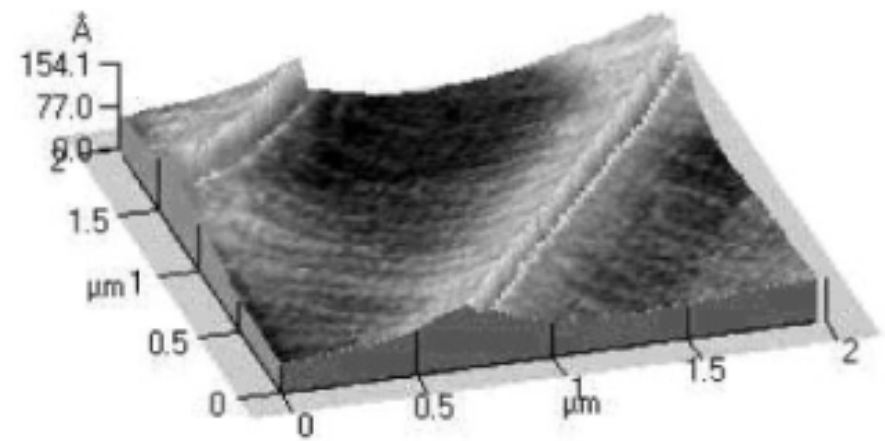
# Nanostructures



## Cracks in InGaAs/InP films



Top view

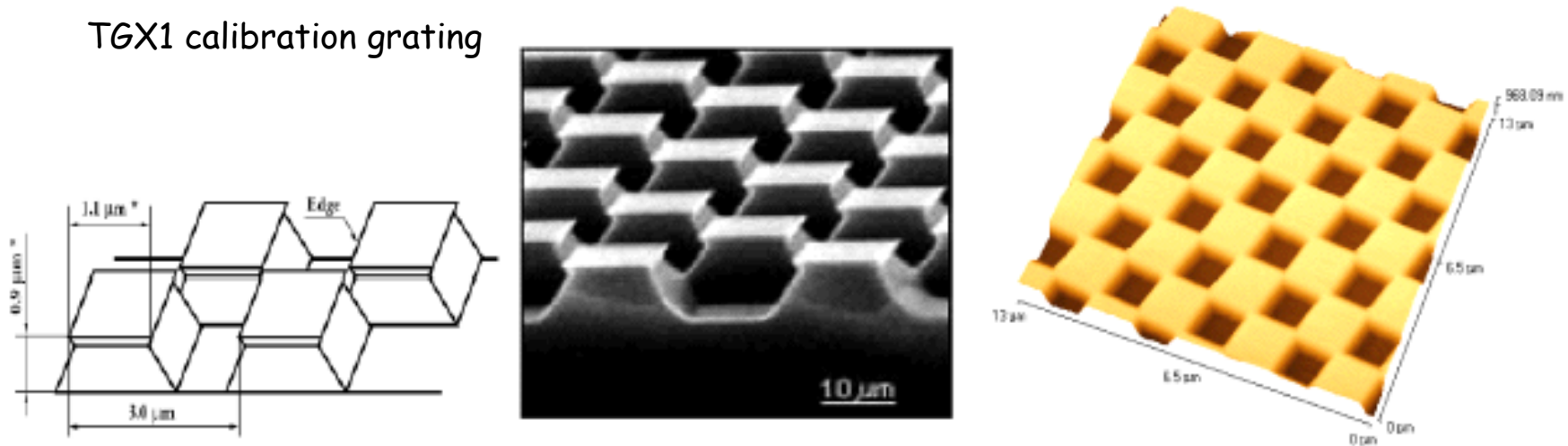


3D view

(note the different scale for x,y and z axes)

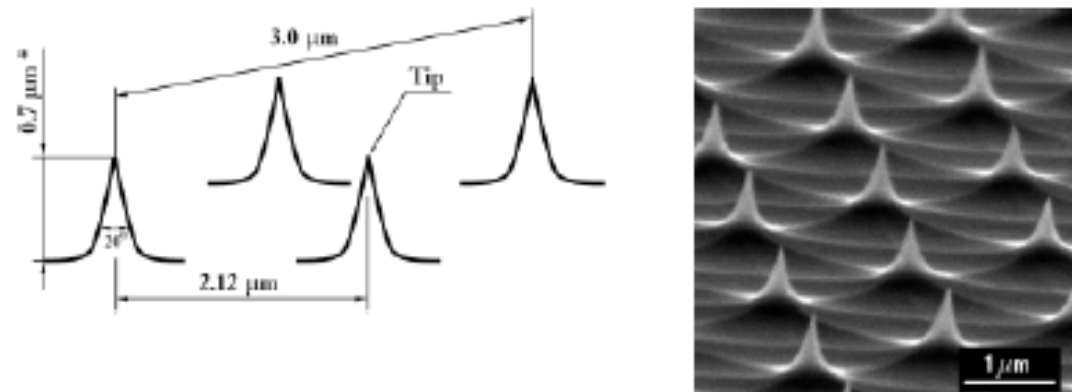
## Calibration grating

TGX1 calibration grating



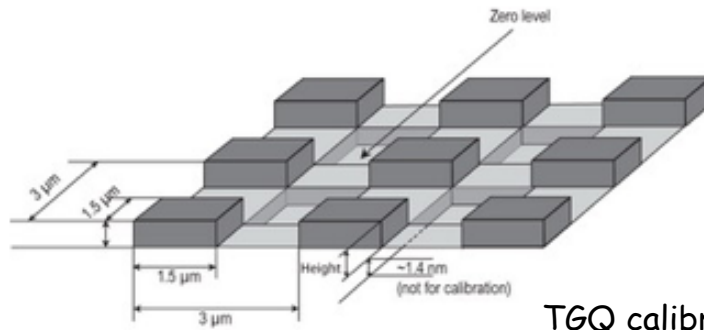
SEM image (left) and SFM image acquired using NanoEducator (right).

TGT calibration grating

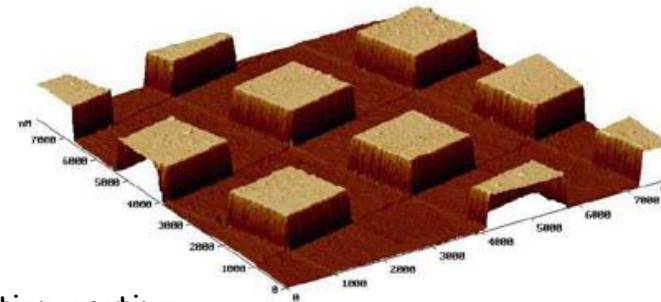




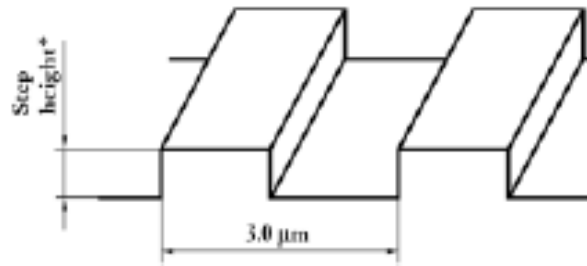
## Calibration grating 2



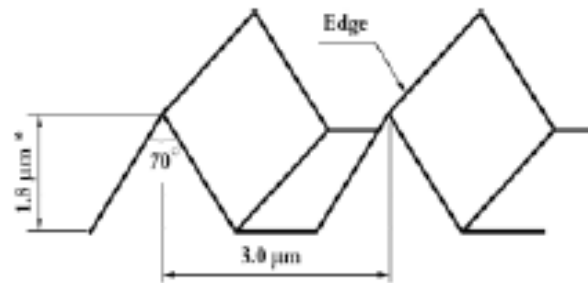
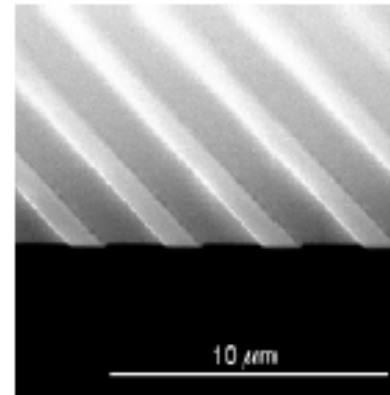
TGQ calibration grating



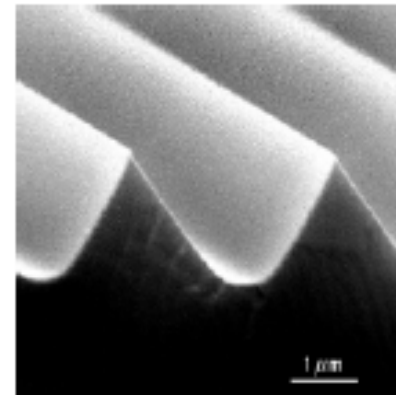
TGQ1



TGZ calibration grating



TGG calibration grating



## Calibration grating producers

[www.vlsistandards.com](http://www.vlsistandards.com) VLSI Standards

[www.vlsistandards.com/products/dimensional](http://www.vlsistandards.com/products/dimensional)

[www.2spi.com](http://www.2spi.com) StructureProbesInc -SPI

[www.2spi.com/catalog/mounts/holographic-diffraction-grating-calibration-SEM-AFM.shtml](http://www.2spi.com/catalog/mounts/holographic-diffraction-grating-calibration-SEM-AFM.shtml)

[www.pacificnanotech.com](http://www.pacificnanotech.com) Pacific nanotechnology

[www.ntt-at.com](http://www.ntt-at.com) NTT Advanced technology

[www.ntt-at.com/products\\_e/nanopattern/index.html](http://www.ntt-at.com/products_e/nanopattern/index.html)

[www.spmtips.com](http://www.spmtips.com) Micromash

[http://www.spmtips.com/test\\_structures](http://www.spmtips.com/test_structures)

[www.emsdiasum.com](http://www.emsdiasum.com) ElectronMicroscopy Standards

[www.emsdiasum.com/microscopy/products/standards/xray.aspx](http://www.emsdiasum.com/microscopy/products/standards/xray.aspx)

[WWW.NT-mdt.com](http://WWW.NT-mdt.com) NT-MDT

[www.ntmdt-tips.com](http://www.ntmdt-tips.com)